THE PREPARATION AND CHARACTERIZATION OF GLASS CAPILLARY GAS CHROMATOGRAPHY COLUMNS CONTAINING CROWN ETHER STATIONARY PHASES

By

DENNIS DALE FINE

Bachelor of Science

Oklahoma State University

Stillwater, Oklahoma

1977

Submitted to the Faculty of the Graduate College
of the Oklahoma State University
in partial fulfillment of the requirements
for the Degree of
DOCTOR OF PHILOSOPHY
December, 1984

THE PREPARATION AND CHARACTERIZATION OF GLASS CAPILLARY GAS CHROMATOGRAPHY COLUMNS CONTAINING CROWN ETHER STATIONARY PHASES

Thesis Approved:

Horacio A Mottola
Thesis Adviser

Harry L. Pearhart II

Warren T. Ford

Linda B. McGown

H. Olin Spivey

Norman N. Durham
Dean of the Graduate College

ACKNOWLEDGEMENTS

I would like to express my sincere gratitude to all the people in the Chemistry Department who have encouraged and supported me during my studies at Oklahoma State University. I realize that several have expressed concern that the time taken for me to complete my degree was longer than normal. This may be true but I assure them that my efforts have always been earnest and feel that the quality of my work has benefited.

The kind and efficient guidance of my advisor, Dr. Horacio A. Mottola, has always been an inspiration to me. He is a true scientist, gentleman, sportsman and friend whose example I hope will be reflected in me in the future. From him I have learned that every plan of study must include a course of action at a nearby lake.

I would like to thank Dr. Harry L. Gearhart II for accepting me into his group and introducing me to glass capillary chromatography. His encouragement that I pursue a Ph.D. degree will always be remembered.

I would also like to thank the other members of my committee, Dr. Warren Ford, Dr. Olin Spivey and Dr. Linda McGown for their advisement during this work.

In any endeavor in life, the paths we take always cross with people whom we wish to continue walking. My special friends in Dr. Mottola's group who have shared their paths with me are Rick Snelling, F. Albahadily, Ramaswamy Gnanaskaran, Suda Varma, Monte Marshall, Ahmad El-

Gendy, Jim Thompsen, Matt Gosnell and Al Goodwin. I wish good luck and God's blessings on each of them and hope that our paths will cross many times throughout our lives.

A special thanks to Fred Rowe of Conoco, Inc., and the analytical chemistry group of Dowell for providing SEM work of the capillary columns. We also appreciate the work of Art Buckholtz at Conoco, Inc., for his DSC and TGA work on the PVB15C5 polymer and Mario Guierrrez for his confirmation of the DSC work.

Support for this thesis was provided in part by the Water Research Institute, Oklahoma State University. Summer support which I received from Conoco, Inc., Dowell and Phillips Petroleum Co. was also greatly appreciated.

My wife, Anne, and my son, Benjamin, have my deepest appreciation for their understanding, help and encouragement. The words and work in this text are dedicated to them and to our Father and Lord Jesus Christ in Heaven. Our lives have received their blessings and we are truly grateful.

TABLE OF CONTENTS

LIST OF TABLES

LIST OF FIGURES

Figure Page

Figure Page

CHAPTER I

INTRODUCTION

Within the last twenty-eight years, the development of capillary gas chromatography columns has enriched gas chromatography technology with a powerful tool which has vastly improved the resolution and separation capability of gas chromatography. Benefits of this increase in column resolving and separating ability are best utilized when capillary columns are applied to situations where difficult sample analyses exist. The majority of capillary column usage occurs in separating components of complex mixtures which are present in samples derived from the environment, foods and flavors, clinical specimens, smoke and exhaust gases. The primary goal here is the determination of the qualitative and quantitative nature of the important components which are present. This necessitates the separation of as many components as possible. The high resolution obtainable with capillary columns is also desirable when the separation of closely related substances such as isomers and the trace analysis of minor components are required. As these benefits are due to the capillary column, a study on the preparation and characterization of glass capillary columns containing crown ether stationary phases is of relevance.

Chapter II of this thesis provides a review of literature which is concerned with capillary column chromatography, column preparation, stationary phases used for capillary chromatography and column evalua-

tion. The section which describes column evaluation was presented as a doctoral qualifier and contains more detail than other sections. Chapter III describes the intention of this thesis and states rationale for choosing crown ethers as stationary phases. This part of the thesis outlines the crown ether synthesis, column preparation and characterization. The chapter on experimental methods, Chapter IV, describes in detail the instrumentation, reagents and synthesis of the crown ether which was used as a stationary phase. The remaining sections of this chapter deal with the step-by-step preparation of eight capillary columns. Chapter V provides discussion on the characterization of each column. The discussion includes comparisons of chromatograms of alkanes and alcohols, retention-temperature plots, efficiency determinations, polarity data, scanning electron micrographs and thermal analysis data. The final chapter, Chapter VI, summarizes the thesis and recommends several crown ether stationary phases for further research.

CHAPTER II

REVIEW OF LITERATURE

Capillary Column Gas Chromatography

When the first capillary open tubular gas chromatography column was invented by M. J. E. Golay (1) in 1956, gas chromatography started developing into a science which was to provide methods to separate components of very complex mixtures such as tobacco smoke as well as very similar mixtures such as deuterated and nondeuterated hydrocarbons. Golay's original column consisted of an open steel tube which was 12 ft in length and had an inner diameter of 0.055 inches. This first capillary column was coated by pulling a cotton swab through a column which had been filled with ethylene glycol. Within two years of this work he also developed the theoretical expression which described the band broadening of solutes as they passed through the coated capillary column (2). This expression, Equation 1, relates the solute band broadening to the time the solute stays in the column ($\bar{v}$ and k'), the dimensions of the column (r_c), the movement of the solute within the liquid and mobile phase (D_L and D_G) and the physico-chemical interactions between the solute and the stationary phase (K and k').

$$H = \frac{2D_G}{\bar{v}} + \frac{(1 + 6k' + 11k'^2)\ r_c^2\ \bar{v}}{24(1+k')^2\ D_G} + \frac{k'^3\ r_c^2\ \bar{v}}{6(1+k')^2\ K^2\ D_L} \qquad (1)$$

where

H = plate height (cm)

D_G = solute diffusion coefficient in the mobile phase (cm^2/s)

$\bar{v}$ = mobile phase linear velocity (cm/s)

k' = partition ratio

r_c = radius of the column (cm)

K = partition coefficient

D_L = solute diffusion coefficient in the liquid phase (cm^2/s)

Many of these parameters are also found in the extended rate theory (van Deemter) equation for packed columns (3). In Equation 2

$$H = 2\lambda d_p + \frac{2\gamma D_G}{\bar{v}} + q\,\frac{k' d_f^2 \bar{v}}{(1+k')^2 D_L} + w\,\frac{k'^2 d_p^2 \bar{v}}{(1+k')^2 D_G} \qquad (2)$$

besides the additional parameters

λ = packing irregularity factor

d_p = particle diameter

γ = tortuosity factor

q = liquid phase configuration factor

w = radial diffusion packing factor

an additional term, $2\lambda d_p$ occurs. The difference between these two equations, which gives the capillary column the advantage in efficiency, results from the random paths that the solute takes around the packing particles (eddy diffusion) and the extent of irregularity of packing. The most significant effect of this difference results in a decreased band broadening of the solute band for the capillary column. This de-

crease in band broadening allows many more peaks to elute within the same period with greater resolution. Table I lists comparisons of various parameters which are typical for capillary and packed columns. The advantages that capillary columns provide include higher efficiency, greater resolution between peaks and shorter retention times. The greatest disadvantage that capillary columns possess is the decreased sample capacity which is caused by the large phase ratio of the capillary column. The presence of small amounts of stationary phase means that much smaller sample sizes must be introduced onto the capillary column and that special injection systems must be utilized. Such systems include split injections where a calculated proportion of the vaporized sample is introduced onto the column and splitless injection where small sample volumes are allowed to vaporize and then reconcentrate on the head of the column in the condensed solvent (4,5). A third sampling system which introduces the smallest quantitative error is on-column injection where syringes with small outer diameter fused silica needles introduce the sample directly onto the column (6). Comparison of the accuracy and precision of these three techniques shows that split and splitless injection introduce more error than on-column injection techniques (7). Large quantitative errors also occur when high boiling compounds are injected in the split mode (8). This is due to low efficiency of the split injection for transferring these compounds onto the column.

Additional equipment is also required in that carrier flow must be added at the end of the capillary to obtain the necessary flow through the detector. This requirement allows the use of capillary columns in packed column gas chromatographs and has been eliminated where detectors designed for capillaries are used.

TABLE I

COMPARISON OF PACKED AND CAPILLARY
GAS CHROMATOGRAPHY COLUMNS

	Packed	Capillary
Length	0.5 - 20 m	10 - 100 m
Inner Diameter	2 - 6 mm	0.15 - 0.50 mm
Particle Size	80 - 100 mesh (177-149 μm) 100 - 120 mesh (149-125 μm)	—
Film Thickness	5 - 10 μm	0.05 - 5.0 μm
% Load	2 - 20%	—
Phase Ratio $(\frac{V_M}{V_L})$	5 - 100	50 - 500
Sample Capacity/ Component	< 20 μg	< 50 ng - 500 ng
Sample Size	0.04 - 20 μℓ	0.004 - 1.0 μℓ (split)
Theoretical Plates	5,000 - 20,000	50,000 - 150,000
Column Linear Velocity	7 - 10 cm/s	16 - 60 cm/s
Flow Rate	10 - 20 mℓ/min	1 - 15 mℓ/min

The disadvantage of low capacity in capillary columns has been lessened recently with the introduction of capillaries with film thicknesses up to 6 μm and wide bore capillaries with inner diameters up to 0.75 mm (9,10). These columns, while having lower efficiencies than narrow bore, thin film capillaries, still possess more efficiency than

packed columns. The thicker films which are stabilized by in situ free radical crosslinking of the coated film provide column capacities which approach that of packed columns. These columns also can withstand larger solvent sample sizes since the stationary phase is nonextractable.

Capillary Column Preparation

Column Materials

Capillary columns have been made from various materials. Early materials include Tygon and Teflon, borosilicate or soda-lime glass, aluminum, nickel, gold, copper, stainless steel, and a stainless steel-nickel alloy (11,12). Of these, borosilicate and soda-lime glass have until recently been the most widely used column materials. Plastics possessed low operating temperatures or as in the case of Teflon possessed a surface that was not wettable by most stationary phases. Metal columns of gold showed excellent efficiency but cost precluded their use. Although metals such as aluminum, copper and nickel gave support surfaces which were wettable by stationary phases, chemical treatment of the metal surface was required to reduce adsorption of solute molecules and decomposition of the stationary phase.

The availability and low cost of borosilicate and soda-lime glass tubing along with the invention of a glass capillary drawing machine by Desty, Haresnape and Whyman (13) in 1960 resulted in the use of glass for the preparation of the majority of capillary columns until recently. The introduction of fused silica capillaries in 1979 provided chromatographers with a flexible column which was easily handled and provided less surface activity than borosilicate or soft glass capillaries (14). This

flexibility was the one feature of fused silica columns that has been responsible for converting packed column users over to capillary columns users.

Much of the literature concerned with the development and preparation of capillary columns can be related to the study of the physical and chemical nature of the glass surface inside the capillary. Desirable properties which are necessary for good columns are wettability of the glass surface by the stationary phase and chemical inertness of the surface toward the stationary phase and solutes injected onto the column. Wettability by the stationary phase can be related to the critical surface tension of the surface and the surface tension of the stationary phase. Stable films of stationary phase are obtained when the surface tension of the solution or stationary phase used to coat the capillary is smaller than the critical surface tension of the glass surface. This criteria has been used to explain why nonpolar stationary phases such as squalane or polydimethylsiloxane are more stable than polar stationary phases when coated on the same unroughened support. Columns containing polar stationary phases have additional requirements of a roughened capillary surface before stable films result. By increasing the surface area of the glass surface, its effective surface tension is increased to a value larger than the surface tension of the polar stationary base. Methods for surface roughening will be covered later.

Chemical inertness of the support material is necessary to prevent chemical or physical adsorption of solutes and for thermal stability of the stationary phases. Inertness of a borosilicate or soda-lime glass surface can be increased by removing metals which are present in the bulk of the glass and chemically deactivating the glass surface. The

bulk of borosilicate glass is composed of 2.5% sodium, 0.2% calcium, 7.0% boron, and 0.8% aluminum (15). These metal oxides act as Lewis acids on the glass surface and must be removed or covered up so that they do not cause adsorption of lone-pair electron donor molecules such as alcohols, ketones or amines and π-bond containing molecules such as aromatic or olefin compounds. The introduction of fused silica glass has eliminated these problems because fused silica contains very low amounts of these metals.

A characteristic of both borosilicate and fused silica glasses is the presence of silanol groups. Silicon-hydroxyl groups are present on the glass surface in different concentrations depending on the thermal treatment of the glass. Geometrical considerations show about eight silanol groups per 100 $\mathring{A}^2$ of glass while experimental determinations show about five groups per 100 $\mathring{A}^2$ (16). Thermal treatment of the glass under vacuum causes the silanol concentration to decrease from 4.8 per 100 $\mathring{A}^2$ at 200°C to 0.7 groups per 100 $\mathring{A}^2$ at 900°C (17). These silanol groups provide proton donor sites which can cause adsorption of molecules which are capable of hydrogen bonding. This means that compounds with π-electrons such as aromatics or unsaturated compounds and free electron pairs on oxygen or nitrogen such as alcohols, amines, carbonyls, and ether compounds are susceptible to adsorption by the silanols. Removal of these silanol groups by high temperature dehydroxylation does not decrease the surface activity since the siloxane bridges, which result after the heat treatment, are more reactive than the free silanol group (18).

Predrawing Treatments

The preparation of glass capillary columns starts with cleaning the glass tube prior to drawing. Among the methods of solvent, chromic acid and hydroflouric acid washing, Onuska, Afghan and Wilkinson (19) has shown that allowing 10% HF to remain in the tube overnight gives the better deactivated column when it is deactivated and coated with Carbowax 20M. This technique serves to remove a layer of the silica from the glass surface and also organic material that is adsorbed to that layer.

Capillary Drawing

Fabrication of capillaries from the cleaned glass tubing is done with a capillary drawing machine. The ratio of speeds of rollers on each side of the drawing oven controls the inner diameter of the drawn capillary. After exiting the drawing oven, the capillary is pushed through a heated coiling tube which forms the capillary into its helical shape. Chemical treatment during the capillary drawing operation has included purging the capillary with oxygen or with very dry argon (15,20). The purge with oxygen was used to oxidize any adsorbed carbon on the surface. The dry argon was used to dehydrate the glass surface and prevent moisture from rehydrating the glass before the capillary was coated with the stationary phase.

Roughening

After the pretreatment and drawing operation, the next step in the preparation depends on the type of stationary phase used. If nonpolar stationary phases are to be coated, then a deactivation step must be in-

cluded before phase coating. When a polar stationary phase is to be coated, a roughening step is required before deactivation. Surface roughening can be accomplished by two approaches. The first involves corrosion of the glass surface with acids such as HF or HCl or bases such as NH_3 or NaOH (21-24). Both of these cause roughening by breaking the Si-O-Si bond in the glass framework. Salts of HF such as KHF_2 and NH_4FHF also can cause corrosion (21,25). In the case of NH_4FHF, silica whisker formation can occur when the salt coated capillary is heated at high temperatures (26). This whisker formation can also be accomplished by fluoroether liquids which decompose at high temperatures and release HF (27). The drawback to these whisker columns is the high surface activity which requires extensive deactivation treatments. One additional type of roughening uses plasma etching where radio frequency discharge causes fluoro compounds to form a plasma (28). The etching of the glass surface by this method is thought to be caused by free radicals which are present in the plasma.

The second type of roughening involves covering the glass surface with a material that increases the inner surface area. This can be accomplished by passing HCl gas through unleached soda-lime capillaries (29). At high temperatures sodium ions migrate to the glass surface, react with HCl, and form NaCl crystals. In addition to surface roughening, silanol groups are also covered and some deactivation occurs. NaCl deposits can also be obtained by coating the capillary with a 10% or saturated solution of NaCl (30,31). Barium carbonate has also been deposited (32). Here a plug of $Ba(OH)_2$ solution was pushed through the capillary with carbon dioxide. Instead of plugging the capillary with barium carbonate, a film and crystals of $BaCO_3$ formed on the capillary

inner wall. This roughening technique caused an increase in surface area and hence good thermal stability of stationary phases, although the basic nature of the carbonate deposit caused adsorption of acidic compounds. Removal of this activity could not be accomplished with Carbowax 20M deactivation as was determined by the adsorption of propionic acid. Other methods of surface roughening include coating the capillary with solid materials such as carbon black, Silanox 101 (a trimethylsilylated fumed silica), Cab-O-Sil (unsilylated fumed silica), amorphous silica, colloidal silicic acid and quartz (33-38). These materials serve only to provide a roughened surface and do not affect the active sites of the glass.

Deactivation and Chemical Modification

Following the roughening step when a polar stationary phase is to be coated or after the capillary drawing for a nonpolar phase, some type of deactivation or chemical modification must be used. For nonpolar phases the first step of deactivation involves acid leaching of the metals from the glass. Grob, Grob and Grob's technique (39) which uses a static leach with 20% HCl at 180°C has been used extensively. Lee, Vassilaros, Phillips, Hercules, Azumaya, Jorgenson, Maskarinec and Novotny (40) have shown that a dynamic leach with a continuous flow of HCl through the capillary at 110°C with intermediate drying steps gives surfaces which are free not only of metals but also of adsorbed carbon. Lee's results revealed that the statically leached glass surface had a carbon contamination of 25%.

After the initial HCl treatment the column should be rinsed with deionized water to remove all traces of HCl and then dehydrated to remove adsorbed water. Removal of the water by carrier flow or vacuum and

heating at 220-250°C for 30-90 min (depending on the glass type) facilitates coating of the capillary by increasing the wettability of the surface and reactivity of the surface toward silylation.

Further deactivation after leaching can be accomplished by coating materials which adsorb on the glass surface, form polymeric coatings over the surface or bond directly to the silanol groups in the glass. Many surfactants have been used where the polar portion of these molecules adsorb to the glass surface of the capillary and deactivate the surface silanol. Examples of these surfactants are trioctadecylmethylammonium bromide, sodium tetraphenylborate and triethanolamine (41-43). Although these surface modifiers have shown good deactivation character, there are drawbacks in the stability of the monolayer of surfactant formed. Since these surfactants are not bonded to the glass surface, thermal stability is poor and replacement of these surfactants by solute molecules can occur.

Polymeric coatings have found wide usage especially for a pretreatment with Carbowax 20M (CW20M) (44,45). When a 2% w/v solution of CW20M in CH_2Cl_2 is dynamically coated in the capillary, the capillary heated at 280°C for 16 hours, and the column exhaustively extracted with solvent, a nonextractable layer of CW20M coats the capillary surface. A thicker film of CW20M or other polar stationary phase can then be coated over this polymeric surface. Though the mechanism for the bonding of the nonextractable Carbowax film has not been determined, the necessity for silanol groups on the glass surface suggests that a chemical bond is formed or that the cumulative effect of hydrogen and Van der Waals bonds between the Carbowax polymer and silanols approaches chemical bond strength. A possible chemical reaction for the deactivation could be the

decomposition of Carbowax into oxirane which reacts with two adjacent silanol groups (46). Surfaces which are deactivated with Carbowax can be coated with thicker films of Carbowax 20M or with nonpolar polydimethylsiloxanes such as OV101 or SP2100. Polymer deactivated surfaces have also been obtained using squalane, ethoxycarbonylpolyphenylene and alkypolysiloxanes. An advantage of polymeric films is the enhanced thermal stability of the coated stationary phase. When alkylpolysiloxanes such as OV1 and OV101 are heated at high temperatures in sealed capillaries and then recoated with the same stationary phase, higher maximum operating temperatures are obtained (47). One disadvantage of these column types is that the underlying polymer film can contribute to retention and effect a change in column polarity different from that expected for the stationary phase.

Deactivation can also be accomplished by chemical bonding groups to the glass surface. Trimethylchlorosilane (TMCS), dichlorodimethylsilane (DCDMS), hexamethyldisilazane (HMDS), diphenyltetramethyldisilazane (DPTMS) and dichlorooctamethyltetrasiloxane are examples of deactivating reagents which react with silanol groups to form bonded silyl ligands on the glass surface. Because different types of silanol groups are present in silica, that is, free, hydrogen bounded, vicinal and geminal, these silanes have different reactivities to each type of silanol group. TMCS reacts with surface silanols in a first order reaction which requires a bimolecular transition state. This mechanism excludes reaction with hydrogen bonded silanols. DMCS which is a bifunctional silane can react with hydrogen bound silanols. HMDS is considerably more reactive towards silanols than either of the chlorosilanes. Novotny, Blomberg and Bartle (48) have shown that improved nonpolar columns can be obtained if gaseous

5:1 mixtures of HMDS and TMCS are used to silanize etched capillary columns. Rutten and Luyten (42) also applied mixtures of HMDS and TMCS but used a coated liquid and heated the sealed capillary at 200°C for several days instead of at 150°C as described by Novotny. This higher temperature silanization gave nonpolar columns which were stable for several months while those treated at 150°C deteriorated rapidly. This trent in high temperature silanization was continued by Welsch, Engewald and Klaucke (49) with silanization temperatures of 300°C for pure HMDS, Grob, Grob and Grob (50) with temperatures of 400°C for diphenyltetramethyldisilazane, and Lee, Wright, Graham and Hercules (51) with temperatures at 400°C for 5:1 mixtures of HMDS and TMCS. The procedure of dynamic chemical treatment using silylating vapors which pass through the heated column has provided better column deactivation than static treatment of sealed capillaries containing films of silylated reagents. Dynamic treatment allows flushing of NH_3 byproducts of disilazanes which can cause regeneration of silanol groups on the silica and HCl byproducts of disilazanes which can cause regeneration of silanol groups on the silica and HCl byproducts of chlorosilanes which can react with metal oxides and also generate silanol groups. One additional chlorosilane, dichlorooctamethyltetrasiloxane, deactivates the column surface by bonding at the two ends of its short siloxane oligomer (51). Heat treatment at 400°C of the sealed capillary provides surfaces which are similar to high molecular polysiloxane deactivated surfaces.

Dynamic and Static Coating

After the surface deactivation step, the column can be coated by a dynamic or static method. Dynamic coating which was first applied by

Dijkstra and De Goey (52) requires that a solution of 2 to 15% v/v stationary phase in volatile solvent be pushed through the capillary column at a constant linear velocity of 1-2 cm/s with helium or nitrogen pressure. The uniformity of the film left inside the column is dependent on many variables, and close attention to detail is required in order to obtain good columns. Since the plug velocity increases as it exits the column and causes thicker films to deposit, buffer columns are attached to the column end. Flow restrictors and syringe pumps functioning as liquid brakes at the end of the column have been used to ensure constant exit of the coating solution (53-54). Even with buffer columns, compression of the pushing gas causes a gradual decrease in coating velocity. Mercury plugs have also been introduced after the coating solution to act as wipers which leave thin films of coating solution (55). Here higher concentrations of coating solution having higher viscosities can be used to obtain thicker films. During the coating operation the alignment of the coils should be vertical so that the coating solution does not collect on the lower portion of each loop. Temperature fluctuations along the column should be minimized to ensure uniform evaporation of solvent and prevent recondensation.

The prevention of droplet or lense formation after the coating has occurred is dependent on the wettability of the surface by the stationary phase and the solution film thickness left after the plug passes through the column. The wettability of the surface can be ensured if the surface tension of the stationary phase is lower than that of the surface. The thickness of the film left on the surface is affected by the column radius (r_c), velocity (v), concentration (C), surface tension (γ), and viscosity (η) of the solvent, volatility and rate of solvent evaporation.

Although Equation 3 which utilizes several of these variables is used to predict the film thickness, other methods are used to calculate the

$$d_f = \frac{r_c C}{200} \left[\frac{v\eta}{\gamma}\right]^{1/2} \quad (3)$$

actual film thickness (56). Examples include determining the volume of coating solution consumed after coating, relating the column radius and partition ratio for a probe on a dynamically coated column to the phase ratio and partition ratio of the same probe on a statically coated column containing the same stationary phase and measuring the weight of stationary phase that can be washed out of the column (57-59).

The method of statically coating capillary columns which was first described by Golay (60) has been shown to produce more efficient columns than the dynamic method and provides a ready determination of film thickness (Equation 4) which is based on the inner diameter and solution concentration (% v/v) (61).

$$d_f = \frac{r_c C}{200} \quad (4)$$

Since a vacuum is applied to one end of the capillary, the solution must be free of dust and degassed so that air or vapor bubbles are not present or do not form later. If an air bubble is formed at the end of the capillary, the coating solution is evacuated instead of the solvent evaporated. A constant column temperature must be maintained during the evacuation if uniform films are to be obtained. A constant room or water bath temperature is sufficient although baths within thermostated baths

for higher temperature evacuation and shorter evacuation times have been described (61). Solvents of low volatility such as methylene chloride, pentane and diethyl ether are recommended so that coating times can be minimized. Typical coating times for solutions in pentane and methylene chloride in a 20 m × 0.3 mm I.D. column are 8 h and 15 h, respectively (62).

The greatest difficulty in static coating is sealing one end of the capillary when the coating solution is present. Simple microtorch sealing of the end cannot be used since vapor bubbles are formed from the flame. Of the various methods including sodium silicate, cements, adhesives, and waxes, a mechanical seal obtained by crimping a copper tube over a piece of heat shrink tubing attached to the column end has been described as the simplest (63). Pressurizing the liquid in the capillary against this seal at 50 psi overnight ensures that vapor bubbles and static coating failures are minimized. In several variations of the static coating method the open end of the capillary is fed into a heated oven or liquid bath where the solvent rapidly evaporates forcing the stationary phase to the column wall (64,65). The pressure of the evaporated solvent which approaches 300 psi produces intimate contact between the glass and stationary phase and more stable columns result. A method of static coating where the coating solution is freeze dried has also been introduced although the method is limited to low viscosity or non-solid stationary phases (66).

Stationary Phase Immobilization

Chemical immobilization of the stationary phase inside the capillary has been accomplished by bonding the phase to the silica surface and/or

crosslinking the molecules of the stationary phase to each other. When the stationary phase is immobilized by either method, the stability of the film increases and the phase becomes nonextractable. As such, phase stripping by large solvent injections is eliminated. Column efficiency which is lessened by non-volatile samples injected onto the column or formed as byproducts from sample decomposition can be restored by rinsing the capillary with solvent.

Though several methods of phase immobilization were introduced from 1966 to 1978 which involved in situ polymerizations of polyolefins and prepolymers, these methods were sophisticated and laborious. In 1981, K. Grob (67) developed an immobilization method which utilized free radical initiators to induce crosslinking in polysiloxane stationary phases. Both the initiator, dibenzoylperoxide, and a low polarity polysiloxane were statically coated in the column and crosslinking induced with temperature programming. After conditioning at 200°C, the column was evaluated, rinsed with two column volumes of methylene chloride and one column volume of pentane and reevaluated to show that only 5% of the stationary phase was lost. The incorporation of surface bonded vinylsilanes has introduced additional phase stability especially when low percentages of vinyl groups are incorporated in the stationary phase. Independent systematic examination of initiators by Grob and Grob (68), Wright, Peaden, Lee and Stark (69), and Richter, Kuel, Park, Crowley, Bradshaw and Lee (70) has shown that dicumyl peroxide, dibenzoyl peroxide and azo-t-butane are initiators that give columns that are highly resistant to phase loss during column washing. One drawback to using dibenzoyl peroxide is the increased column activity (tailing) which is caused by adsorption of initiator decomposition products. Although

dicumyl peroxide has been shown to give less active columns, it and dibenzoyl peroxide are limited to stationary phases which do not have oxidizable groups such as cyanopropyl or tolyl groups. For such stationary phases, azo-t-butane was the initiator of choice.

Crosslinking can also be accomplished by exposing the coated capillary to γ-radiation. Schomburg, Husmann, Ruthe and Herraiz (71) and Bertsch, Pretorius, Pierce, Thompson and Schnautz (72) have described simple methods of effecting immobilization using a cobalt 60 gamma source. This technique has advantages over azo or peroxide initiators in that no functional groups are added to the stationary phase. This ensures no change in polarity or loss in efficiency due to activity of initiator byproducts.

Column Conditioning

The final step in column preparation involves temperature conditioning the column under carrier flow. This removes any solvent left in the column after coating. Since gas chromatographic grade stationary phases have very narrow ranges of high molecular weight, the capillary column needs to be conditioned only for one to two hours at temperatures slightly above the desired operating temperature (73). The practical operating temperature limit for stationary phases used in capillary columns is about 50°C lower than the supplier's recommended temperature limit (74). This difference in temperature limit is due to the lower thermal stability of the coated film on the capillary wall as compared to the film on the support particle in the packed column.

Stationary Phases for Capillary Chromatography

Materials which are used as stationary phases in capillary chromatography must have good thermal stability and low vapor pressure, a wide working temperature range, high permeability to solute vapors, high viscosity and especially be able to form stable, uniform films on the capillary wall. Of the many types of stationary phases that have been evaluated, polysiloxanes which are available in a wide range of polarities and polyethylene glycols provide these characteristics. The wide range of polarity for polysiloxanes is obtained by attaching different functional groups such as methyl, phenyl, tolyl, vinyl, trifluoropropyl, cyanopropyl or cyanoethyl groups to the silicon of the siloxane polymer (75). A wide range of operating temperatures for polysiloxanes which can extend from 30 to 350°C for polydimethylsiloxanes is due to the polymeric chain flexibility and thermal stability of the Si-O-Si and Si-C bonds. As more polar groups are attached to the siloxane, the lower working temperature increases to 100°C for 100% cyanopropyl or cyanoethyl silicone oils. Polyethylene glycols have working ranges of 50 to 280°C and are medium to high polarity. The structures of polysiloxanes and polyethylene glycol are given in Figure 1.

Column Evaluation

After a capillary column has been prepared or purchased it should be characterized to determine the column efficiency, resolving ability, adsorption character and thermal stability. Once an initial evaluation has been determined, changes in column or instrument performance can be

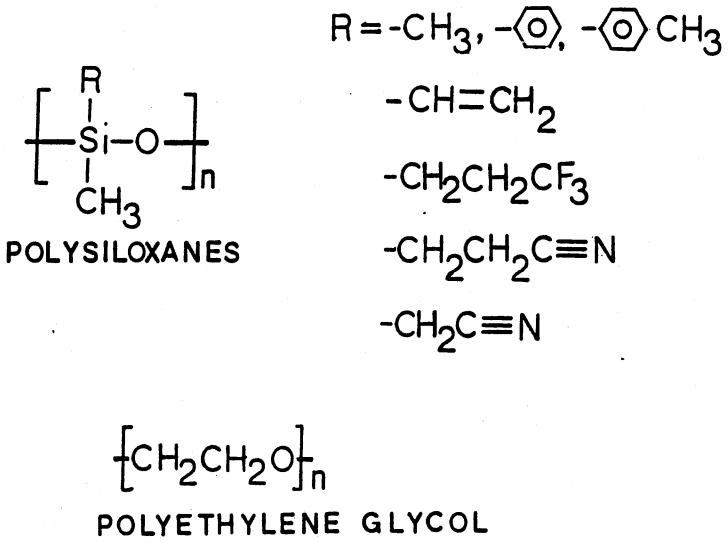

Figure 1. Structures of Polysiloxanes and Polyethylene Glycol

diagnosed by additional evaluation.

(The following section on column evaluation was presented in 1979 as a critical review to fulfill requirements for doctoral candidacy. This qualifier is included with moderate changes and contains more detail than other parts of the introduction.)

Column Efficiency

The measurement of the efficiency of a gas chromatography column involves a relationship between the peak broadening tendency of the eluted solute and the retention of this peak in the column. When two columns of similar type and length are compared, the highly efficient column would elute peaks with smaller widths.

Theoretical Plate Number. The first measure of column efficiency

in gas chromatography, the number of theoretical plates, was suggested by Martin and Synge (76) in 1941 when they realized the similarity between distillation and gas chromatography. In the distillation column the number of theoretical plates corresponds to the number of separate equilibrations which the solute experiences between the liquid and vapor phases. Each of the plates in the distillation column consists of a physically separate condensation and vaporization step. Borrowing this concept from distillation, they derived a theoretical plate number expression for the chromatography column. Their derived expression,

$$n = \frac{2\pi\ h_t^2\ t_R^2}{A^2} \tag{5}$$

(where h_t is the peak height, t_R is the time of the peak maximum and A is the peak area) assumed linear, ideal chromatography, in other words 1) that the partition coefficient, K, was constant throughout the column and independent of concentration, 2) that rapid equilibration of the solute occurred between phases, 3) that longitudinal diffusion was negligible in the column, 4) that the column consisted of a number of identical column elements where equilibration occurred and 5) that the flow of the mobile phase was considered to be discontinuous, that is, the mobile phase was added in stepwise sequence. This last assumption was considered unsatisfactory by Glueckauf (77) who derived a plate number expression based on a continuous flow model. His assumptions were similar to Martin and Synge's in that he also assumed linear ideal chromatography. The difference in Glueckauf's model was that he assumed zero volume increments of flowing mobile phase or continuous flow of the mobile phase. Solution of the material balance differential equation

that results from this continuous flow situation using boundary conditions specified by Glueckauf results in the following expression:

$$C_m = C_m(\max) \cdot \exp\left[\frac{-n'(V_R - V)^2}{2V_R V}\right] \tag{6}$$

(where C_m is the concentration of solute when a volume of mobile phase, V, is eluted from the column, $C_m(\max)$ is the maximum C_m value, V_R is the total retention volume and n' is the difference between the true number of theoretical plates and the number of plates in the original band width). An expression for n'

$$n' = 2\,\frac{V_e V_R}{(V_R - V_e)^2} \tag{7}$$

is obtained by considering that when $C_m/C_m(\max) = 1/e$, the exponential term equals -1 and V becomes the retention volume corresponding to the point along the elution curve located at 1/e times the peak height, V_e (See Figure 2). By replacing $(V_R - V_e)$ with one-half of the width of the peak at 1/e times the peak height, $\beta'/2$, and assuming that $n' \approx n$ (n is the number of theoretical plates) and $V_R \approx V_e$', Equation 7 becomes

$$n = 8\left[\frac{V_R}{\beta'}\right]^2 \tag{8}$$

This expression can be changed directly into

$$n = 8\left[\frac{t_R}{w_e}\right]^2 \tag{9}$$

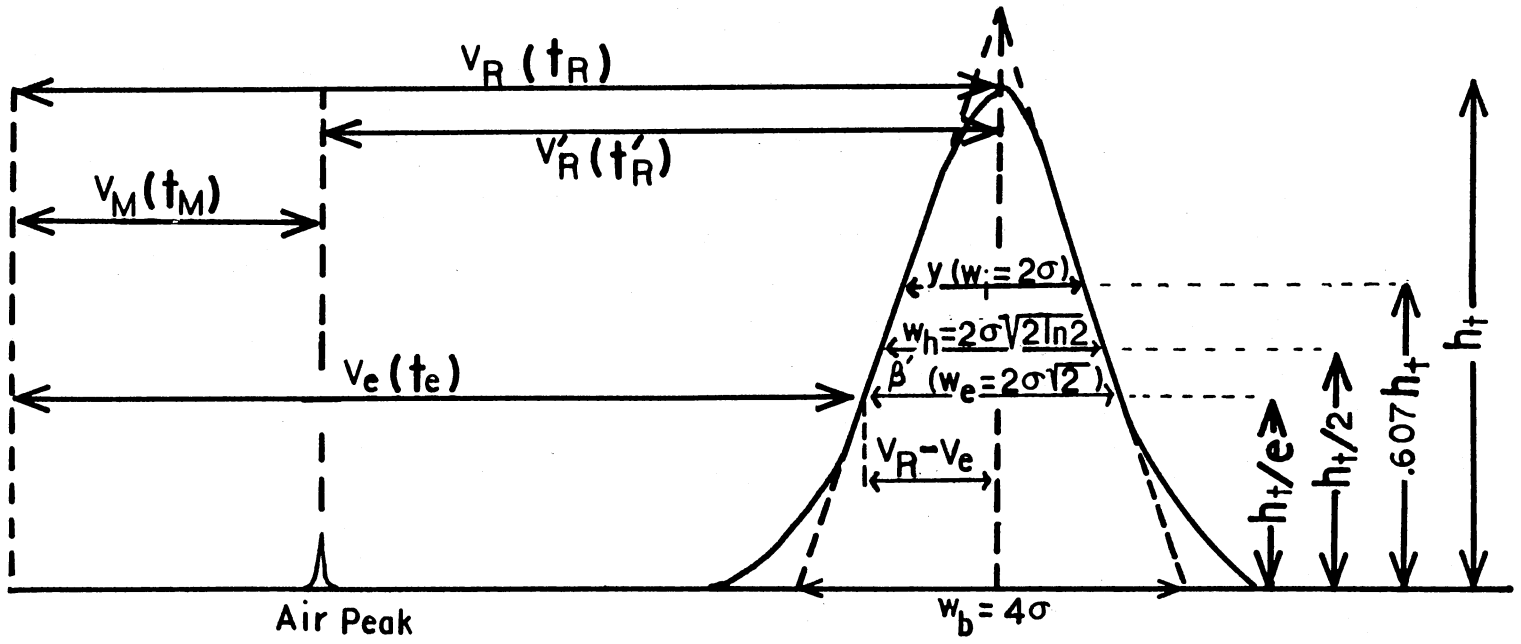

Figure 2. Characteristic Data Calculated for a Chromatogram

where t_R is the retention time and w_e is the width of the peak at 1/e times the height. Modification of this equation into more easily calculable expressions occurs when the elution curve has the form of a Gaussian distribution (provided n is large). With this assumption, the widths of the eluted peak at different peak heights can then be expressed in terms of the standard deviation of the peak, σ. Substitution of w_e where $w_e = 2\sigma\sqrt{2}$ results in

$$n = \left[\frac{t_R}{\sigma}\right]^2 \tag{10}$$

Substituting σ in Equation 10 with expressions containing the peak widths at half height ($\sigma = w_h/(2\sqrt{2\ \ell n\ 2})$), at the inflection point ($\sigma = w_i/2$), and at the intersection of the tangents at the inflection points and the base of the elution curve ($\sigma = w_b/4$) results in the following:

$$n = 8\ \ell n\ 2 \left[\frac{t_R}{w_h}\right]^2 \tag{11}$$

$$n = 4 \left[\frac{t_R}{w_i}\right]^2 \tag{12}$$

$$n = 16 \left[\frac{t_R}{w_b}\right]^2 \tag{13}$$

It should also be noted that when the expression for the standard deviation of a Gaussian peak expressed in terms of peak area and height,

$$\sigma = \frac{A}{2\pi h_t} \tag{14}$$

is substituted into Equation 10, Martin and Synge's original plate number expression, Equation 5, is obtained. This shows that although the assumptions of Glueckauf and Martin and Synge differed, both theories give equivalent mathematical expressions when the number of theoretical plates is large.

Purnell (78,79) has shown that two limiting situations should be considered before the number of theoretical plates can be used to measure the efficiency of a gas chromatography column. The first requires that the feed volume, or the initial volume of the vaporized sample, be less than one-quarter of the average band width of the solute peak as it leaves the column. Approximations in Glueckauf's derivation require this. Based on an average band width of 2σ at the inflection point, the maximum feed volume, V_F, is given by

$$V_F < \frac{\beta}{4\sqrt{2}} = \frac{V_R}{2\sqrt{n}} \qquad (15)$$

From this equation we see that 1) the more efficient column, that is, the one with the larger n value, requires a smaller feed volume and that 2) as the retention volume increases, the acceptable feed volume can also increase. The second limiting situation set by Purnell (78) maintains that the size of the retention volume must be much greater than the free column volume in order for the number of theoretical plates to be a true measure of the column's separating efficiency. This implies that the theoretical plate number should be determined for components whose retention time is much larger than the gas hold-up time. Besides these two limiting situations, the number of theoretical plates should only be calculated when band spreading is not dominated by non-equilib-

rium conditions between the solute and the stationary phase or solid support. According to Glueckauf (77), this occurs in gas-liquid chromatography when the height equivalent to one theoretical plate is determined entirely by gas-phase diffusion along the column length or by channeling effects in the column, and/or when equilibrium is established by use of very small particles and low flow rates.

Although there is a tendency to apply the theoretical plate number expression directly to real chromatography columns, the theoretical column that was discussed by Glueckauf and others does not consider the band broadening by extra column components. Extra column effects due to the injector, column connections and detector contribute to the retention time and peak width of the eluted peak and should be quantitated and subtracted from the actual peak parameters if a true efficiency indicator is to be obtained. Guiochon (80) has suggested a means of accounting for these extra column contributions by replacing the column to be evaluated with a short capillary column which has a very small inner diameter. An expression for the theoretical plate number corrected for the retention time and peak width of the component on the "null" volume column with pressure corrections is shown below:

$$n = \frac{16\left(t_R - \frac{j_0}{j_c} t_{R,0}\right)^2}{w_b^2 - \frac{g_0}{g_c} w_{b,0}^2} \qquad (16)$$

(j_0 and j_c are the values of the correction coefficient of James and Martin (81) for the column of null gas volume and the column studied, g_0 and g_c are the values of correction coefficient of Giddings, Seager,

Stucki and Stewart (82) for the column of null gas volume and the column studied, $T_{R,0}$ is the retention time in the column of null gas volume and $w_{b,0}$ is the width at the base of the peak recorded at the outlet of the null volume column). The underlying assumption in the use of this expression is that the contributions of the short, small inner diameter column to the retention time and peak width be negligible compared to the extra column contributions. A requirement of identical gas flow rates in the two columns actuates this assumption because of the high linear velocity present in the small column. Though simple in concept, actual matching of gas flow rates through the two columns is difficult since comparable pressure drops are required.

Effective Plate Number. In 1960 Purnell (79) first demonstrated a modification of the theoretical plate number expression when he defined the separation factor, S

$$S = 16\left[\frac{t'_R}{w_b}\right]^2 \quad \text{or} \quad S = 8\,\ell n\,2\left[\frac{t'_R}{w_h}\right]^2 \tag{17}$$

where t'_R is the adjusted retention time ($t'_R = t_R - t_M$, t_M is the gas hold-up time). This equation not only corrects for the gas hold-up time in Equation 13 but also eliminates the extra column dead time. It provides a measure of the column efficiency which Purnell prefers instead of the theoretical plate number. His preference for S arises because large unrealistic theoretical plate numbers occur for peaks which elute early. This effect is more strongly evident in capillary columns where longer gas hold-up times exist than in packed columns.

Desty, Goldup and Swanton (83) defined an expression identical to

Purnell's equation which they called the effective plate number, N. They also defined the effective plate number as Equation 18.

$$N = n \left[\frac{k'}{1+k'}\right]^2 \tag{18}$$

where k' is defined as

$$k' = \frac{t'_R}{t_M} = \frac{t_R - t_M}{t_M} \tag{19}$$

Real Plate Number. Another modification to the theoretical plate number expression occurred in 1976 when Kaiser (84-89) defined his real plate number, n_{real}, as

$$n_{real} = 8 \ln 2 \left[\frac{t_M}{a}\right]^2 \tag{20}$$

where a is the slope of the linear expression that describes the increase of the peak width, w_h, at one-half peak height with respect to the partition ratio, k'. This linear equation is expressed as

$$w_h = ak' + w_{ho} \tag{21}$$

where w_h is the peak width at half height for a peak with partition ratio, k', and w_{ho} is the starting peak width at k' = 0. We can see the relationship between n_{real} and the theoretical plate number, n, by expressing the t_R and w_h terms that are found in Equation 11 in terms of k'. From Equation 19 we obtain

$$t_R = t_M + t_M k' \tag{22}$$

Substituting Equations 21 and 22 into Equation 11, the following results:

$$n = 8 \ln 2 \left[\frac{t_R}{w_h}\right]^2 = 8 \ln 2 \left[\frac{t_M k' + t_M}{ak' + w_{ho}}\right]^2 \qquad (23)$$

By comparing this equation to Equation 20, it becomes evident that Kaiser's equation is obtained by subtracting t_M from the numerator and w_{ho} from the denominator in the squared term whereby the partition ratio cancels. By eliminating t_M as was done in the effective plate number equation and w_{ho}, the extrapolated peak width at $k' = 0$, Kaiser obtained a measure of the column efficiency which is relatively independent of the nature of the substance, the injection technique and the connection details. He claims that this expression measures the actual peak broadening due to the column alone. This concept is based on the experimental fact that peak widths at half height increase with almost complete linearity as the partition ratio increases. Kaiser claims that this observation occurs if isothermal, isobaric and non-overloaded gas chromatographic analysis occurs under optimum conditions. Hence when non-stabilized temperature conditions, non-constant gas flow, overloading of the column or the detector, too low a temperature for sampling and separation or too widely differing chemical classes are used as probes for column testing, non-linearity in Equation 21 occurs.

The measurement of a and w_{ho} is accomplished by linear regression analysis of the peak width and partition ratio for a number of compounds (usually more than five from a series of homologs) that exhibit symmetrical profiles. Appropriate measures of the quality of the linear regression, that is, the regression coefficient, r^2, the regression

angle, α_R, and the standard deviations of a and w_{ho} are necessary before realistic w_{ho}, a, n_{real} and other resulting column characteristics should be calculated. If r^2 values significantly less than 1.000 and α_R values greater than 0.000° are obtained, then linearity of Equation 21 is lacking and application to real plate number calculations and other column evaluation characteristics, which will be covered in later sections, become complex.

Plate Number Comparison. Comparison of the three plate number expressions presented in the preceeding sections, theoretical, effective, and real, is best seen by expressing each plate number equation in terms of the partition ratio, k' (88). Each corresponding plate number equation is then defined as

$$n = 8 \ell n 2 \left[\frac{t_R}{w_h}\right]^2 = 8 \ell n 2 \left[\frac{k't_M + t_M}{ak' + w_{ho}}\right]^2 \tag{24}$$

$$N = 8 \ell n 2 \left[\frac{t_R - t_M}{w_h}\right]^2 = 8 \ell n 2 \left[\frac{t'_R}{w_h}\right]^2 = 8 \ell n 2 \left[\frac{k't_M}{ak' + w_{ho}}\right]^2 \tag{25}$$

$$n_{real} = 8 \ell n 2 \left[\frac{t_R - t_M}{w_h - w_{ho}}\right]^2 = 8 \ell n 2 \left[\frac{k't_M}{ak'}\right]^2 = 8 \ell n 2 \left[\frac{t_M}{a}\right]^2 . \tag{26}$$

In Equation (24) we see that as k' approaches zero, the expression takes on the following form:

$$n = 8 \ell n 2 \left[\frac{t_M}{w_{ho}}\right]^2 \tag{27}$$

Also as k' approaches ∞, the theoretical plate number, the effective plate number, and the real plate number all become equal (90,29). The tendency for the theoretical plate number to decrease as the partition ratio increases has been graphically demonstrated as in Figure 3a by several sources (85,92). Figures 3b and 3c show new theoretical relationships between n and k' which result in an increasing and constant theoretical plate number. The tendency for n to increase, decrease or remain constant depends upon the respective sizes of the ratios, t_M/w_{ho} and t_M/a. If the value of w_{ho} is larger than a, then the number of theoretical plates will increase as k increases until it becomes as large as n_{real} (Figure 3b). As Figures 3a, 3b and 3c show and as Equation 25 predicts, the effective plate number equals zero at k' = 0 and approaches the number of real plates as k' approaches infinity. The relationship between N and n is governed by Equation 18. Figure 3a shows the special case where the number of theoretical plates equals the number of real plates. This independence of k' which has been observed by Nilsson (91) occurs when w_{ho} and a are equal. It should be noted that even though the theoretical plate number is constant, the effective plate number still asymptotically approaches n_{real} as is predicted by Equation 18. Figures 3a, 3b and 3c were constructed to show the converging tendency of the three plate number expressions. It should be noted that the high values of the partition ratio represented in these graphs are seldom if ever approached in actual chromatography and that realistic k' values range from 0 to 10.

Criticism of Real Plate Number. The reliability and applicability of Kaiser's real plate concept has been challenged by several authors.

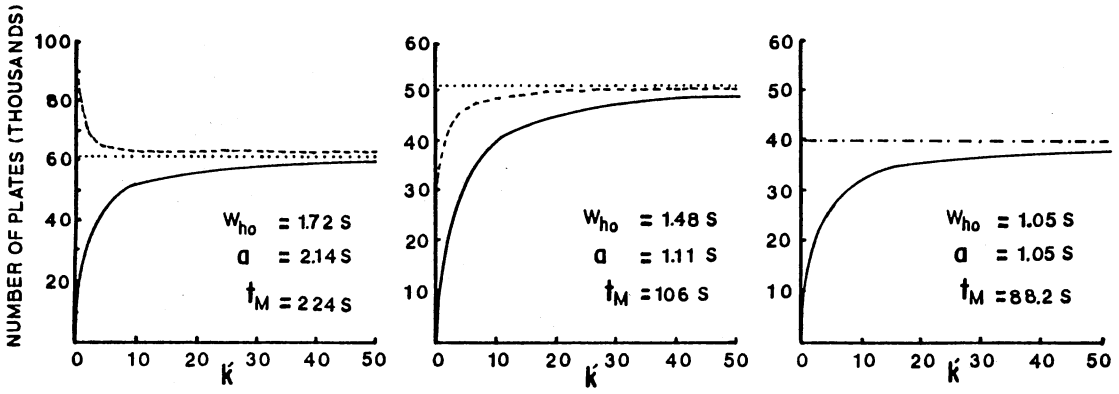

Figure 3. Theoretical Relationship of the Number of Theoretical Plates (n), Effective Plates (N) and Real Plates (n_{real}) with Respect to Partition Ratio (k') when a) $w_{ho} < a$, b) $w_{ho} > a$, and c) $w_{ho} = a$

In 1977 Franken (93) pointed out that the peak width due to extra column contributions, σ_{ex} (expressed as a standard deviation), and the peak width due solely to the separation processes, σ_c, are related quadratically to the square of the experimentally observed total peak width, σ_T.

$$\sigma_T^2 = \sigma_{ex}^2 + \sigma_c^2 \tag{28}$$

It is assumed that this quadratic expression, an example of the variance additivity principle, is valid because the processes which cause broadening of the peak width, extra column contributions and column separation processes, are statistically independent of each other (94). When Gaussian shaped peaks are assumed, this equation can be converted readily into Equation 29.

$$w_h^2 = w_{hex}^2 + w_{hc}^2 \tag{29}$$

It is easily seen that the contribution of w_{hex} to w_h becomes more important as w_{hc} becomes small. Franken demonstrated that Kaiser's Equation 25 does not produce constant n_{real} values for the same column and column conditions when w_{hex} values are increased by using slower injection rates and decreased injection depths.

Kaiser's reply (86) revealed that Franken's data failed to fulfill the basic requirement of linearity between peak widths and partition ratios which must be qualified by regression coefficients, regression angles and standard deviations of w_{ho} and a values. Kaiser was convinced that the excellent long range linearity that he had found in hundreds of analyses provided a practical evaluation for this column efficiency method even though the concept was not theoretically complete. Apparent-

ly, the extra column contributions to broadening which were present in Kaiser's data were small enough so that a linear relationship between w_{hc} and k' occurred within Kaiser's limits.

Guiochon (95) also has attacked Kaiser's concept in that he took Kaiser's experimental observation and placed it in the theoretical realm. Beginning with the Golay equation, Equation 30, and an expression of the theoretical plate height in terms of base line peak width, Equation 30, Guiochon derived Equation 33.

$$h = \frac{2D_G}{\bar{v}} + \frac{1 + 6k' + 11k'^2}{(1+k')^2} \cdot \frac{d_c^2 \bar{v}}{96D_G} + \frac{2k'd_f^2 \bar{v}}{3(1+k')^2 D_L} \tag{30}$$

$$h = \frac{2D_G}{\bar{v}} + f(k')\, C\, \bar{v} + g(k')\, C'\bar{v} \tag{31}$$

$$h = \frac{B}{\bar{v}} + C_G\, \bar{v} + C_L\, \bar{v} \tag{32}$$

where

h = height of a theoretical plate

$\bar{v}$ = average mobile phase velocity

k' = partition ratio

d_c = column inner diameter

d_f = average film thickness of the liquid phase

D_G = diffusion coefficient of the vapor of the solute in the carrier gas

D_L = diffusion coefficient of the solute in the stationary phase

and

$$f(k') = \frac{1 + 6k' + 11k'^2}{(1+k')^2} \qquad C = \frac{d_c^2}{96D_G} \qquad B = 2D_G$$

$$C_G = f(k')C$$

$$g(k') = \frac{k'}{(1+k')^2} \qquad C' = \frac{2}{3}\frac{d_f^2}{D_L} \qquad C_L = g(k')C'$$

From Equations 13 and 30 he obtained

$$w_b = 4t_R \left[\frac{2D_G}{L\bar{v}} + \frac{1+6k'+11k'^2}{(1+k')^2} \cdot \frac{d_c^2\,\bar{v}}{96D_G L} + \frac{2k'\bar{v}}{3(1+k')^2\,D_L L}\right]^{1/2} . \qquad (33)$$

Using this equation Guiochon stated that he had found no theoretical basis for an exact linear relationship between the peak width at the base and the partition ratio, although linearity could occur when the diffusion coefficients in the gas phase, D_G, were identical for all components. He also showed that linearity is possible when the diffusion coefficients for a series of components, D_G and D_L, varied regularly with k' and/or when the band broadening due to resistance to mass transfer in the liquid phase was negligible. By plotting theoretical values of w_b (calculated from the Golay equation) and k' for data given by Kaiser (88), he showed that linearity was found to hold in practice for k' values greater than 0.30. Although Guiochon admitted that the determination of n_{real} at an optimum flow rate might provide the best characterization of a column, he claimed that Kaiser's method was useless because of the inaccurate determination of a and w_{ho}. He stated that positive deviations from linearity due to ubiquitous extra column contributions occur as k'

approaches zero and that the linear extrapolated w_{ho} value would underestimate the true w_{ho} value. Guiochon's incorrect interpretation of Kaiser's definition of w_{ho} also contributed to his criticism of the n_{real} concept. Guiochon believed that Kaiser attributed only extra column effects to w_{ho} and not peak broadening due to the intracolumn longitudinal diffusion of the non-retained peak.

Kaiser (89) has responded to Guiochon by reiterating his confidence in his concept and by re-explaining his theory. He stated that linearity must occur before conclusions about his efficiency measure can be obtained.

Several authors have continued the discussion of the experimental results of linear w_h versus k' plots and have extended their concern to the measurement of w_{hex} and its effect on linearity (96-100). Several opposing views of w_{hex}'s effect are presented. Although determination of w_{hex} is a critical parameter for correction of the peak width, the methods used by the authors are theoretical and experimentally determined w_{hex} values at low k' were not provided.

Plate Height. Three ralated parameters which follow from each type of plate number previously discussed are the height equivalent to a theoretical plate (h), effective plate (H), and a real plate (h_{real}). These parameters, defined as

$$h = \frac{L}{n} \tag{34}$$

$$H = \frac{L}{N} \tag{35}$$

$$h_{real} = \frac{L}{n_{real}} \tag{36}$$

are traditional measures of column efficiency. The theoretical plate height concept allows comparison of columns based on relative peak broadening which is independent of column length.

By taking the expression for the number of theoretical plates expressed in units of time (Equation 10) and converting it into units of column length, the following equation results.

$$n = \left[\frac{L}{\sigma_L}\right]^2 \tag{37}$$

Substituting this into Equation 34, an expression for plate height in terms of the variance of the peak and the column length is obtained.

$$h = \frac{\sigma_\ell^2}{L} \tag{38}$$

Because of the statistical property of additivity of variances, a plate height equation can be expressed as the summation of all the independent processes which contribute to peak broadening, provided the column acts as a Gaussian operator on the processes (94,100,101). Equation 38 can then be expressed as

$$h = \frac{\sigma_{\ell 1}^2}{L} + \frac{\sigma_{\ell 2}^2}{L} + \frac{\sigma_{\ell 3}^2}{L} + \ldots \tag{39}$$

Golay (102) has used this equation as the basis for his derivation of the theoretical plate height expression for the capillary column which was presented earlier in Equations 30 and 31. Each of the three terms in this expression correspond to one of the peak broadening processes that occur in the column. The first term, B, is due to static or longitudinal

molecular diffusion of the solute zone in the mobile phase. As can be seen from the plate height expressions, this peak broadening term decreases with increase of the average mobile phase velocity. The second term, dynamic diffusion or resistance to mass transfer in the gas phase, C_G, is due to the distribution of the molecules across the laminar flow profile. Those molecules which are located near the center of the capillary move ahead in the band while those located near the capillary wall lag behind. The third term, resistance to mass transfer in the liquid phase, C_L, is the zone broadening which is due to wandering of molecules in the stationary phase without instantaneous movement into the mobile phase. Both of these last two peak broadening terms decrease with decreasing average mobile phase velocity. Because of the two opposing effects which the average mobile phase velocity has on the plate height, a minimum plate height, h_{min}, occurs at the optimum average mobile phase velocity, $\bar{v}_{opt}$, for each solute that elutes from the column. Experimental determination of these minimum plate heights, $h_{expt(min)}$, which reflect optimum peak efficiency for the column with regard to a particular solute, is accomplished by plotting experimental plate height values versus their corresponding average mobile phase velocities. Obviously, $h_{expt(min)}$ occurs at the minimum h value obtainable from the h versus $\bar{v}$ curve. The discussion of plate height versus linear mobile phase velocity curves presented so far has been concerned with theoretical plate heights. This does not mean that the effective plate height or real plate height cannot be plotted versus $\bar{v}$. Desty and Goldup (103) have discussed such H versus $\bar{v}$ plots and also have modified the Golay equation so that it contains the effective plate height instead of the theoretical plate height. Plots of h_{real} versus $\bar{v}$ have not been dis-

cussed by Kaiser.

When Equation 32 is differentiated with respect to $\bar{v}$, an expression for the minimum theoretical plate height, Equation 40, is obtained.

$$h_{theo(min)} = 2\,[B(C_G + C_L)]^{1/2} \tag{40}$$

Assuming that the C_L term and peak broadening due to pressure gradients are negligible, Ettre (12,104) has shown that

$$h_{theo(min)} = 2\,[BC_G]^{1/2} = \frac{d_c}{2}\left[\frac{1+6k'+11k'^2}{3(1+k')^2}\right]^{1/2} \tag{41}$$

This equation provides a means of determining the minimum plate height and maximum plate number for each of the three plate concepts for a specific partition ratio, column length and inner diameter.

Coating Efficiency. The coating efficiency (CE%) or utilization of the theoretical efficiency (UTE%) incorporates the $h_{theor(min)}$ and the $h_{expt(min)}$ values which were discussed earlier into the following expression

$$CE\%\ (UTE\%) = \left[\frac{h_{theo}}{h_{expt}}\right]_{min} \times 100 \tag{42}$$

This expression was originally proposed by Ettre for use in measuring the column quality by comparing the experimental plate height with the theoretically predicted value, but Cramers, Wijnheijmer and Rijks (105, 106) have demonstrated that this expression fails to measure the column quality in many practical situations. They have revealed that the fol-

lowing observations account for this failure.

1) The CE% as calculated by Equation 41 is not independent of the carrier gas type or the ratio of the inlet to outlet pressures.
2) The predicted effect of the partition coefficient, K, of the solute on the CE% is different from the experimental results.
3) CE%'s for columns of large radius are higher than for small columns.

Cramers et al (106) have used the Golay equation which was extended by Giddings (107) for pressure drop across the column, Equation 43,

$$h = \left[\frac{2D_{G,o}}{v_o} + \frac{1+6k'+11k'^2}{24(1+k')^2} \cdot \frac{r_c^2 v_o}{D_{G,o}}\right] f_1 + \frac{2}{3}\frac{k'}{(1+k')^2} \cdot \frac{d_f^2 v_o}{D_L} f_2 \qquad (43)$$

$$f_1 = \frac{9}{8}\frac{(P^4-1)(P^2-1)}{(P^3-1)^2}, \qquad f_2 = \frac{3}{2}\frac{P^2-1}{P^3-1}, \qquad P = \frac{P_I}{P_o}$$

(where P_I is the inlet pressure, P_o is the outlet pressure, and terms which have a subscript o are determined at the column outlet) to arrive at a new $h_{theo(min)}$ expression.

$$h_{theo(min)} = 2\,[Bf_1(C_G f_1 + C_L f_2)]^{1/2} \qquad (44)$$

Cramer et al used this new expression which accounts for the pressure drop and C_L term to show that coating efficiencies calculated with it are always higher than those calculated with Equation 41. Due to the lack of tabulated values of the molecular diffusion coefficients of the solute in the stationary phase, D_L, the calculation of the theoretical C_L term becomes limited. When such D_L values are tabulated in the

literature or are determined by the chromatographer, then deviations from a 100% coating efficiency can be obtained using Equation 44, but if such D_L values are not obtainable, then errors associated with the original CE% expression must be accepted.

Efficiency Comparison. Of the three plate numbers, theoretical, effective and real, the real plate number in operational use best describes the efficiency of the capillary column because it reflects the number of plates available in the column which are due only to the partition processes of the column. In the theoretical plate number expression, the non-partition contributions, that is, the dead time, the width of the non-retained air peak and any extra-column effects are included in the retention time and peak width ratio. These non-partition effects contribute most to the value of n when the eluted peak has a small retention time. The attempt to correct these contributions by simply eliminating the dead time in the effective plate number expression failed to consider those contributions which cause the low N values when k' decreases. As these contributions to the peak width become smaller in comparison to the peak width contributions due to the partition processes, N tends toward the value of the real plate number.

The criticisms of the real plate number do not provide strong enough evidence to lessen the reliability or applicability of this concept. Linearity in the relationship between the peak width and partition ratio does occur in reality. The theoretical explanation for this occurance has been demonstrated using the rate theory expression for the plate height. Theory predicts that linearity will occur when the ratio of the diffusion coefficients of the solute in the gas and stationary phase for

a homolog series varies regularly with the partition ratio. Though evidence of this relation has not been presented in the articles reviewed, Kaiser's requirement that the efficiency probes be homolog series such as alkanes and his observance of linearity with these probes alone, increases the likelihood of such a relationship.

Although extra column contributions to band broadening do not contribute significantly to the peak width at large retention times, their effect on the slope between the peak width and partition ratio for peaks with low retention times is important.

The plate height expressions which have been presented are intended to provide a comparison of column efficiency between columns of different length. From this efficiency measure it could be surmised that if a column containing 3000 plates per meter was doubled in length, twice as many plates would be present. In reality this does not occur because the increased pressure drop in the longer column causes a larger deviation from the optimum carrier gas velocity across the column. Although plate height Equation 43 shows the correction for this pressure drop, the calculation of plate height is not usually determined with this expression because of the difficulty in determining the diffusion coefficients of the solute in the gas and stationary phase. Accurate determination of the $h_{theo(min)}$ used in the coating efficiency expression also requires these coefficients.

For the efficiency measures which have been presented to be valid it is required that the concentration profile of the elution curve follow the distribution set by Glueckauf in Equation 6 and that this distribution also be Gaussian. All the derived expressions presented after Glueckauf's distribution require this assumption. The applicability of

these expressions rests first on the positive correlation between the concentration distribution of the experimental peak and Glueckauf's concentration distribution and then between the actual peak distribution and a Gaussian distribution.

Resolution, Separating Power and Performance

The combination of column resolution, resolving power and performance into one section is done for convenience's sake because of the various inter-relationships between the six column evaluation parameters which are to be presented. Column resolution and resolving power are related in that a measure of the resolution between peaks is usually required before the resolving power of the column can be determined. The resolving power provides information on the column's ability to separate one component from another. The performance of the column relates a desired quantity such as resolution or the number of effective plates to a quantity which the chromatographer "trades in" such as the retention time.

Resolution. The measure of the separation which occurs between two adjacent peaks which elute from the column is expressed by the resolution, R. One resolution expression which is shown below and was established at the 1958 Amsterdam Symposium (108) is calculated from the retention time of the peaks and the average peak width at the base expressed in time units.

$$R = \frac{2(t_{R2} - t_{R1})}{w_{b2} + w_{b1}} \tag{45}$$

For practical purposes exact separation of the adjacent peaks, implying

a complete baseline separation with a cross contamination of less than 1.5%, occurs when $R \geq 1.5$. Other expressions for R have been presented which make the approximation that the width of the first peak (Equation 46) or the width of the second peak (Equation 47) is equal to the average base width.

$$R = \frac{t_{R2} - t_{R1}}{w_{b1}} \tag{46}$$

$$R = \frac{t_{R2} - t_{R1}}{w_{b2}} \tag{47}$$

Resolution equations which allow the calculation of the maximum possible resolution using a given number of theoretical plates, separation factor, α, and partition ratios, k_1' and k_2', were derived for each of the three equations above by Said (109), Knox (110), and Purnell (79). For Said: from Equation 45

$$R_S = \frac{\sqrt{n}}{2}\left[\frac{\alpha - 1}{\alpha + 1}\right]\left[\frac{k'}{1 + k'}\right] \quad \text{where} \quad k' = \frac{k_1' + k_2'}{2} \tag{48}$$

For Knox: from Equation 47

$$R_K = \frac{\sqrt{n}}{4}(\alpha - 1)\left[\frac{k_1'}{k_1' + 1}\right] \tag{49}$$

For Purnell: from Equation 47

$$R_P = \frac{\sqrt{n}}{2}\left[\frac{\alpha - 1}{\alpha}\right]\left[\frac{k_2'}{k_2' + 1}\right] \tag{50}$$

The expression derived by Said, Equation 45, is an exact equation in that the approximation mentioned above is not involved in its derivation. Said (111,112) has also introduced another exact resolution Equation 51.

$$R_S = \frac{\sqrt{n}}{4} \ln\left[\frac{k_2' + 1}{k_1' + 1}\right] \tag{51}$$

which is derived from a resolution definition which accounts for the increase in peak width with increase of retention volume or time. He has shown by comparing $\frac{R}{\sqrt{n}}$ values calculated from resolution Equations 48, 49, 50 and 51 for different values of α and k_1' ($k_2' = \alpha k_1'$) that the exact Equations 48 and 51 lead to almost identical $\frac{R}{\sqrt{n}}$ values while values calculated from Equations 49 and 50 give increasingly larger absolute deviations as α and k_1' increase.

Separation Number. A characteristic of the column, called the separation number (SN) or Trennzahl (TZ), which is related to the resolution of the column has been developed by Kaiser in several articles since 1962 (113,84-89). This separation number is defined as the number of base to base peaks with resolution equal to 1.0 which can be placed between two chromatographed peaks. The first expression introduced by Kaiser (113), denoted as TZ,

$$TZ = \frac{t_{R2} - t_{R1}}{w_{h2} + w_{h1}} = 1 \tag{52}$$

is an approximate expression. Kaiser later presented three correct SN equations which involve logarithms and the a, w_{ho}, and n_{real} concepts. These equations which are listed below provide separation numbers for

homolog pairs ($SN_{homolog}$), for a range of partition ratios, $k' = 0$ to $k' = 10(SN_{real})$ and for the complete chromatogram with a partition ratio range of $k' = 0$ to k'_e, where k'_e is the partition ratio for the last chromatographed peak ($SN_{0-k'_e}$).

$$SN_{homolog} = \frac{\log \frac{w_{h2}}{w_{h1}}}{\log \left| \frac{\sqrt{\frac{n_{real}}{8 \ln 2}} + 1}{\sqrt{\frac{n_{real}}{8 \ln 2}} - 1} \right|} - 1 \qquad (53)$$

$$SN_{real} = \frac{\log \frac{10a + w_{h0}}{w_{ho}}}{\log \left| \frac{\sqrt{\frac{n_{real}}{8 \ln 2}} + 1}{\sqrt{\frac{n_{real}}{8 \ln 2}} - 1} \right|} - 1 \qquad (54)$$

$$SN_{0-k'_e} = \frac{\log \frac{k'_e a + w_{h0}}{w_{h0}}}{\log \left| \frac{\sqrt{\frac{n_{real}}{8 \ln 2}} + 1}{\sqrt{\frac{n_{real}}{8 \ln 2}} - 1} \right|} - 1 \qquad (55)$$

The introduction of a and w_{ho} into the SN_{real} and $SN_{0-k'_e}$ expressions permits the calculation of substance independent separation numbers. The t_R and w_h parameters which are present in the TZ and SN expressions impart on these expressions a dependence on the polarity of the column and the selection of the substance pair.

Resolution Versus Retention Time Plots. In 1974 Ettre and March (114) developed three methods of comparing columns which involve the resolution between a pair of peaks and the retention time of the second peak. They felt that these methods provide a true measure of the performance of a column and applied the method by comparing wall-coated open tubular (WCOT), surface-coated open tubular (SCOT), and packed columns containing the same stationary phase. They suggested 1) comparison of the retention time of each column that corresponds to the same resolution, 2) comparison of the resolution of each column that corresponds to the same retention time and 3) comparison of plots of resolution versus retention time. The third method provided a visual comparison of the resolution and retention time and is considered by Ettre and March to be the best way to compare the performance of different columns. In this method the gas holdup time, t_M, the retention times, t_{R2} and t_{R1}, and the peak widths at half height, W_{h2} and W_{h1} are obtained at different column flow rates. From this data Ettre and March calculated the resolution between two peaks using Equation 50 for the different flow rates and then plotted each resolution against its corresponding retention time. Plots of resolution versus retention time for methyl stearate and methyl oleate on packed and wall coated capillary columns containing the same stationary phase showed that the best performance that the packed column could attain was baseline resolution within 27 to 30 minutes. The capillary column provided much better resolution in much less time.

Separating Power. Kaiser (84-89) has introduced a measure of the resolving power of the capillary column, SN_t, which is obtained when the separation number for $k' = 0$ to 10 (Equation 54) is divided by the retention time of the $k' = 10$ peak. Since $t_R = (k' + 1)t_M$, this retention

time equals $11t_M$. Therefore:

$$SN_t = \frac{SN_{real}}{11\ t_M} \tag{56}$$

SN_t provides the chromatographer with the number of totally separated peaks that elute from the column per unit time with a resolution of $R = 1.0$. By adjusting the temperature and gas flow of the column, this column quality indicator can be optimized so that maximum separation power of the column is obtained. It should be noted that the optimum average mobile velocity for SN_t can be different from the one obtained from the h versus $\bar{v}$ plot discussed earlier. The h versus $\bar{v}$ plot optimum velocity is found for one solute and provides a ratio of the smallest peak spread relative to the distance migrated for this solute. The SN_t optimum velocity provides the largest number of resolved peaks per unit time that the column can attain. This information is very useful when the mixture to be analyzed consists of many components which elute over the partition ratio of $k' = 0$ to $k' = 10$.

Ratio of Effective Plate Number to Retention Time. A measure of the column performance which follows directly from the effective plate number is presented by Desty et al (83) as the rate of production of effective plates, N/t_R. The maximum value of the ratio occurs when the average mobile phase velocity is the optimum value obtainable from the H versus $\bar{v}$ plot. While this ratio provides a means for optimizing a column's performance, comparison of the maximum N/t_R values between columns for the same solute requires that some column conditions between columns be identical. Ettre and March (114) have shown that N/t_R can be expressed as

$$\frac{N}{t_R} = \frac{\bar{v}}{h} \cdot \frac{k^2}{(1+k)^3} \tag{57}$$

This expression shows a dependence of N/t_R upon the partition ratio of the solute. Because of this dependence, Ettre and March maintain that the partition ratio of the solute be identical on both columns in order for the comparison to be of value. This criterion requires that the inner radius of the capillary and the film thickness of the stationary phase be the same. If these criteria are met, the column that exhibits the larger N/t_R or $\bar{v}/h$ ratio according to Desty et al (83) has the better performance.

Performance Index. When Golay (102) derived his plate height equation for the wall-coated open tubular column, he also developed an equation for measuring the performance of the column. The following expression which he called the performance index, PI,

$$PI = \left(\frac{w_h}{t_R - t_M} \right)^4 \left[\left(\frac{t_R - t_M}{t_R} \right)^4 \left(\frac{t_M}{t_R - \frac{15}{16} t_M} \right) \right] t_R \Delta p \tag{59}$$

requires that the four parameters, w_h, t_R, t_M and Δp, be obtained at the optimum carrier gas velocity. This expression which has the dimension of viscosity consists of three terms which affect the value of PI. The first term contains the reciprocal of the ratio found in the effective plate number equation. This expression and the third one, which contains the product of the retention time and the pressure drop, should decrease if the desired low performance index value is to be obtained. The middle term which is dimensionless will increase in value when the

first and third terms decrease. Ettre (12) gives a value of PI of 0.1 as the value expected for open tubular columns.

Comparison. In summarizing the merits of the equations which have been presented to calculate column resolution, resolving power and performance, it must be said that all of the resolving power and performance equations are of value and each provides different information regarding the column separation and performance capabilities. With regard to the resolution equations, Equation 45 is an exact equation which involves no approximations. When the maximum possible resolution for a given number of theoretical plates is required, Equations 48 or 51 give the most accurate results.

With regard to each resolving power and performance determination, one feels a need to ask, "How does this column quality indicator, this separation number, or this performance index compare to values obtained from other columns or to the optimum value?" Each of the five resolving power and performance qualities provides a means for comparison of columns. When the TZ or SN parameter is calculated, the number of resolved peaks which can be placed between two reference peaks is obtained. This powerful column quality indicator speaks loudly to someone who has many components in his sample. When SN_{real} is divided by a retention time element or the "waiting time", SN_t or the rate of peak production is obtained. When resolution between two peaks which elute close to one another is important, R versus t_R plots can show the resolution which is obtainable and the "waiting time" required to obtain it. Although N/t_R ratios also include this time element, this quality measure speaks of efficiency and is not as practical as the number of peaks separated per

unit time or resolution attained at a certain retention time. Golay's performance index presents a unique measure of column performance in that the pressure drop is included. The dimension of his column parameter, viscosity, which is expressed in dynes·sec/cm^2, is quite different from other resolving power or performance dimensions such as number of peaks separated per second.

Peak Shape

One assumption which is present in almost all of the theoretical expressions presented so far has been that the shape of each peak be Gaussian. For a peak to be Gaussian, its concentration distribution with time must fit the Gaussian distribution described by (94).

$$C(t) = C_0\left(\exp -(t - t_0)^2/2\sigma^2\right) \quad \text{for} \quad -\infty < t < +\infty \tag{59}$$

When non-Gaussian peaks occur, equations which are used to calculate plate numbers, plate heights, resolution, and so on, become invalid simply because within their derivation, Gaussian shaped peaks are assumed. In each equation where a Gaussian shaped peak is assumed, measurement of a peak width at the base, 1/e times the peak height, half height, or the inflection point is required. These widths are related to each other through the standard deviation, σ, of the peak. Equations which show this relation were presented earlier. Kaiser (115) has demonstrated that errors of approximately 16% can occur when measured peak widths are used to determine the standard deviation, σ, of a skewed HPLC peak which was recorded under optimum technical conditions.

Tailing Factor. A simple measure of the peak symmetry called the tailing factor, TF%, is defined below for the peak in Figure 4 (116,117).

$$TF\% = \frac{a}{b} \times 100 \qquad (60)$$

Measured at 10% of the peak height, a and b provide a ratio which is unity when the investigated peak is symmetrical. Said (118) has also provided three measures of asymmetry called asymmetry indexes which provide information which is similar to the tailing factor.

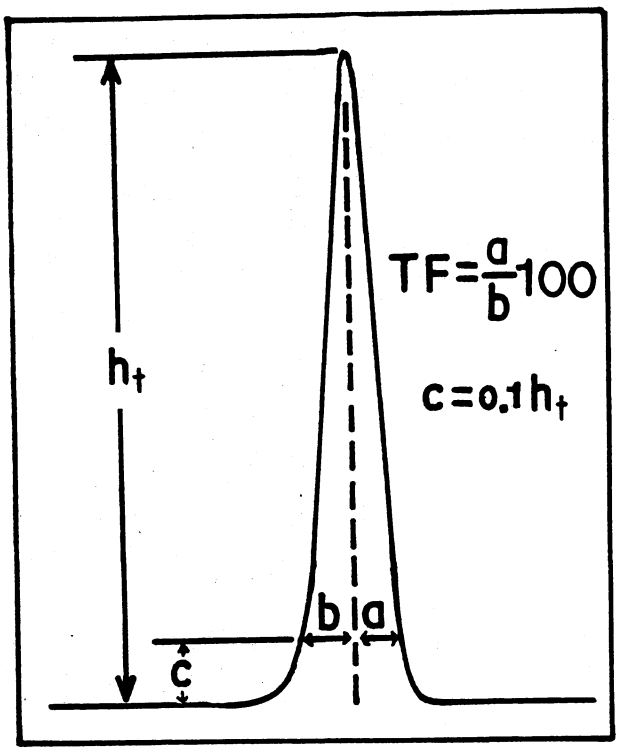

Figure 4. Definition of Tailing Factor (TF%)

Moment Analysis. Since the elution curve can be considered to be a probability distribution, the shape of the chromatographed peak can be described statistically by determining its statistical moments (119). The first statistical moment, M_1, represents the center of gravity or mean of the distribution curve and is defined by

$$M_1 = \frac{\int_0^{+\infty} t\,C(t)\,dt}{\int_0^{+\infty} C(t)\,dt} \tag{61}$$

where C(t) is the concentration at time t. The center of gravity corresponds to the peak maximum when the distribution is symmetrical. The second, third, and fourth statistical moments, M_2, M_3, and M_4, respectively, are defined by:

$$M_k = \frac{\int_0^{+\infty} C(t)\,(t - M_1)^k\,dt}{\int_0^{+\infty} C(t)\,dt} \tag{62}$$

When k = 2 as is the case for M_2, the variance of the probability density distribution curve is determined. The standard deviation, σ, is easily determined from the square root of the variance. The third statistical moment, M_3, provides curve asymmetry information. The skewness, S, indicates leading or trailing edge tailing according to the sign of

$$S = \frac{M_3}{\sigma^3} \tag{63}$$

skewness. Positive skewness implies tailing away from Gaussian symmetry toward positive values of time with respect to the center of gravity, M_1. The fourth statistical moment enables the calculation of the excess, E.

$$E = \frac{M_4}{\sigma^4} - 3 \qquad (64)$$

This result allows the comparison of the pointedness or flatness of the elution curve with that of the Gaussian distribution with the same standard deviation. Excess values which are larger than zero predict chromatographic peaks which are sharper than Gaussian distribution peaks. This concept is important in that it points out that the tailing factor and asymmetry indexes can determine if a peak is symmetrical but each fails to indicate if the symmetrical peak is Gaussian. Only an accurate excess calculation can distinguish between the two.

Exact determination of the moments described by the integral Equations 62 and 63 require that the distribution function of the concentration profile, C(t) be known. If such a situation exists, the integration can usually be calculated by formula or by numerical methods. Knowledge of the mathematical description of the elution curve is usually the exception and moment analysis involving analog to digital conversion of the peak profile data and computer computation is necessary. Grubner (120) and Gruska, Myers, Schettler and Giddings (121) have provided summation approximations of Equations 61 and 62 that can be used to arrive at the moments, skewness and excess from data points generated in the digital form. These approximations require that the detector output be divided into finite intervals and digitized.

Chesler and Cram (122,123) have reported on the accuracy of the generated statistical moments. They have shown that significant errors in the skew and excess can occur as a result of errors in the lower moments and the limits of integration. The rate of data acquisition and

number of data points stored also affect the precision of the moment calculation and are especially important in calculating the skew and excess.

Cram, Yang and Brown (124) have applied computerized data handling to moment analysis of capillary peaks and have reported that the analog to digital converter clock rate which regulates the number of data points collected per peak must be at least 50 in order that the peak shape be characterized accurately. They see this to be critical especially for peaks which elute early ($k' < 5$) with small peak widths.

Adsorption Indicators. Although moment analysis can provide a very sensitive, descriptive characterization of the chromatographic and physicochemical processes occurring in the column, Grob, Grob and Grob (125) have chosen not to use moment analysis for evaluation of peak distortions that can occur in the glass capillary column. Of the four types of peak distortions, namely, 1) broadened peaks of Gaussian shape, 2) tailing peaks of constant area, 3) reasonably shaped peaks of reduced area and 4) misshapen peaks of correct area but increased retention, Grob et al (125) state that moment analysis fails to observe irreversible adsorption in the Case 3 situation where part of the component doesn't elute from the column but the peak shape looks Gaussian. Instead of calculating a parameter related to peak shape, Grob et al (125) determine an adsorption indicator by measuring the height of the eluted peak and comparing this height to the height which is expected for a complete undistorted elution. To simplify the height observation, a test mixture is prepared so that the peak areas of all the components are identical. Since their testing procedure employs linear temperature programming with standard-

ized program rates, most of the eluted peaks will have widths which are approximately equal. Since the areas are equal, the peak heights for non-adsorbed components are also equal. A 100% line is drawn by connecting all the non-adsorbing peaks (n-alkanes and methyl esters). When the height of the adsorbed peak is expressed as a percentage of the distance between the baseline and the 100% line, a measure of the adsorption is obtained.

Column Character Probes

Column character testing of the capillary column requires a myriad of probing components. From the interaction of the functional groups present on these different solutes with the stationary phase and inner surface of the capillary, indications of the adsorption, polarity, acidity and basicity of the column can be observed. Quantitative measurement of the peak shape by methods provided previously indicate the presence or absence of these interaction sites in the column when the functional group of the probe is specific. Often adsorption of a probe can indicate that several active sites are present. Table II lists many of these probes and includes the expected interactions and purposes (125-127).

One test to be noted which determines the acidity-basicity of the column, requires that the test mixture contain 1:1 by weight 2,6-dimethylaniline (or 2,4-dimethylaniline) and 2,6-dimethylphenol (124-126). Comparison of the peak heights of these components with the heights expected for complete elution provides acid-base adsorption information of the column.

Because the solid support of the capillary column, the glass capillary wall, is the chief contributor to the quality of the column, evaluation of its surface activity-adsorption characterisitcs are necessary

TABLE II

COLUMN CHARACTER PROBES AND
EXPECTED INTERACTIONS

Component	Interaction/Purpose
Alkanes (C_{10} - C_{18})	Instrumental effects, separation efficiency, adsorption
Methyl esters (C_{10} - C_{18})	
Naphthalene	Metal adsorptive sites
Alcohol (1-octanol, 2,3-butanediol 2-propyl cyclohexanol)	Hydrogen bonding, basicity, adsorption, senses active silanol groups
Aldehydes (n-nonanal)	Hydrogen bonding, adsorption independent
Ketones (2-octanone, 5-nonanone, dibutylketone)	Adsorption to surfaces that act as Lewis acids
Acids (propionic acid, 2-ethyl hexanoic acid)	Adsorption-chemisorption
Amines (2,6-dimethylaniline, 2,4-dimethylaniline, dicyclohexylamine)	Basicity
Phenol (2,6-dimethylphenol)	Acidity

if improvement is expected. Schomburg, Husmann and Weeke (128) have reported on a method of testing the uncoated capillary column. When a precolumn of high quality is placed between the injector and the column to be tested, perfectly shaped, separated elution bands are allowed to pass into the uncoated column. Comparison of the chromatograms of the components eluted from the precolumn and the precolumn-test column pair permit quality control of the uncoated capillary prior to coating with the stationary phase.

The influence of the activity of the inner wall of the coated capillary on column performance can be measured by calculating the relative retention, α, for a pair of components. Hartigan and Ettre (130) and Hartigan, Billieb and Ettre (131) have shown that when compounds of different polarity such as 1-hexanol and n-nonane or 1-hexanol and isopropylbenzene are used as probes, the relative retention of these probes will change between columns if the surface activity in one of the columns is greater. The difference arises because the polar compound is retarded more on the active column while the retention of the nonpolar compound remains unchanged.

Conclusion

From the chromatogram which occurs as a result of testing the newly purchased or produced capillary gas chromatography column, information is available which can be used to determine the efficiency, resolving power and performance of the column. This information consists of the retention time, gas hold-up time, width, area, shape, and concentration profile of the peak or peaks eluted from the column. The applicability of this peak information to the determination of efficiency, resolving

power and performance depends upon the column's adsorption character. When distorted, asymmetric peaks are obtained, the functional groups on the probe can suggest possible interaction sites that might be present in the column. If Gaussian shaped peaks are determined as a result of peak moment analysis, meaningful efficiency information is obtained. The efficiency measures which have been presented use the peak width, retention time, adjusted retention time and gas hold-up time to determine how the peak broadens. This broadening which is described by Kaiser's a and w_{ho} values can be used along with the gas hold-up time to describe completely the three plate number efficiencies. The resolving power of the column provides information on how well the column separates peaks or how many resolved peaks can be separated between two reference peaks. The performance relates resolving power to how long each peak is retained. This information is the most useful aspect of the column evaluation procedures discussed and answers two essential questions of chromatography: How well does the column separate the components in the mixture and how long will it take for elution to occur?

A summary table of the column evaluation techniques (Table III) which have been presented is provided on the following pages. This summary considers each technique and attempts to evaluate each with regard to parameter and chromatographic requirements, assumptions, applications, advantages and disadvantages.

Stationary Phase Evaluation

The previous sections have dealt with evaluation techniques which are applied to columns where the stationary phase has been well characterized. When new stationary phases are prepared, characterization should

TABLE III

SUMMARY OF COLUMN EVALUATION TECHNIQUES

Method	Information/Data/ Processing Required	Chromatographic Requirements	Assumptions	When Applied	Why Applied/ Advantages	Disadvantages	References
I. Efficiency							
A. Plate Number							
1. Theoretical $n = 2\frac{V_e V_R}{(V_R - V_e)^2}$	Retention time at peak maximum and at 1/e times peak height	Isothermal and isobaric conditions; low feed volume; $t_R > t_M$ (large k′); one probe	Linear ideal chromatography; Glueckhauf's concentration profile; all plates equivalent	Packed columns, large k′	Concentration distribution is not Gaussian; to determine a measure of the peak broadening with respect to peak retention	Includes gas hold-up time, peak width, and extra coluan contributions; n is too large when k′ is small	71
$n = 8 \ln 2 \left[\frac{t_R}{w_h}\right]^2$	Retention time; peak width at half height or at other locations	As above	As above; Gaussian peaks; $V_R >> V_e$	As above; Gaussian peaks	Ease in calculation	As above	78,79
2. Effective $n = 8 \ln 2 \left[\frac{t'_R}{w_h}\right]^2$	Gas hold-up time; retention time; peak width at half height or at other locations	Isothermal and isobaric conditions; low feed volume; large k′; one probe	Linear ideal chromatography; Glueckhauf's concentration profile; all plates equivalent; Gaussian peaks; $V_R >> V_e$	Capillary columns, large k′	To correct for dead time; to determine a measure of the peak broadening with respect to peak retention	Includes gas hold-up time and extra coluan contributions in peak width	78,79,83
3. Real $n_{real} = 8 \ln 2 \left[\frac{t_R}{a}\right]^2$	Retention time; dead time; peak width at half height; slope of peak width vs k′; starting peak width; linear regression coefficient and angle; standard deviation; programmable calculator	Isothermal and isobaric conditions; low feed volume; 5 - 6 homolog probes	As above; linearity of peak width between half height and ki extra coluan contributions are negligible	Any coluan type	Substance independent; more than one probe used; based on statistical calculation; provides maximum number of plates available; independent of k′; free of extra coluan effects and dead time; to determine a measure of the peak broadening with respect to peak retention	Does not apply if peak width is not linear with respect to k′; requires more calculation	84-89

TABLE III (Continued)

Method	Information/Data/ Processing Required	Chromatographic Requirements	Assumptions	When Applied	Why Applied/ Advantages	Disadvantages	References
B. Plate Height							
1. Theoretical $h = \frac{L}{n}$	Column length, n	As in n(b) above	As in n(b) above; n increases proportionally with column length	As in n above; differences in column length are not large; evluation of parameters of the plate height equation is desired	Allows comparison of columns of various lengths	Assumptions fail when large Δp occurs (h is not constant along the column); very small plate heights occur at low k'	78,83
2. Effective $H = \frac{L}{N}$	Column length, N	As in N above	As in N above; N increases proportionally with column length	As in N above; differences in column length are not large	Allows comparison of columns of various lengths	Assumptions fail when large Δp occurs (H is not constant along the column); very large plate heights occur at low k'	78,83
3. Real $h_{real} = \frac{L}{n_{real}}$	Column length, n_{real}	As in n_{real} above	As in n_{real} above; n_{real} increases proportionally with column length	As in n_{real} above; differences in column length are not large	Corresponds to H and h values at large k'	Assumptions fail when large Δp occurs (h_{real} is not constant along column)	84-89
C. Coating Efficiency							
1. $CE\% = \frac{\frac{d_c^2}{2}\left[\frac{1+6k'+11k'^2}{3(1+k')^2}\right]}{h_{expt(min)}} \times 100$	Column inner diameter; k'; plot of h_{expt} vs. average linear gas velocity; $h_{expt(min)}$ from plot	As in n above	C_s term in plate height equation is negligible; peak broadening due to pressure gradients are negligible	Seldom; only when 5% to 40% error is acceptable	To compare efficiency of prepared column to that of the theoretical column of same inner diameter	Assumptions do not apply in general; when assumptions fail, CE% > 100% can occur	12,104
2. $CE\% = \frac{2\left[B f_1 (C_G f_1 + C_L f_2)\right]^{1/2}}{h_{expt(min)}} \times 100$	Column inner diameter and film thickness; k'; inlet and outlet pressures; diffusion coefficients for solute in gas or liquid phase; plot of h_{expt} vs. average linear gas velocity; $h_{expt(min)}$ from plot	As in n above	As in n(b) above	When comparison of efficiency of prepared column to that of the theoretical column is desired	Provides information about the uniformity of the film thickness of the stationary phase	D_L and D_G for solute in gas and stationary phase may not be available	105,106
II. Resolution, Resolving Power and Performance							
A. Resolution							
1. $R = \frac{2(t_{R2} - t_{R1})}{w_{b2} + w_{b1}}$	Retention time; peak widths at half height	Symmetrical peaks	None; the widths of two peaks are different	Whenever the resolution between two peaks is desired	This expression makes no assumptions about the peak widths; it is an exact equation	None	108

TABLE III (Continued)

	Method	Information/Data/ Processing Required	Chromatographic Requirements	Assumptions	When Applied	Why Applied/ Advantages	Disadvantages	References
2.	$R_s = \frac{\sqrt{n}}{2}\left[\frac{\alpha-1}{\alpha+1}\right]\left[\frac{k'}{1+k'}\right]$	Adjusted retention time; retention time gas hold-up time; n	Symmetrical peaks; two peaks	n is the same for peak 1 and peak 2	Before the chromatograph run	Used to determine the resolution obtainable based on a given n, α, and k'	Not for coluan evaluation (prediction of R only)	118,111,112
3.	$R_s = \frac{\sqrt{n}}{6}\ln\left[\frac{k_2'+1}{k_1'+1}\right]$	Retention time; gas hold-up time; n	Symmetrical peaks	n is the same for the two peaks	As above	Takes into account continuous peak broadening with increase of retention time	As above	111,112
B.	Separation Number							
1.	$TZ = \frac{t_{R2}-t_{R1}}{w_{h2}+w_{h1}} - 1$	Two probes; retention time; peak width	Temperature programming; symmetrical peaks	Peak widths of test pair are equal	When the number of peaks that can be chromatographed between two peaks with R = 1 is desired	Provides a measure of coluan efficiency	When used with an isothermal run, peaks should be close together or assumption fails	113
2.	$SN_{homolog} = \frac{\log\frac{w_{h2}}{w_{h1}}}{\log\left[\frac{\sqrt{\frac{n_{real}}{5\ln 2}}+1}{\sqrt{\frac{n_{real}}{5\ln 2}}-1}\right]} - 1$	As in n_{real}	As in n_{real}	As in n_{real}	As above but the two peaks are a homolog pair	As above	Requires long calculation	113,84-89
3.	$SN_{real} = \frac{\log\frac{10\alpha + w_{h0}}{w_{h0}}}{\log\left[\frac{\sqrt{\frac{n_{real}}{5\ln 2}}+1}{\sqrt{\frac{n_{real}}{5\ln 2}}-1}\right]} - 1$	As in n_{real}	As in n_{real}	As in n_{real}	As above but the two peaks would occur at $k' = 0$ and $k' = 10$	As above	As above	113,84-89
4.	$SN_{0-k'_a} = \frac{\log\frac{k'_a + w_{h0}}{w_{h0}}}{\log\left[\frac{\sqrt{\frac{n_{real}}{5\ln 2}}+1}{\sqrt{\frac{n_{real}}{5\ln 2}}-1}\right]} - 1$	As in n_{real}	As in n_{real}	As in n_{real}	As above but the two peaks would be the air peak and the last peak chromatographed	Provides an efficiency measure over entire run	As above	113,84-89

TABLE III (Continued)

Method	Information/Data/ Processing Required	Chromatographic Requirements	Assumptions	When Applied	Why Applied/ Advantages	Disadvantages	References
C. Resolution vs. Retention Time Plots	Two peaks; retention time peak widths; flow rates	Isothermal; changes in flow rates for each run	Symmetrical peaks	When resolution between peaks and retention time are important; applicable to isomer separation	Allows selection of fastest flow rate for the minimum resolution acceptable; very practical for optimizing separations; not based on Glueckhauf or Gaussian profiles; allows comparison of different type columns	Not applicable for efficiency measurements	114
D. Separation Power $SN_t = \frac{SN_{real}}{11\ t_N}$	As in SN_{real} above retention time and separation distance are standardized	As in SN_{real} above	As in SN_{real} above	When the number of separated peaks per unit time is desired; comparison of column performance	Since retention time and separation distances are standardized, SN_t allows comparison between columns practical for optimizing mixture separations	Does not account for extra column contributions in peaks of small k'	84-89
E. N/t_R	As in N above	As in N above	As in N above; optimum carrier flow	Seldom; for column comparison of performance	Provides a measure of the efficiency available with respect to the time spent	Depends on k' (different N/t_R for different retention times); not as practical as SN_t or R vs t_R plots; as in N above	83,114
F. Performance Index $PI = \left(\frac{n_h}{t_R - t_M}\right)^h \left[\left(\frac{t_R - t_M}{t_R}\right)^h \left(\frac{t_M}{t_R - \frac{11}{10} t_M}\right)\right]^{t_R \Delta P}$	Peak width; retention time; gas hold-up time; pressure drop	Isothermal and isobaric conditions	Optimum carrier flow; symmetrical peaks	Seldom; for column comparison of performance	Combines resolving power, time of analysis and pressure drop into one evaluation expression	Units of PI (viscosity) are awkward; application to resolution, separation or efficiency concepts is difficult	12,102
III. Peak Shape							
A. Tailing Factor $TF\% = \frac{a}{b} \times 100$	Chromatograph tracing	Measurable peak width; temperature programming is possible	None	When symmetry measure of tailing peak is desired	Simple; requires only a ruler	Cannot detect peak adsorptions which cause broadened Gaussian shaped peaks or symmetrical peaks with reduced area	116-118

TABLE III (Continued)

Method	Information/Data/ Processing Required	Chromatographic Requirements	Assumptions	When Applied	Why Applied/ Advantages	Disadvantages	References
B. Moment Analysis	Analog to digital converters with clock rates of 50 points per peak; computer/data system with 24K core memory and large word bulk storage	Automatic sample injection	Integrals which occur in moment expressions are approximated as summations	When a comparison of the experimental peak is desired; also provides center of gravity, variance and asymmetry of peak	Fast data reduction; other parameters, e.g. n, can be calculated with ease	Computer system required; cannot detect peak adsorptions which result in broadened Gaussian shaped peaks or symmetrical peaks with reduced area	119-124
C. Adsorption Indications	Peak heights	Concentration of component test mixture adjusted so that peak areas are same; temperature programming	Temperature programming at constant rate produces peaks of same width	When adsorption, polarity, acidity, or basicity character of column is desired	Adsorption which does not result in asymmetry or non-Gaussian peaks can be detected	Temperature programming prohibits efficiency measurements in same chromatograph run	125

be done so that the material can be compared with existing stationary phases. These characterizations should include determination of minimum and maximum allowable operating temperatures, phase transition studies, retention indices and McReynolds' constants. The minimum allowable operating temperature occurs at the temperature where the efficiency of eluted peaks starts to decrease and adsorption causes retention to change with sample size. These effects usually occur at the melting point of the stationary phase. Differential scanning calorimetry can provide melting and glass transition temperatures of bulk stationary phases. If the stationary phases are prepared inside the column, the gas chromatograph can give this information. This technique, called inverse phase gas chromatography, determines the properties of the stationary phase using known molecular probes whereas conventional chromatography utilizes a well characterized stationary phase to determine properties of unknown solutes. When the logarithm of the partition ratio, k', or the specific retention volume, V_g, for a molecular probe is plotted versus inverse temperature (1/T(K)), a linear relationship results as long as no change in phase occurs (132-134). When the temperature of the column increases and a melting transition occurs, a decrease in slope results because the stationary phase becomes more liquid and partitioning increases. Along with the change in trend of retention, an increase in efficiency results because band broadening due to adsorption is reduced and more efficient partitioning processes occur. Maximum operating temperatures are temperatures above which column bleed becomes excessive or where continued use causes large decreases in retention. Such temperatures are determined from temperature retention studies or by following baseline shifts during temperature programming and setting temperature limits where bleed becomes

excessive.

Stationary phase polarity can be compared with other stationary phases by calculating the McReynolds' constants and comparing them with published values (135-137). To calculate McReynolds' constants, retention indices for the McReynolds' probes: benzene, 1-butanol, 2-pentanone, pyridine and 1-nitropropane are first calculated by

$$I^{phase}_{120°C}(Probe) = 100 \frac{\log k'_{probe} - \log k'_{C(Z)}}{\log k'_{C(Z+1)} - \log k'_{C(Z)}}. \quad (65)$$

Here $k'_{C(Z)}$ and $k'_{C(Z+1)}$ are the partition ratios for the homologous n-alkanes with carbon number Z and Z+1 which elute before and after each probe. This equation which is based on the partition ratio instead of the net retention volume can be derived from Kovat's retention index equation (138). McReynolds' constants, ΔI, were calculated using Equation 66,

$$\Delta I = I^{phase}_{120°C}(Probe) - I^{squalane}_{120°C}(Probe) \quad (66)$$

where $I^{squalane}_{120°C}$ was the absolute value of the retention index of each probe on squalane as reported by McReynolds (139). Comparison of the average value of the McReynolds' constants and the retention sequence of the five probes with the values for other stationary phases in McReynolds' table gives information about the average polarity and selectivity of the stationary phase.

CHAPTER III

DIRECTION OF RESEARCH

Crown Ethers as Stationary Phases

Crown ethers have been used in analytical chemistry as solvent extractions reagents for alkali and alkaline earth metal ions, the basis for ion selective electrodes and stationary phases or mobile phase complexing agents in liquid chromatography (140-142). In each of the analytical applications of crown ethers which were found in the literature, it was the cation complexing ability of the crown ether that was utilized. As a gas chromatography phase, crown ethers could provide a unique phase where the polarity would be localized within the center of the ring formed by the crown ether oxygens. Instead of metal cations, polar compounds such as alcohols, amines and carboxylic acids and compounds with methyl groups attached to electron withdrawing substituents such as acetonitrile or nitromethane should interact with the localized polarity that a crown ether would provide. Such interactions have been observed in the stable nonionic host-guest complexes that have been prepared from organic molecules such as acetonitrile, nitromethane, dimethylcarbonate, dimethylsulfate, aniline, cyanamide and malonitrile and the crown ether, 18-crown-6 (143-145). The polarity of a stationary phase containing crown ethers should be similar to polyethylene glycol because of the similar $-CH_2-CH_2-O-$ units, although crown ethers should be more

selective toward polar molecules due to the localized polarity.

The selection of suitable crown ethers for this study was limited to those crown ethers which were commercially available or whose synthesis was published. Two sila crown ethers available from Petrarch Systems, Inc. (Bristol, Pennsylvania), vinylmethylsila-17-crown-6 and vinylmethylsila-14-crown-5, were selected because of the polymerizable vinyl groups which were present in each compound. Poly(vinylbenzo-15-crown-5) whose synthetic route was published by Kopolow, Hogen Esch and Smid (146) was selected for its similarities to polystyrene and relative ease in systhesis. The structures of these crown ethers are given below in Figure 5.

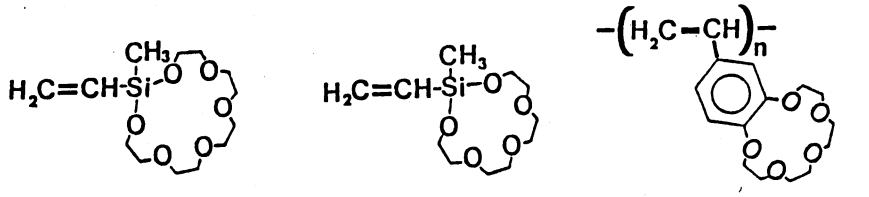

Figure 5. Crown Ether Structures

Although the polymeric backbone of these crown ethers, polyethylene and polystyrene, would have glass and melting transitions well above the lower operating temperatures of typical stationary phases (See Table IV), chromatographic characterization of columns prepared with these crown ethers could provide rationale for synthetic work on more promising crown ether stationary phases.

TABLE IV

GLASS AND MELTING TRANSITION TEMPERATURES AND COLUMN OPERATING TEMPERATURE RANGES OF FOUR POLYMERS

Polymer	Glass Transition Temperature (T_g) (148)	Melting Transition Temperature (T_M) (148)	Column Operating Temperature Range (76)
Polydimethyl-siloxane	-127°C	-40°C	0 - 200°C
Polyethylene glycol	-41°C	66°C	80 - 250°C
Polyethylene	-125°C	137°C	-
Polystyrene	100°C	240°C	-

The experimental studies which will be discussed involve the synthesis of poly(vinylbenzo-15-crown-5), the preparation of glass capillary columns containing polystyrene, vinylmethylsila-17-crown-6, vinylmethylsila-14-crown-5, and poly(vinylbenzo-15-crown-5) and the characterization of these capillary columns. The synthesis of polyvinylbenzo-15-crown-5 involves the four steps shown in Figure 6. Reaction 1 which was described by Parish, Stott, McCausland and Bradshaw (148) is an acylation of benzo-15-crown-5 with acetic acid using Eaton's reagent (phosphorous pentoxide dissolved in anhydrous methanesulfonic acid). Reactions 2, 3 and 4 were described by Kopolow et al (146) and involve a reduction of the ketone using sodium borohydride, a dehydration using p-toluene sulfonic acid and finally polymerization of vinylbenzo-15-crown-5 to

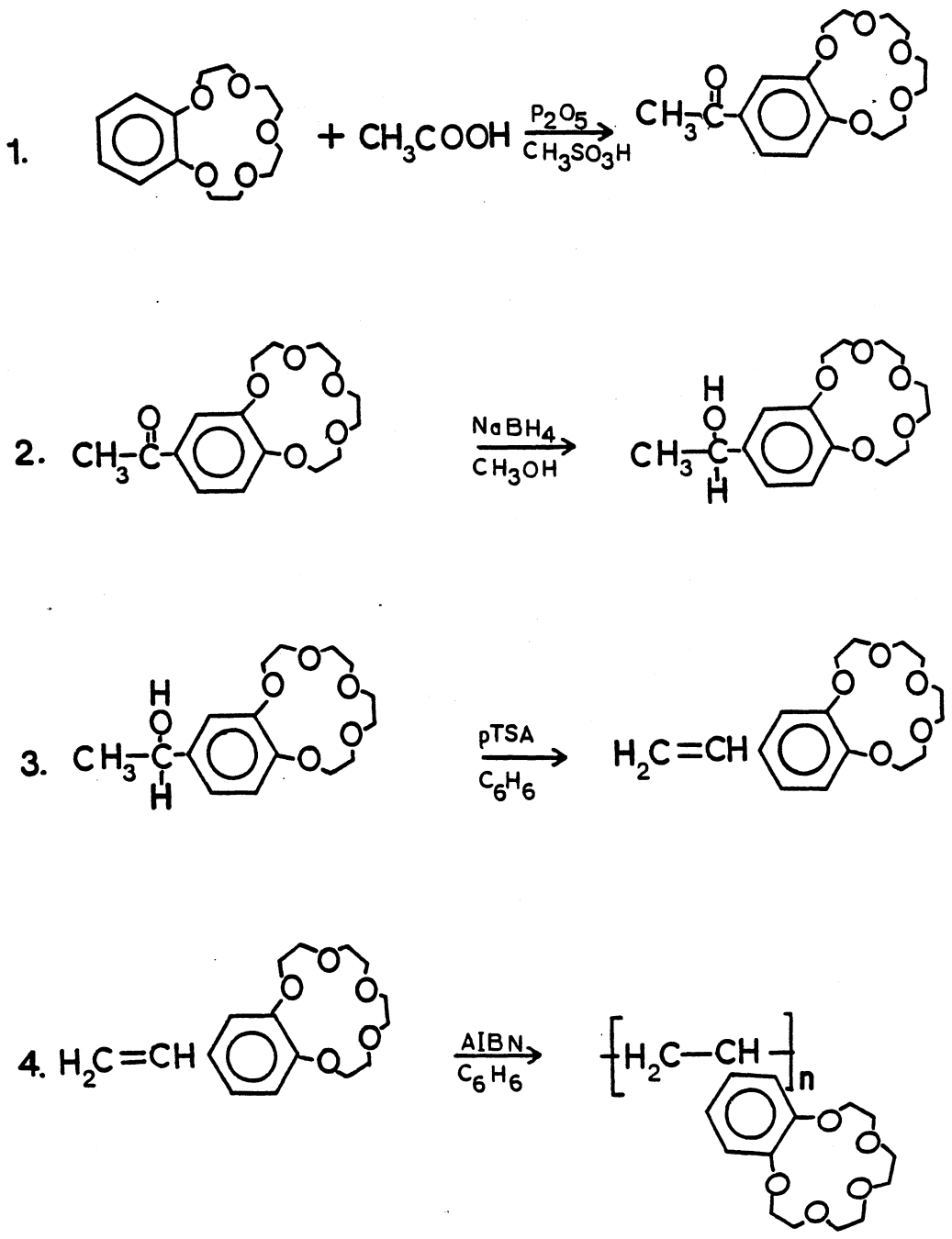

Figure 6. Reaction Steps for Synthesis of PVB15C5

poly(vinylbenzo-15-crown-5).

Column Preparation

Glass capillary columns were prepared in two ways. The first involved a polymerization of the vinyl crown ether inside the capillary. Before this in situ polymerization, the HCl leached capillaries were treated with γ-methyacryloxypropyltrimethoxysilane (MAPTMS). This silane provided methacryloxy groups which can copolymerize with the vinyl crown ethers (149,150). Hydrolysis of the methoxy groups on the silane provide silanols which bond to the glass surface. Figure 7 shows this silane as it is bonded to the glass surface. Figure 8 shows how the vinyl silacrown ethers might be crosslinked to the MAPTMS surface and crosslinked with divinylbenzene. Preliminary studies involving in situ bonding, crosslinking and polymerization of styrene in capillary columns was done before attempting polymerization with vinyl crown ethers.

The second method of capillary preparation involved statically coating poly(vinylbenzo-15-crown-5) inside a roughened, deactivated capillary. The roughening was achieved by a NH_4FHF etch (25). This was followed by deactivation of the capillary with a thin nonextractable film of Carbowax 20M (45).

Column Characterization

Chromatographic characterization was done by comparing the separation of mixtures of alcohols, aromatics and alkanes on each column. Various sample sizes and isothermal column temperatures or temperature programs were utilized. Phase transitions for each column were studied by inverse phase gas chromatography. Differential scanning calorimetry

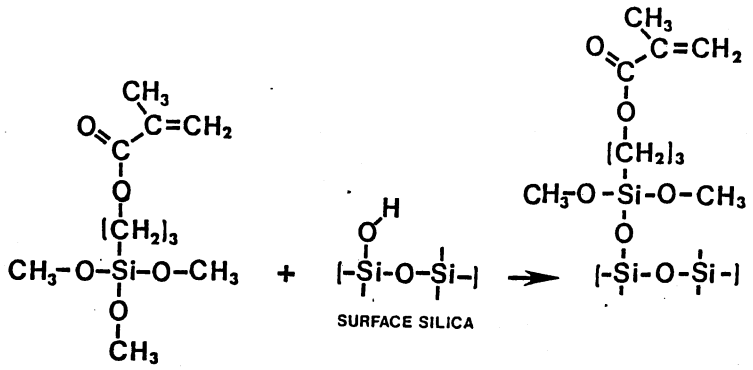

Figure 7. Surface Silanization with γ-(Methacryloxy)propyl-trimethoxysilane

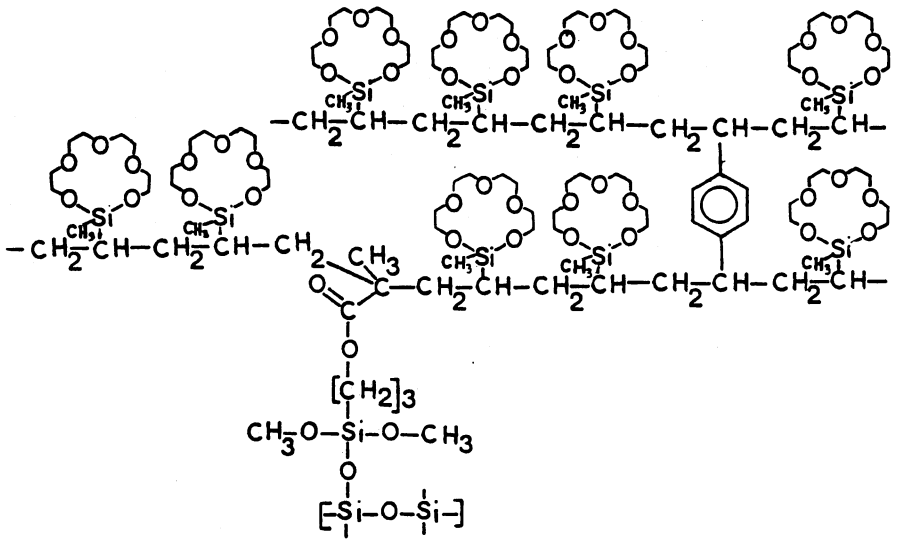

Figure 8. Copolymerization of Surface Bonded Groups with Vinylmethylsila-14-crown-5 and Divinylbenzene

was used to confirm phase transitions of PVB15C5 which were determined by gas chromatography. Thermogravimetric analysis of this polymer was also obtained and was compared with that of Carbowax 20M. Minimum and maximum operating temperatures, column efficiencies and McReynolds' constants were also compared on several of the columns. In addition, differences in efficiency and retention of homologous series of alkanes, alcohols and diols on the PVB15C5 column were compared. Scanning electron micrographs of the inner surface of the polystyrene columns showed the effect of column treatments and allowed measurements of film thickness of deposited films.

CHAPTER IV

EXPERIMENTAL METHODS

Instrumentation

A Hewlett Packard 5880A gas chromatograph equipped with Level 4 integrator and computer system, capillary split injection and a flame ionization detector was used. Pyrex glass capillaries were drawn on a Hewlett Packard 1045A capillary drawing machine. A Shimadzu MCT-1A micro-column treating stand was used to prepare the glass capillary columns. Verification and purity of the crown ethers were determined with Varian XL-100 and XL-300 NMR spectrometers and with a Perkin Elmer 681 IR spectrophotometer. A DuPont differential scanning calorimeter with a single crucible cell and a scanning rate of 10°C/min was used to determine phase transitions of poly(vinylbenzo-15-crown-5). Thermogravimetric analysis of the PVB15C5 and Carbowax 20M samples was done on a DuPont 951 thermogravimetric analyzer. Micrographs of the inner capillary surface was done on a JEOL JSM-35, a Cambridge 250 and an AMR 100A.

Reagents

Vinylmethylsila-17-crown-6 (VMSi17C6) and vinylmethylsila-14-crown-5 (VMSi14C5) were obtained from Petrarch Systems, Inc. (Bristol, Pa.) and were used without further purification. NMR and IR spectroscopy showed

that impurities were present in both samples. The VMSi17C6 sample was ∿80% pure. NMR spectroscopy showed that the impurity which was present contained methylsilyl groups. The VMSi14C5 samples was ∿60% pure with tetraethylene glycol as the predominate impurity. Benzo-15-crown-5 was obtained from Parish Chemical Co. (Orem, Utah) and Chemalog, Chemical Dynamics Corporation (South Plainfield, N.J.). γ-Methacryloxypropyltrimethoxysilane (MAPTMS) was obtained from Dow Corning (Midland, Michigan). All other chemicals used for column preparation and characterization were analytical reagent grade.

Synthesis

4'-Acetobenzo-15-crown-5

For the synthesis of 4'-acetobenzo-15-crown-5, a mixture of 15.1 g (0.056 mol) of benzo-15-crown-5 and 3.6 ml (0.082 mol) glacial acetic acid was added to a stirring mixture of 70 g of distilled methane sulfonic acid and 5.6 g of phosphorus pentoxide. After stirring for 6 hours, the mixture was poured into 280 ml of distilled water, neutralized with sodium bicarbonate and then extracted four times with 80 ml portions of methylene chloride. When the combined extract was washed with water, dried with anhydrous sodium sulfate and its solvent removed, a reddish brown oil was obtained. Extraction with hot hexane and crystallization yielded 4.2 g (24%) of 4'-acetobenzo-15-crown-5, m.p. 96-97°C (lit. (148) mp 96-97°C).

4'-(1"-Hydroxyethyl)benzo-15-crown-5

To a stirring solution of 27.6 g of 4'-acetobenzo-15-crown-5 was

slowly added 4.9 g of sodium borohydride. After stirring for 24 hours, the solution was poured into 540 ml of water, neutralized with acetic acid, and extracted four times with 500 ml portions of chloroform. This extract was washed with water, dried with sodium sulfate and the chloroform evaporated. To the gold brown oil that resulted a minimum amount of diethyl ether was added. Crystallization of this solution in a salt-ice water bath yielded 8.76 g of 4'-(1"-hydroxyethyl)benzo-15-crown-5, m.p. 63-65°C (lit. (146) 65-66°C).

4'-Vinylbenzo-15-crown-5

To a 250 ml round bottom flask containing 200 ml of benzene and a trace of p-toluene sulfonic acid was added 1.0 g of 4'-(1"-hydroxyethyl) benzo-15-crown-5. The benzene was refluxed through a Soxhlet extractor which contained a thimble of calcium chloride for removal of water. After 24 hours, the benzene was removed and the oily residue that resulted was placed on top of a column that contained 50 ml of acidic alumina in benzene. 4'-Vinylbenzo-15-crown-5 was eluted with acetone and was recrystallized with petroleum ether to give 0.65 g, m.p. 42-43.5°C (lit. (146) 43-44°C).

Poly(vinylbenzo-15-crown-5)

To a solution of 0.75 g of VB15C5 in toluene was added 1.0 ml of 0.5% w/v 2,2 azobis(isobutyronitrile) (AIBN) in toluene. Ater toluene was added so that the total volume was 15 ml, the solution was placed in a Pyrex ampule. The ampule was degassed using a mechanical pump and ultrasonic bath, cooled in a dry ice/acetone bath and then sealed under vacuum. After the ampule was heated at 70°C for 24 hours, the solution

was slowly poured into 300 ml of petroleum ether. The white precipitate was filtered off and reprecipitated to give 0.29 g of material after vacuum drying.

Capillary Column Preparation

The following section describes the preparation of eight capillary columns. Table V outlines the treatments which each capillary received and gives the stationary phase present in each column.

TABLE V

STATIONARY PHASES AND TREATMENTS USED FOR COLUMN PREPARATION

Column	Stationary Phase	Treatment			
		HCl Leached	Surface Roughening	Deactivation/ Bonded Silane	Coating
1	Styrene	Yes	NH_4FHF(450°C)	MAPTMS	In Situ Polymerization
2	Styrene	Yes	NH_4FHF(450°C)	MAPTMS	In Situ Polymerization
3	VB15C5	Yes	None	MAPTMS	In Situ Polymerization
4	None	Yes	None	None	None
5	None	Yes	None	MAPTMS	None
6	VMSi17C6	Yes	None	MAPTMS	In Situ Polymerization
7	VMSi14C5	Yes	None	MAPTMS	In Situ Polymerization
8	PVB15C5	Yes	NH_4FHF(RT)	Carbowax 20M	Static

Column 1: In Situ Polymerization of Styrene

Thirty-one meters of capillary with an inner diameter of 0.41 mm was rinsed with one column volume of concentrated HCl. The column was then filled with the concentrated HCl and the open end of the capillary sealed. A vacuum applied to the open end aspirated the HCl out of the column until 8% of the sealed portion of the coil was empty. The end attached to the vacuum was then sealed and the coil placed in an oven. After heating overnight at 80°C, the leaching solution was aspirated out and the column rinsed with 10 ml each of deionized water, acetone, and diethyl ether. The capillary was then attached to a nitrogen regulator set at 15 psi and the capillary was flushed overnight. A 5% w/v NH_4FHF solution in methanol was then aspirated into the column (26). The solution was allowed to remain in the capillary one hour before being pushed out at a linear velocity of 6 cm/min. This linear velocity was obtained by using a piece of crimped 0.01" inner diameter stainless steel tubing and a nitrogen pressure of 31 psi. A buffer column which was longer than the coil containing the NH_4FHF solution was attached to the end of the column so that a uniform linear velocity could be maintained. When the NH_4FHF plug exited the coil, the restrictor was removed and nitrogen flow continued at a pressure of 10 psi. After 15 min the coil turned milky white throughout. Both ends of the coil were then sealed and the coil was placed on a mandril. The coil and mandril were placed in an annealing furnace and the temperature of the furnace set at 450°C. When this temperature was reached, the coil remained in the furnace for 3 h. The coil ends were then broken open in a fume hood and 20 ml of methanol aspirated through the coil. The coil was then connected to a nitrogen

regulator set at 10 psi and dried overnight. The column was then filled with an aqueous solution of 0.1% v/v MAPTMS and 0.1% v/v acetic acid. After this solution remained in the column for one hour, the column was washed with 20 ml of distilled water. A monomer solution of 5% v/v distilled styrene, 0.8% v/v distilled divinylbenzene and 0.8% w/v AIBN in toluene was placed in an ultrasonic bath and vacuum deaerated before being introduced into the capillary. When the ends were sealed, the capillary was placed in an oven and heated at 70°C for 24 h and then 90°C for 48 h. A buffer column was attached to the column and the solvent was slowly removed. A crimped restrictor and a nitrogen pressure of 14 psi maintained a constant linear velocity. After the solvent exited the column, the nitrogen flow continued until the next day. Before attaching the column to the gas chromatograph for conditioning, 20 ml of methylene chloride was aspirated through the column. The capillary was conditioned at 200°C with a helium flow rate of 8.1 ml/min for 3 h.

Column 2: In Situ Polymerization of Styrene

This column was leached and treated with NH_4FHF in a manner similar to the treatment of column 1 except that the NH_4FHF solution was pushed through the column at a linear velocity of 12 cm/min instead of 6 cm/min. After the whisker growth treatment and solvent rinse, the column was heated at 200°C for 3 h with nitrogen flowing through the column at a regulator pressure of 20 psi. A 0.1% v/v MAPTMS solution was prepared by first adding enough glacial acetic acid to 50 ml of deionized water so that a pH between 3.5 and 4.5 was obtained. A volume of 0.05 ml of MAPTMS was added and the solution was stirred for 15 min before introduction into the capillary column. The MAPTMS plug was pushed out of the

column through a buffer column at a linear velocity of 3 cm/s. After the plug exited, the coil was placed in an oven with nitrogen passing through the coil at 2 psi. The initial oven temperature, 60°C, was slowly increased to 106°C. After this temperature was maintained for 15 min, the oven was turned off and nitrogen flow continued overnight. A monomer solution of 48% v/v styrene, 1% v/v divinylbenzene and 0.09% w/v AIBN in toluene was ultrasonicated and vacuum deaerated before the solution was introduced into the capillary. The ends of the capillary were then sealed and the capillary placed in an oven set at 60°C. A vial which contained several milliliters of the monomer solution was also placed in the oven. After approximately four hours, the monomer in the vial started to become viscous. This indicated that the monomer solution in the capillary should be pushed out as plugging of the column due to gelation would soon occur. A nitrogen pressure of 50 psi was required for a slow flow of the monomer solution out of the capillary. After the monomer solution exited, the column was conditioned with a helium pressure at the head of the column of 2 psi and a temperature which increased from 40°C to 162°C at 5°C/min. The oven temperature was then lowered to 100°C and conditioning continued overnight. Before evaluation, the column was conditioned at 200°C for 2 h.

Column 3: In Situ Polymerization of Vinylbenzo-15-crown-5

Following an HCl leach and dehydration as described earlier, the column was filled with 5% w/v NH_4FHF using a syringe pump at a coating velocity of 4.4 cm/s and emptied using N_2 pressure at 3.0 kg/cm^2. After evaporating the solvent from the capillary, the column ends were switched

and the NH_4FHF coating was repeated in the opposite direction. After solvent evaporation, the ends were sealed and the column was heated using the following temperature program: 50°C to 200°C at 5°C/min; hold isothermal for 2 h; 200°C to 350°C at 1°C/min; hold isothermal for 12 h; then cool oven at 5°C/min to 50°C. The column was again HCl leached and dehydrated before it was silylated with MAPTMS. After drying, the column was filled with a 10% w/v VB15C5, 0.2% v/v DVB, and 0.07% w/v AIBN solution in benzene, its ends sealed and then heated at 70°C for 24 h. After the solution was emptied through a buffer column at 0.1 cm/s, the column was conditioned as in earlier columns.

Column 4: HCl Leached, 5: HCl Leached and MAPTMS Treated, 6: In Situ Polymerization of Vinylmethylsila-17-crown-6 and 7: In Situ Polymerization of Vinylmethylsila-14-crown-5

The capillaries containing the two silacrown ethers were prepared in the same manner. Pyrex capillaries were first leached with 20% HCl at 180°C for 16 h. After flushing with one column volume of distilled water, the capillary was dehydrated at 300°C for 1 h with a helium flow of 5 cm^3/min. The capillary was then dynamically coated at 3 cm/min with a 0.5% v/v MAPTMS solution. After the solution exited, the column was dried at 115°C for 15 min with a helium flow of 1 cm^3/min. A solution of 20% v/v VMSi17C6 (column 6) or VMSi14C5 (column 7), 0.5% v/v divinylbenzene and 0.1% w/v 2,2 azobis(isobutyronitrile) in benzene was degassed using a water aspirator and a sonic bath. After filling all but 8% of the capillary with this solution, the sealed capillary was

heated at 60°C for 72 h. The capillary was then attached to a buffer column and the liquid was pushed out at a linear velocity of 5 cm/min. Conditioning of the capillary was accomplished by a temperature program up to 200°C with an isothermal hold for 3 h. Helium flow was maintained at 5 cm^3/min. In addition to these silacrown ether columns, two capillaries were prepared at different stages of completion. The treatment of column 4 was stopped after the HCL leach and dehydration. Column 5 was stopped after the MAPTMS coating and drying.

Column 8: Static Coating of Poly(Vinylbenzo-15-crown-5)

This column was HCl leached and dehydrated as described for column 6. Roughening of the capillary was done by a room temperature etch with 5% w/v NH_4FHF in methanol. Ten ml of this solution was pushed through the capillary at 0.5 cm/s. After all the solution exited, the capillary was rinsed with 10 ml of methanol, a gradient of methanol to water over 20 ml total volume and then 10 ml of water. After a second HCl leach and dehydration, the capillary was deactivated with Carbowax 20M (CW20M). The capillary was dynamically coated by pushing four column loops of 5% w/v CW20M in CH_2Cl_2 through the capillary at 2 cm/s. After the solvent was evaporated, the ends were sealed and the capillary was heated at 280°C for 24 h. The capillary was then rinsed with 15 ml of CH_2Cl_2 and 15 ml CH_3OH. For static coating, a solution of 0.020 g PVB15C5 in 3.0 ml of CH_2Cl_2 was degassed over an ultrasonic bath using a water aspirator until a final volume of 2.0 ml (1.2% w/v PVB15C5) was reached. The capillary with open Teflon heat shrink tubing attached to one end was filled with coating solution. After the solution began to empty out the column,

the column was sealed by crimping a piece of copper tubing around the Teflon tubing. A nitrogen pressure of 3.7 kg/cm^2 was maintained on the column overnight. The column was then placed in a water bath and attached to a vacuum pump (vac. 0.35 mm Hg). The solution meniscus evaporated smoothly when the vacuum was applied, and the solvent was evacuated from the column by the next day. Initial column conditioning consisted of a temperature program up to 150°C at 5°C/min with an isothermal hold for 3 h. Helium flow was set at 3 ml/min before temperature programming started.

CHAPTER V

RESULTS AND DISCUSSION

Column 1 and 2: In Situ Polymerization of Styrene

Characterization of Column 1 consisted of carbon analysis and scanning electron microscopy of capillary sections taken from the column after each of the six steps in the capillary preparation. The column treatment, carbon analysis in ppm and corresponding micrograph figure numbers are given in Table VI. Carbon analysis showed an increase in total carbon content after the HCl leach which remained essentially the same after the NH_4FHF treatment and MAPTMS silanization. Although the carbon content increased as expected after the styrene and divinylbenzene polymerization, it fell below previous levels after the column was washed with 20 ml of methylene chloride. This showed that the film of polystyrene-divinylbenzene was not bound to the glass surface. Visual observation of the surface with scanning electron microscopy confirmed this in Figures 9, 10, 11, 12, 13 and 14. Figures 12, 13 and 14 show the buildup and subsequent loss of the polymer on the NH_4FHF roughened surface. The film thickness of the polymer can be measured from the micrograph and is estimated to be between 0.2 and 0.5 μm. Figure 9 and 10 show that the HCl leach treatment gives an additional benefit in that

TABLE VI

CARBON ANALYSIS AND CORRESPONDING SCANNING ELECTRON MICROGRAPHS FOR TREATED SECTIONS OF COLUMN 1: IN SITU POLYMERIZATION OF STRYENE

	Treatments	Carbon Content (PPM)	SEM Figure Number
1.	Bare Pyrex capillary after drawing	5	9
2.	After HCl leaching, water rinse	20	10
3.	After NH_4FHF treatment, methanol, acetone and diethyl ether rinse	26	11
4.	After MAPTMS treatment, water rinse	25	12
5.	After styrene-divinylbenzene polymerization	112	13
6.	After methylene chloride rinse	8	14

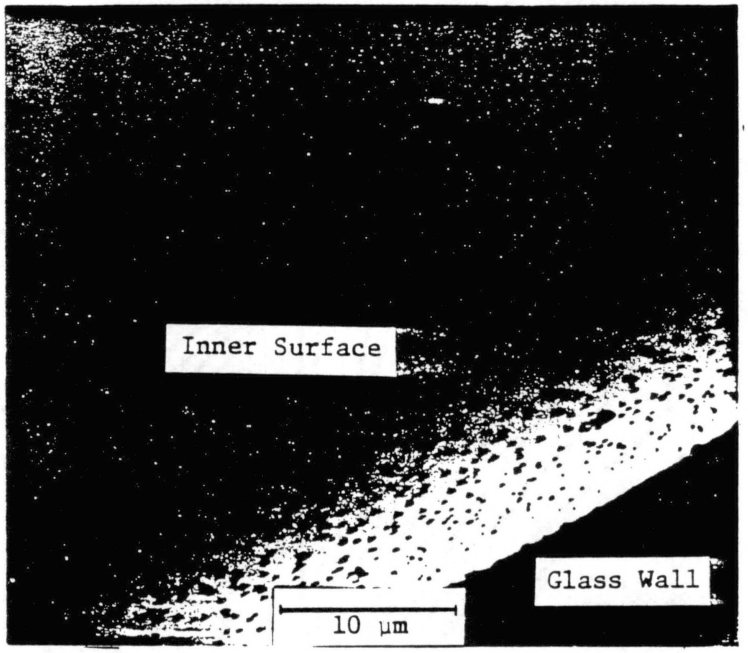

a. Edge View of Inner Surface and Fractured Glass Wall. Magnification X2400.

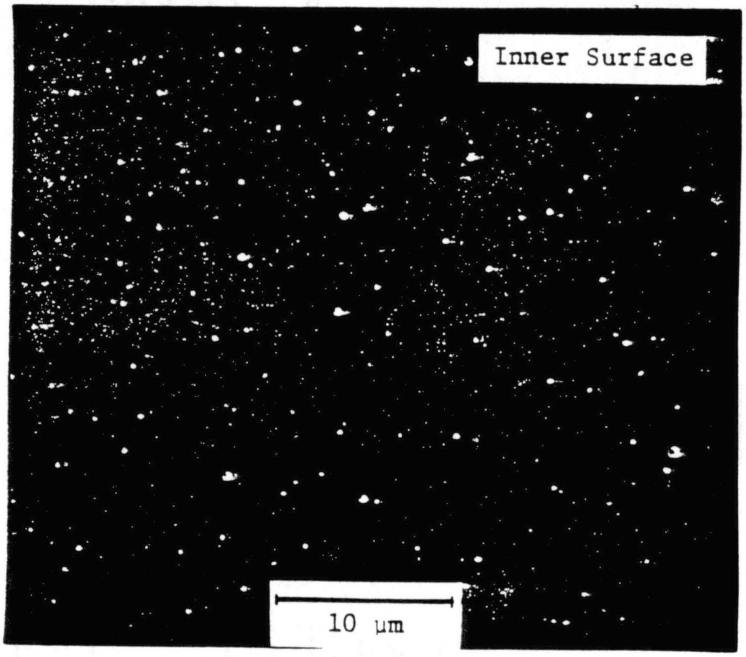

b. Inner Surface Viewed From Above. Magnification X2400.

Figure 9. Scanning Electron Micrograph of Column 1 After Drawing

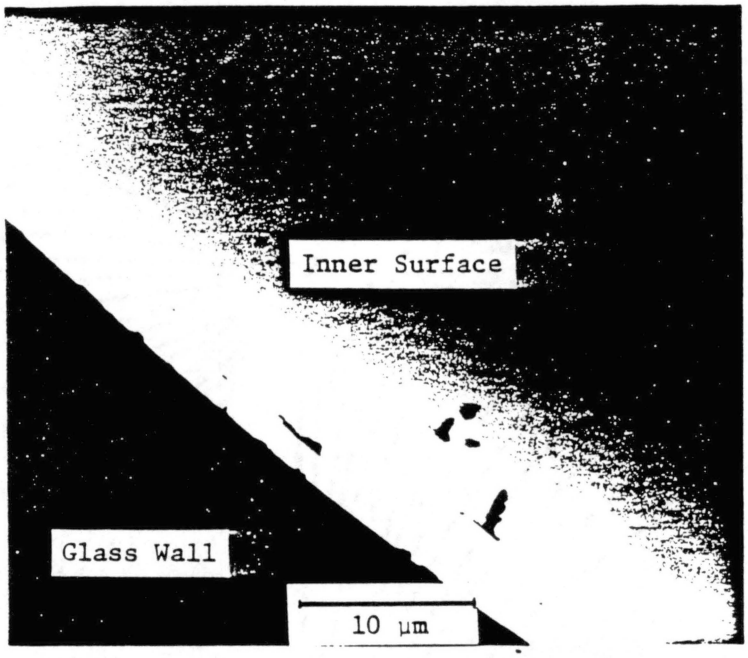

a. Edge View of Inner Surface and Fractured Glass Wall. Magnification X2400.

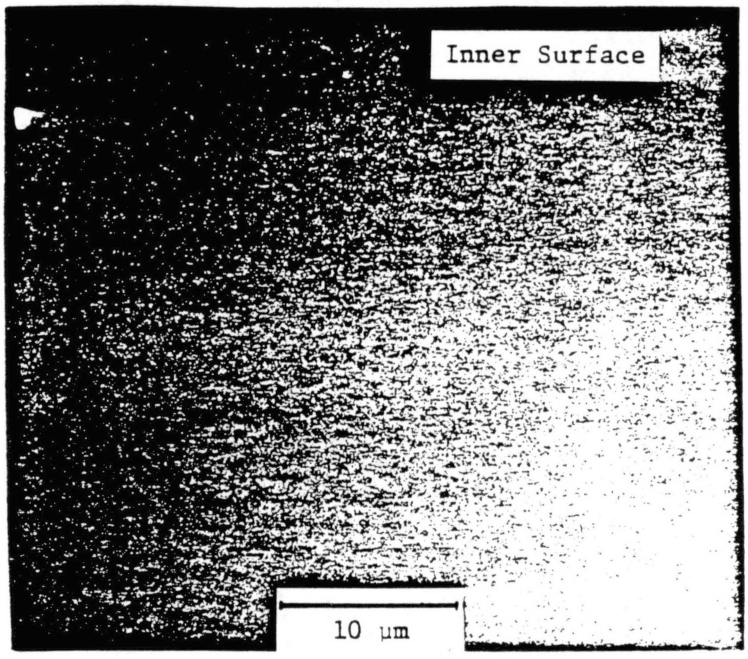

b. Inner Surface Viewed From Above. Magnification X2400.

Figure 10. Scanning Electron Micrograph of Column 1 After HCl Leach

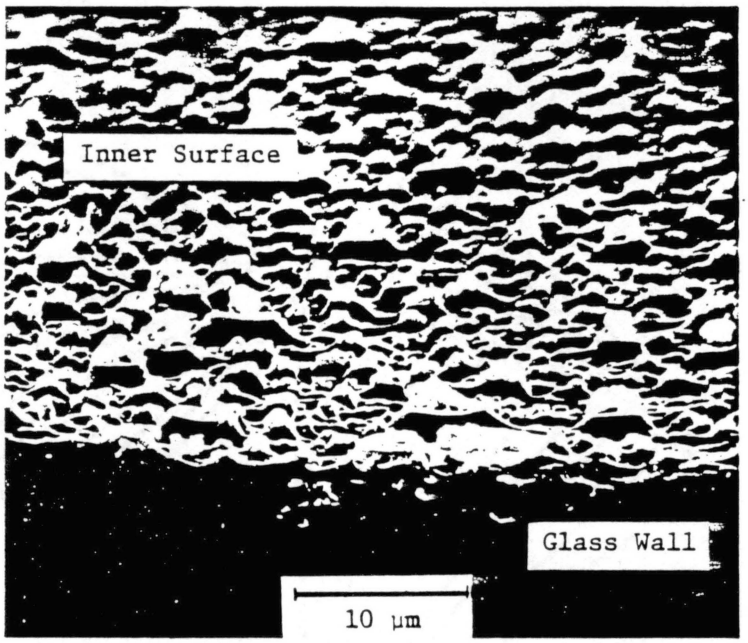

a. Edge View of Inner Surface and Fractured Glass Wall. Magnification X2400.

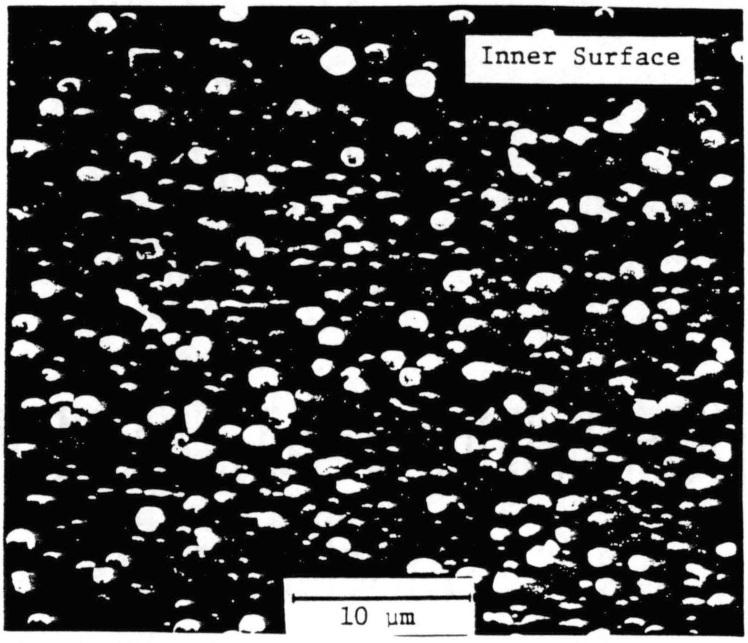

b. Inner Surface Viewed From Above. Magnification X2400.

Figure 11. Scanning Electron Micrograph of Column 1 After NH_4FHF Treatment

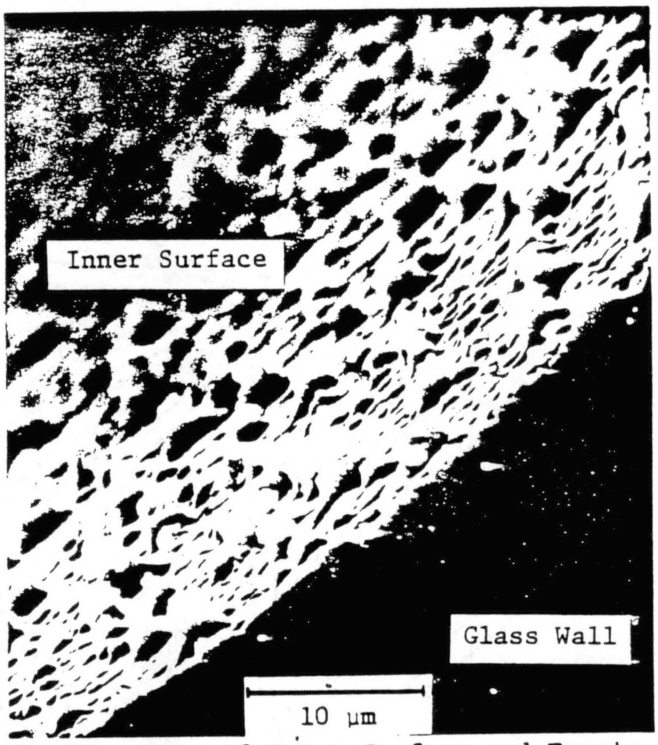

a. Edge View of Inner Surface and Fractured Glass Wall. Magnification X2400.

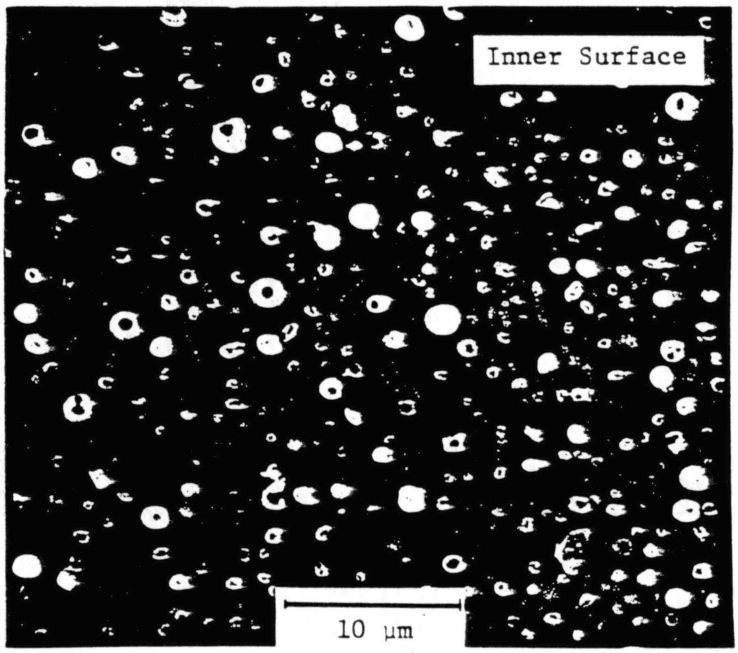

b. Inner Surface Viewed From Above. Magnification X2400.

Figure 12. Scanning Electron Micrograph of Column 1 After MAPTMS Silanization

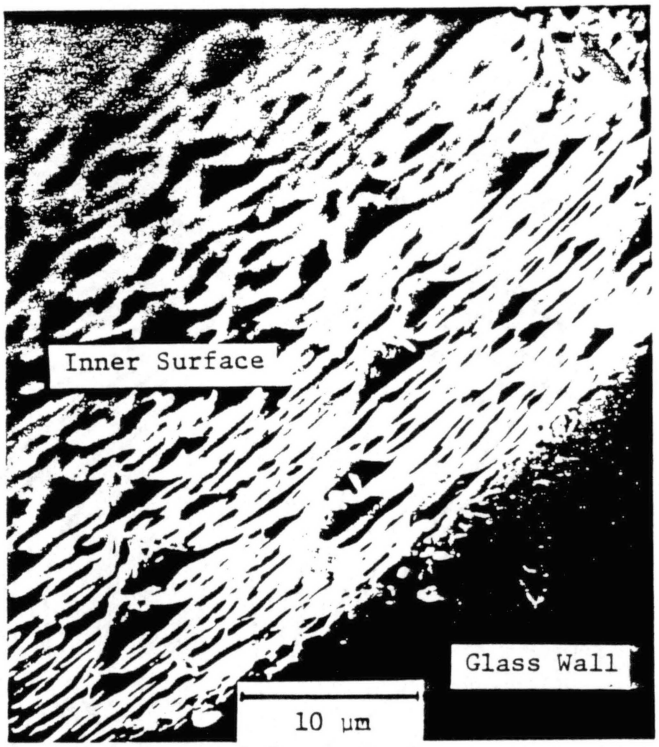

a. Edge View of Inner Surface and Fractured Glass Wall. Magnification X2400.

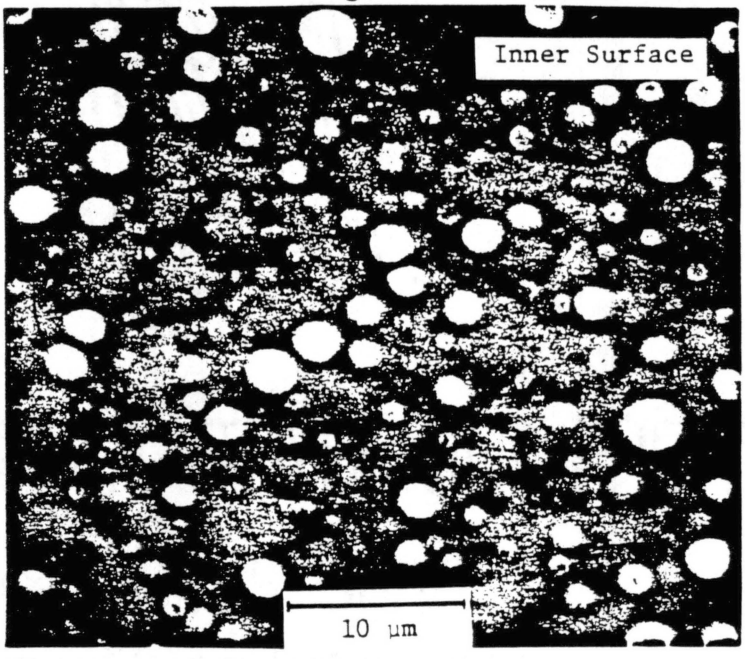

b. Inner Surface Viewed From Above. Magnification X2400.

Figure 13. Scanning Electron Micrograph of Column 1 After Styrene-Divinylbenzene Polymerization

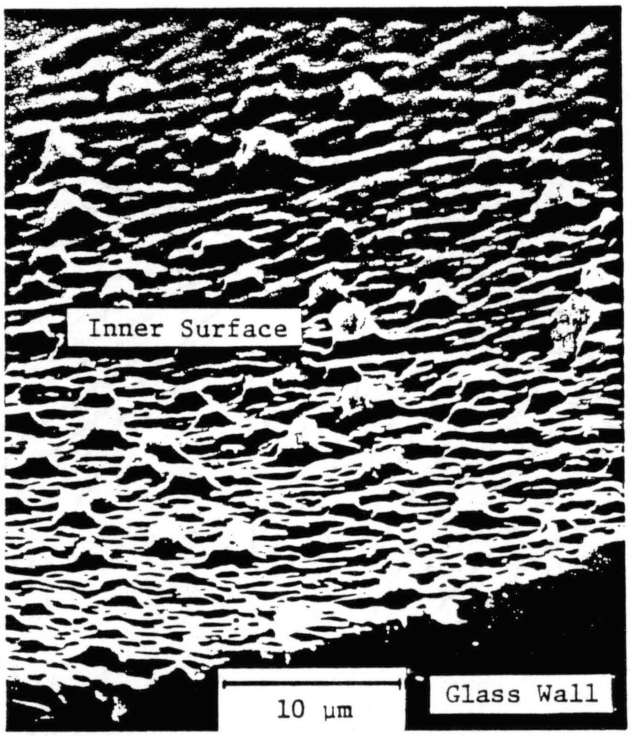

a. Edge View of Inner Surface and Fractured Glass Wall. Magnification X2400.

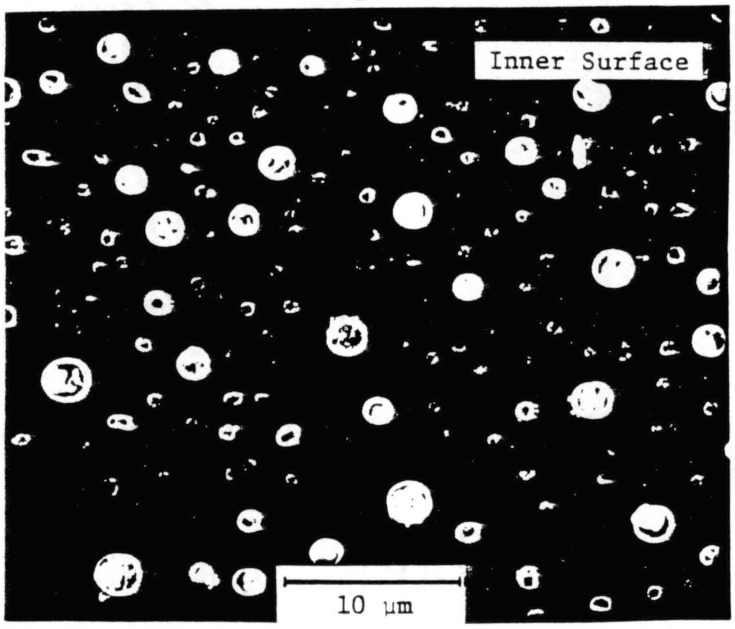

b. Inner Surface Viewed From Above. Magnifiaation X2400.

Figure 14. Scanning Electron Micrograph of Column 1 After Methylene Chloride Rinse

it cleans the glass surface of small particles. The effect of the NH_4FHF treatment is seen in Figure 11 and 12. Instead of the expected silica whiskers with heights of 8 to 10 μm as reported by Onuska (26), short stubs of about 2 μm were obtained.

Column 2 was evaluated by SEM to observe NH_4FHF roughening effects and polymer film thicknesses and by gas chromatography to determine the phase transition temperature and column efficiency. Scanning electron micrographs were taken of capillary sections after the NH_4FHF treatment and also after the polymerization. Figure 15 shows that silica whisker growth can vary within the same section of capillary. Non-uniformity of the NH_4FHF which was coated inside the capillary and of the temperature within the furnace used to heat the capillary can cause this variation. Figure 16 shows silica whiskers which are 3.5 μm in height at a magnification of ×5000. SEM of the glass wall and polymer interface allowed the determination of the film thickness and also shows evidence of film stability. The calculated film thickness for Figures 17 and 18 ranged from 4.2 to 4.4 μm. Figure 19 shows whiskers protruding slightly into the polymer surface. Scanning electron micrographs in Figures 20 and 21 show the polymer and glass interface before and after the capillary was washed with 20 ml of methylene chloride over 3 1/2 hours. The micrographs in Figures 20 and 21 were taken of the same end of the column. The film thicknesses measured from the micrographs are 1.9 ± 0.1 μm (n=5) before washing and 1.7 ± 0.1 μm (n=5) after washing. Though the difference in the film thicknesses may not be considered significant, a 0.014 g weight loss in the 8.4 m capillary showed that some of the stationary phase was lost. The difference in film thickness measurements, $\sim$ 4 μm for Figures 17 and 18 and $\sim$ 2 μm for Figure 20 was due to a

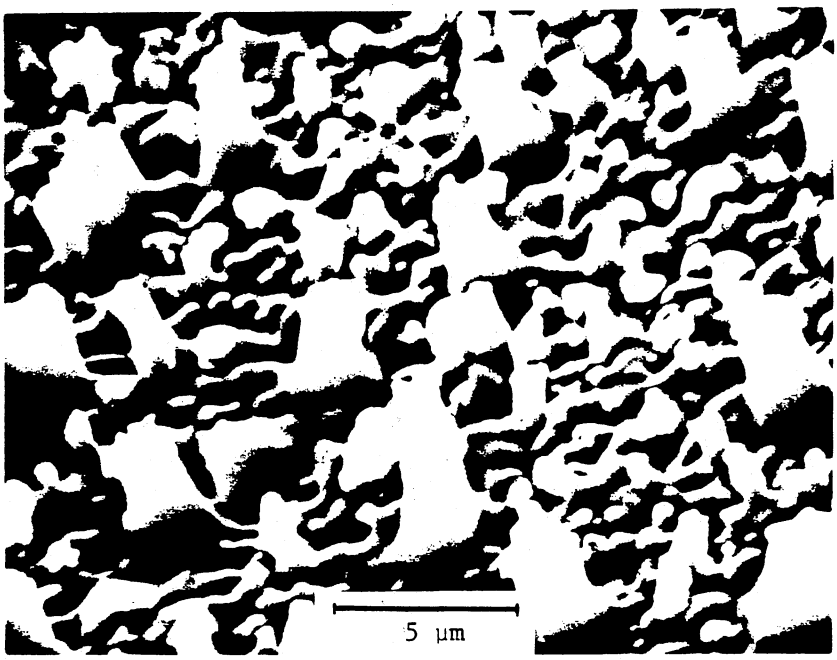

Inner Surface of Pyrex Capillary Tube. Side View Magnification X2500.

Figure 15. Scanning Electron Micrograph of Column 2 After NH_4FHF Treatment

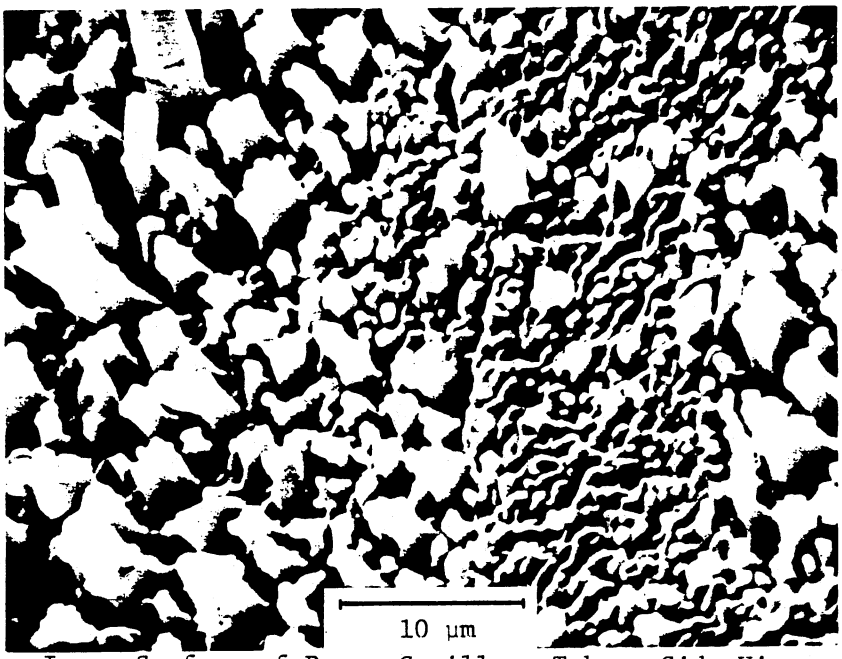

Inner Surface of Pyrex Capillary Tube. Side View.
Magnification X5000.

Figure 16. Scanning Electron Micrograph of Column 2 After NH_4FHF Treatment

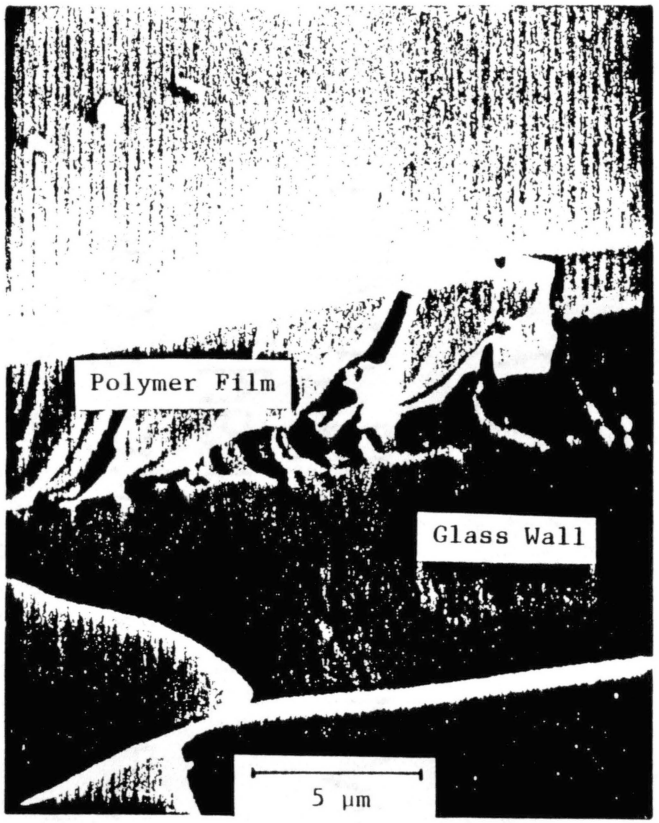

Edge View of Polymer-Glass Interface.
Magnification X4600.

Figure 17. Scanning Electron Micrograph of Column 2 After Styrene-Divinylbenzene Polymerization

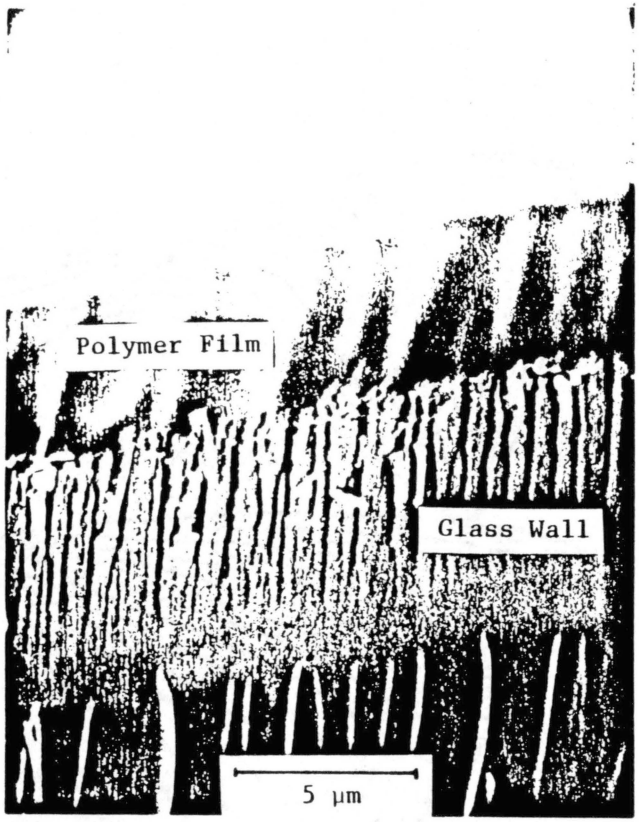

Edge View of Polymer-Glass Interface.
Magnification X5000.

Figure 18. Scanning Electron Micrograph of Column 2 After Styrene-Divinylbenzene Polymerization

Inner Surface of Polymer-Glass Interface.
Magnification X1000.

Figure 19. Scanning Electron Micrograph of Column 2 After Styrene-Divinylbenzene Polymerization

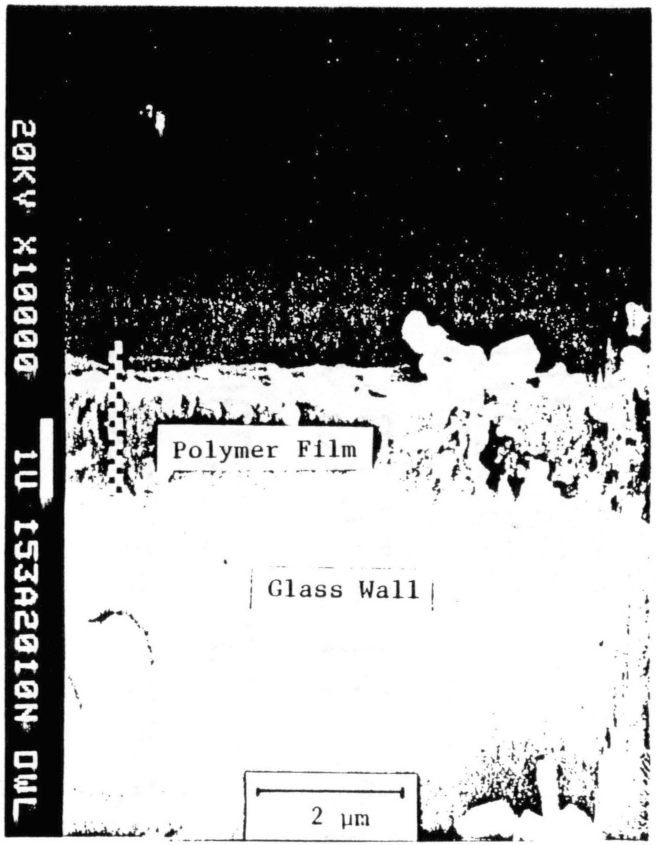

Edge View of Polymer-Glass Interface.
Magnification X10000.

Figure 20. Scanning Electron Micrograph of Column 2 Before Methylene Chloride Rinse.

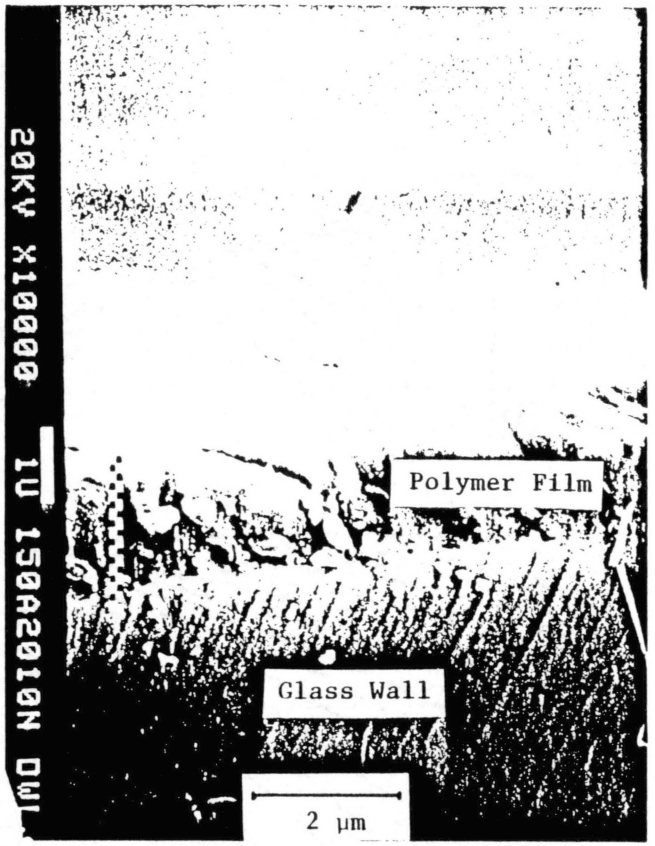

Edge View of Polymer-Glass Interface.
Magnification X10000.

Figure 21. Scanning Electron Micrograph of Column 2 After Methylene Chloride Rinse.

thicker film of polymer on one end of the capillary compared to the other.

The greater stability of the polystyrene-divinylbenzene film in Column 2 can be attributed to the increased silica whisker height and the lower initiator to monomer ratio. From the monomer solution compositions, 5% v/v styrene, 0.8% v/v divinylbenzene and 0.8% w/v AIBN for Column 1 and 48% v/v styrene, 1% v/v divinylbenzene and 0.09% w/v AIBN for Column 2, the crosslink percentage of 14% for Column 1 and 2% for Column 2 can be determined. This indicates that both films would be insoluble in the methylene chloride rinse. However, because the initiator to monomer ratio for Column 2, 1/544, is lower than for Column 1, 1/7, the polymer in Column 1 would have much shorter chain lengths and would be more soluble in the solvent used for the column rinse.

Chromatographic evaluation of Column 2 included the determination of the phase transition of the polymer from the partition ratio (k') of methylene chloride at temperatures that ranged from 50°C to 170°C. The discontinuity between the two linear portions of Figure 22 corresponds to the second order glass phase transition of polystyrene. The temperature of this transition, 93°C, was determined at the point where the first deviation from linearity (as temperature increased) occurred (133).

The HETP plot in Figure 23 shows that a minimum theoretical plate height for methylene chloride of 1.9 cm occurs at an optimum linear velocity of about 5 to 8 cm/s. This corresponds to 568 theoretical plates or 28 effective plates. When compared to the calculated minimum theoretical plate height, 0.18 mm, for a capillary with the same inner diameter and solute partition ratio, a difference of two orders of magnitude between these plate heights results.

This poor efficiency is due to the thick film of polystyrene which

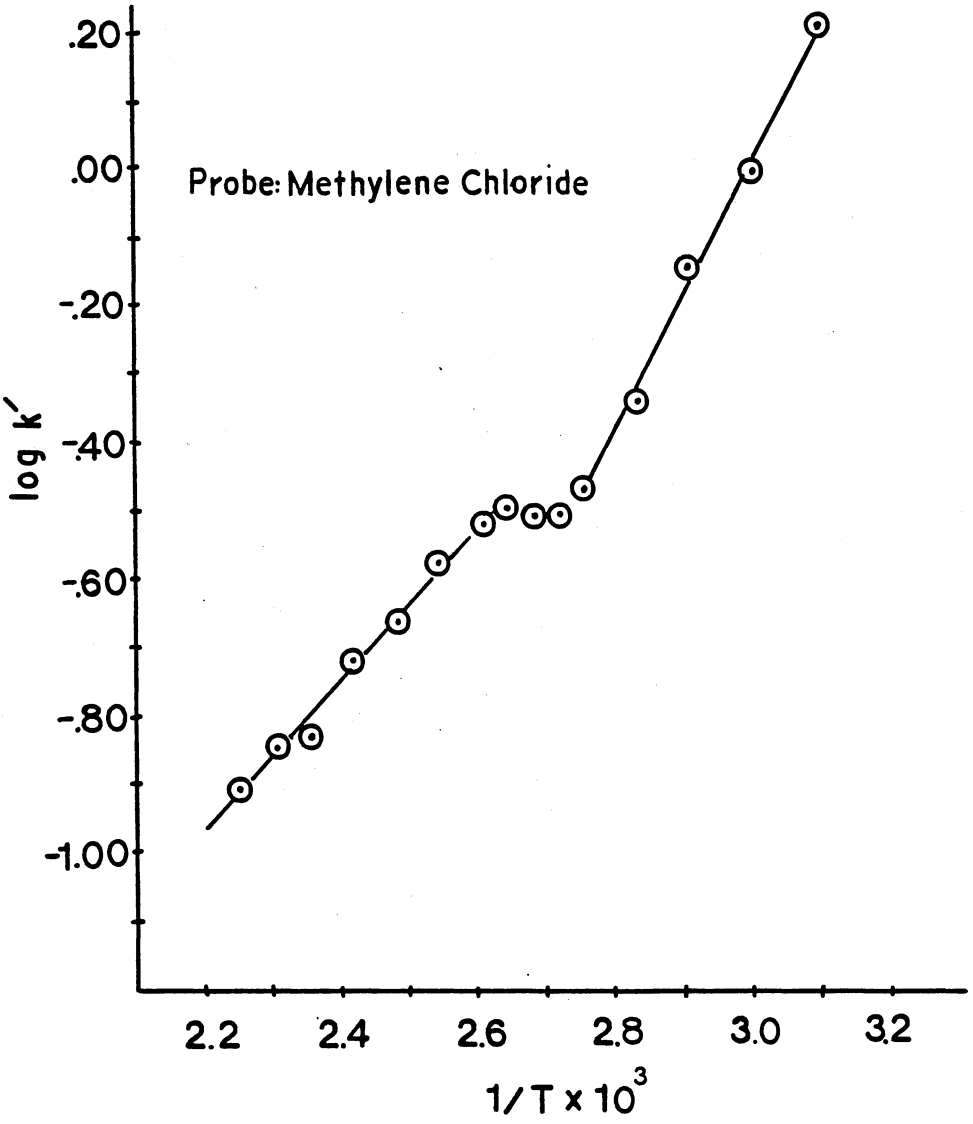

Column length: 10.8 m; I. D.: 0.41 mm
Sample size: 0.1 µm
Split ratio: 1/150
Initial linear velocity (50°C): 20.0 cm/s

Figure 22. Relationship of log k' and 1/T for Polystyrene-divinylbenzene Capillary (Column 2)

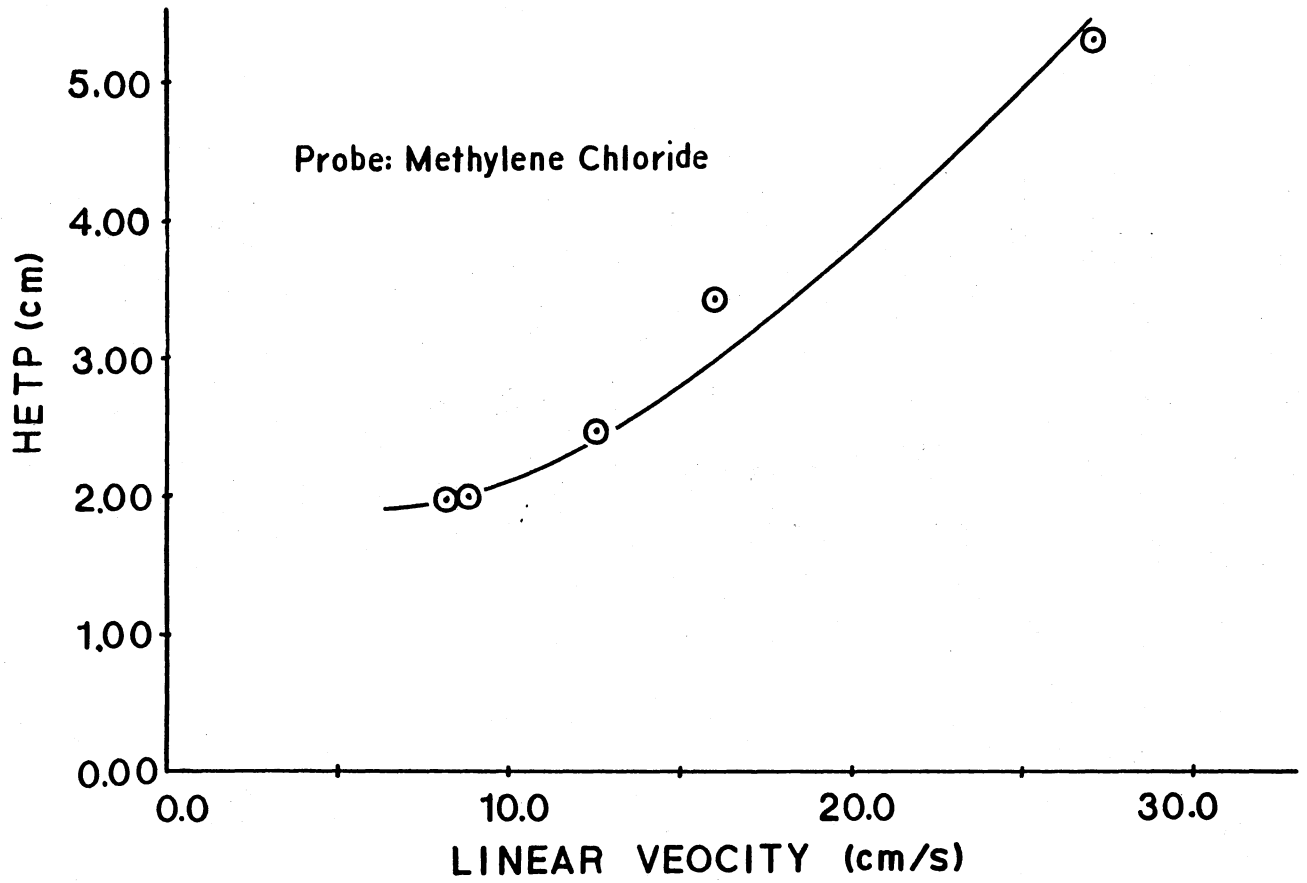

Column length: 10.8 m I. D.: 0.41 mm Probe: Methylene Chloride (k' = 0.29)
Sample size: 0.1 µm Split ratio: 1/150 Column temperature: 120°C

Figure 23. Relationship of HETP and Linear Velocity for Polystyrene-divinylbenzene Capillary (Column 2)

causes excessive band broadening due to resistance to mass transfer in the stationary phase. The poor correlation between measured and calculated minimum plate heights occurs because Equation 41 assumes that this band broadening is negligible.

Column 3: In Situ Polymerization of Vinylbenzo-15-crown-5

Chromatographic characterization of Column 3 included alcohol and alkane chromatograms, an HETP plot of n-C_{32} and determination of McReynolds' constants. Figure 24 (a, b and c) shows chromatograms of a 0.2% v/v mixture of n-pentanol, n-hexanol n-heptanol and n-octanol in n-pentane. Improvements in this alcohol separation will be seen later for a statically coated PVB15C5 column which contains a thicker film. These effects are diminished when higher column temperatures are utilized to separate components which have higher boiling points. Figure 25 shows baseline separation of a mixture of six alkanes from n-C_{20} to n-C_{36} at a column temperature of 150°C. An HETP plot (Figure 26) for n-C_{32} gives a minimum theoretical plate height of 0.18 cm. This corresponds to a column efficiency of 9100 theoretical plates or 5100 effective plates. The % utilization of theoretical efficiency (%UTE) for this 0.30 mm I.D. column was 13%.

The McReynolds' constants, retention indices and partition ratios for the McReynolds' probes are given in Table VII. While the McReynolds' constants for column 3 are similar to those obtained for the statically coated PVB15C5 column (See Table XII), the partition ratios for the McReynolds' probes in column 3 are $\sim$14 times smaller than those calculated for the statically coated PVB15C5 column. This means that the film

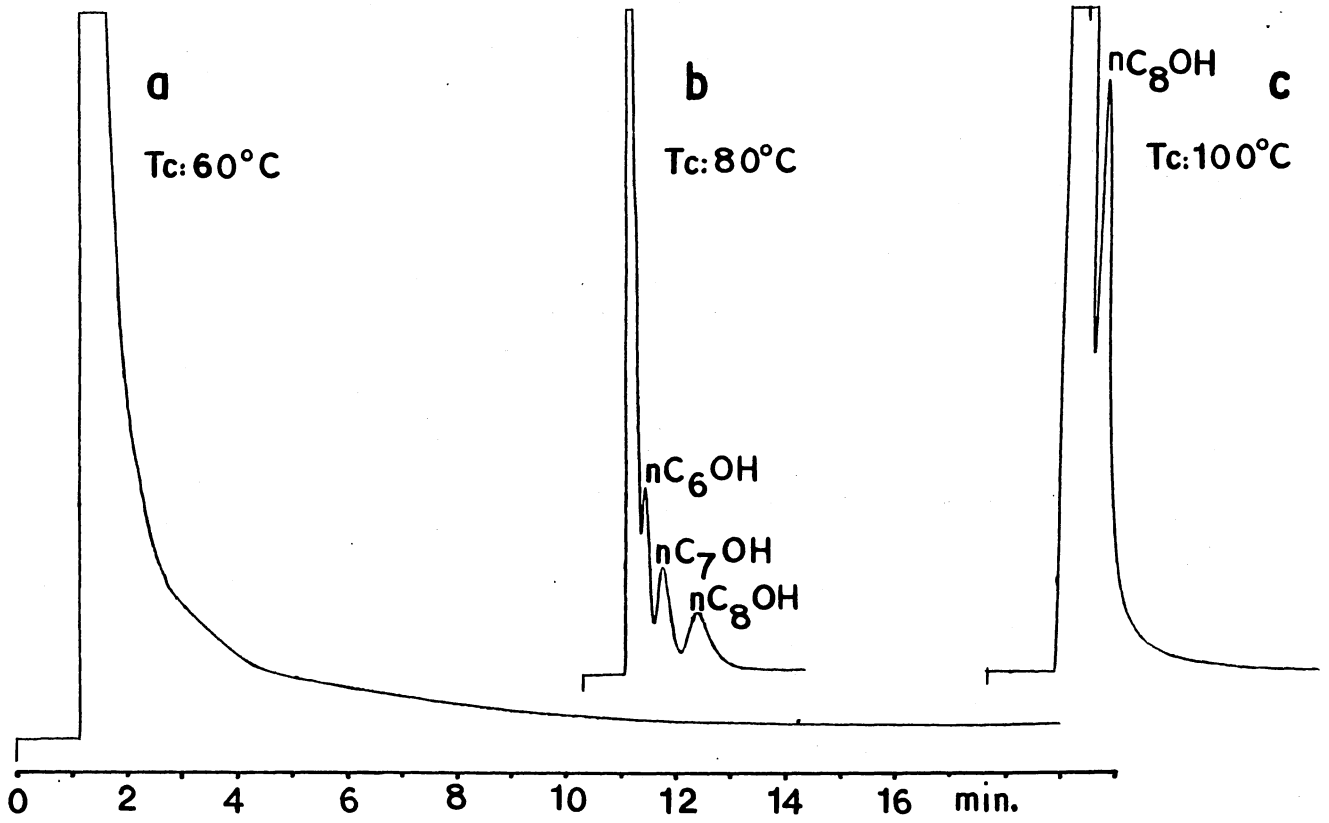

Column length: 16.4 m; I.D.: 0.30 mm; Sample: nC_1 to nC_8OH, 0.2% v/v in pentane

a) Attenuation: 2^1; Sample Size: 0.01 µl; Split ratio: 1/40; $\bar{v}$: 22.7 cm/s

b) Attenuation: 2^4; Sample size: 0.04 µl; Split ratio: 1/40; $\bar{v}$: 33.6 cm/s

c) Attenuation: 2^1; Sample size: 0.01 µl; Split ratio: 1/40; $\bar{v}$: 21.0 cm/s

Figure 24. Chromatograms of Alcohol Mixture on In Situ Polymerized VB15C5 Capillary (Column 3)

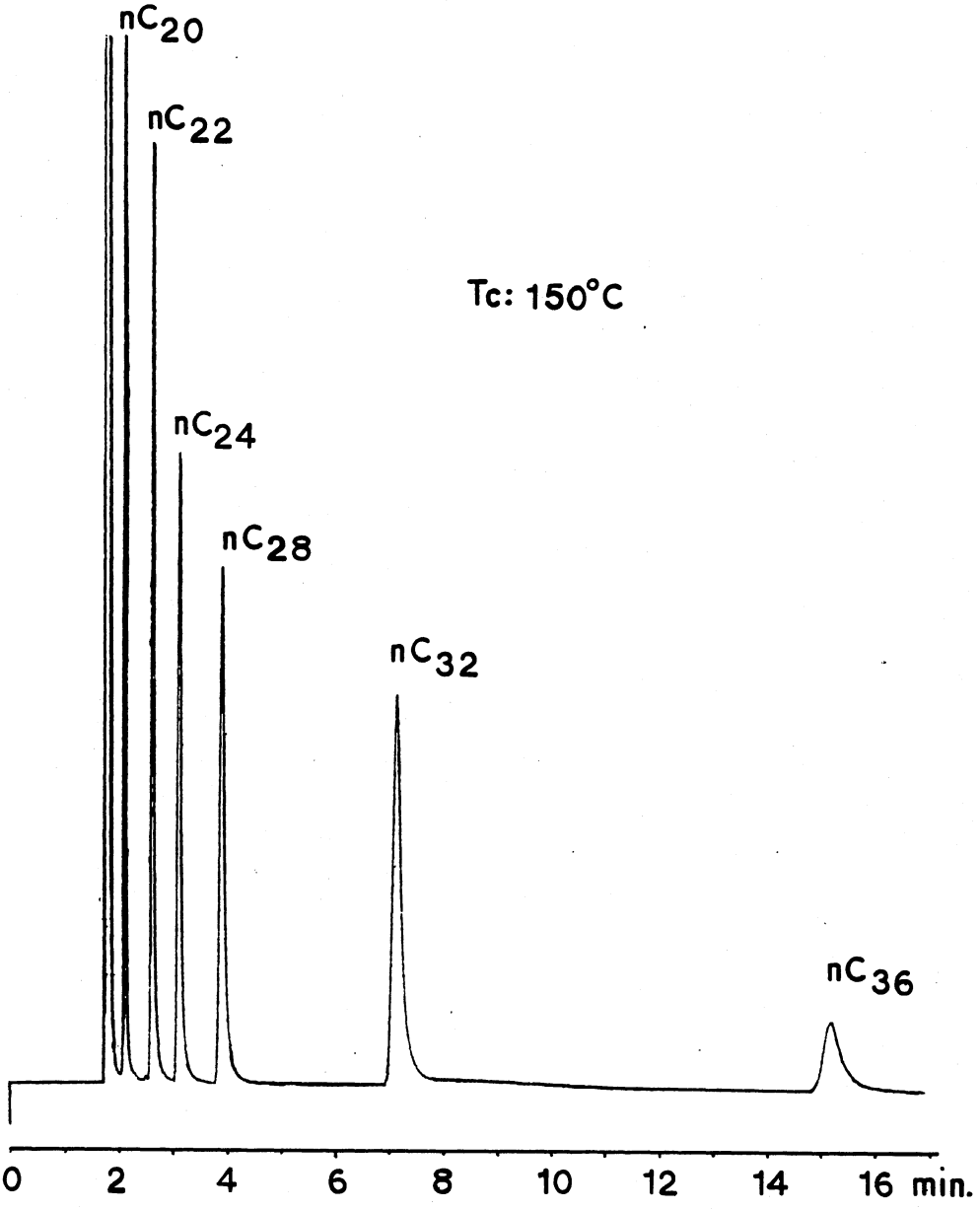

Alkane mixture: 0.2% v/v $nC_{20,22,24,28,32,36}$ in pentane
Attenuation: 2^1 Sample size: 0.4 µl
Split ratio: 1/26 $\bar{v}$: 20.2 cm/s

Figure 25. Chromatogram of Six Alkanes on In Situ Polymerized VB15C5 Capillary (Column 3)

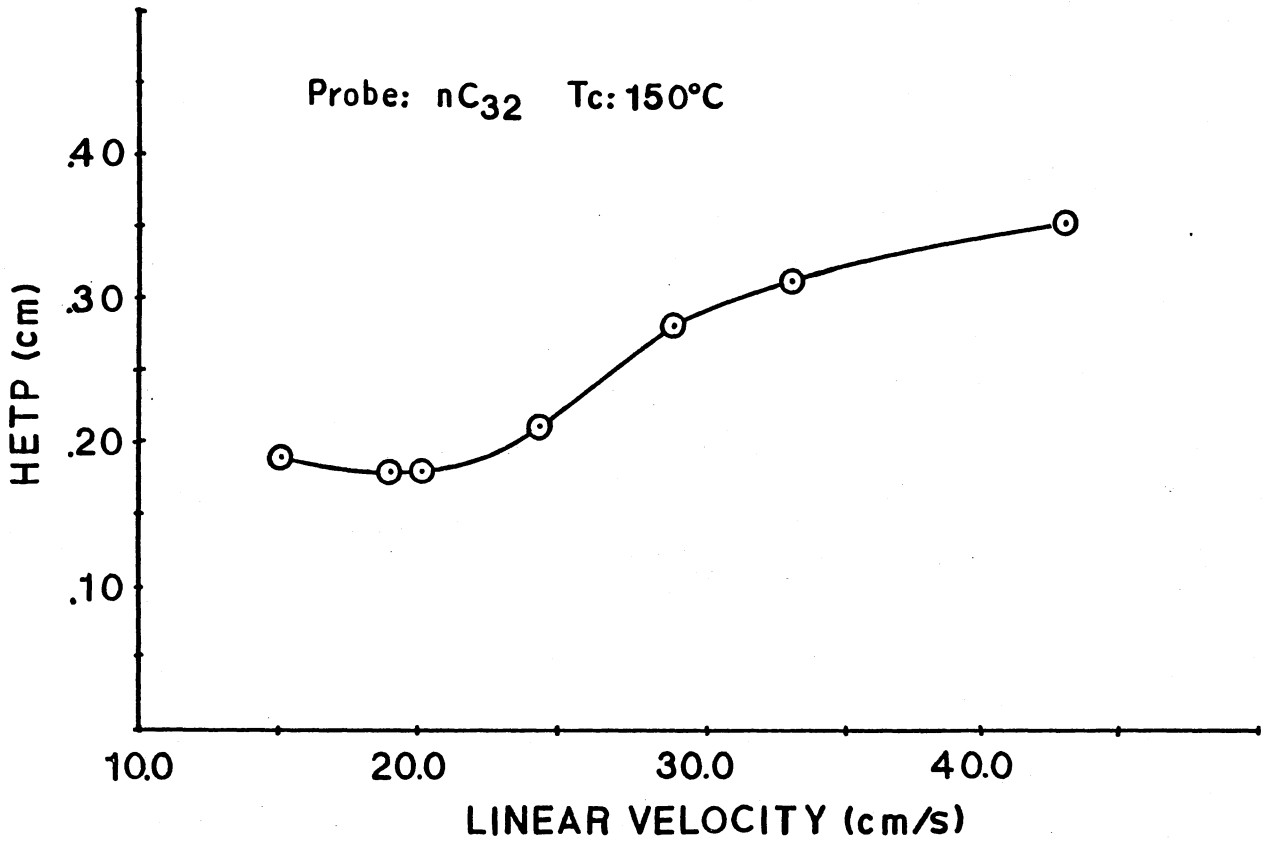

Sample size: 0.4 µl of 0.2% v/v nC_{32} in pentane

Split ratio: 1/26 Partition ratio of nC_{32}: 3.00

Figure 26. Relationship of HETP and Linear Velocity for In Situ Polymerized VB15C5 Capillary (Column 3)

thickness in column 3 is smaller than the 1 μm film thickness in column 8. From the average ratio of the partition ratios of these two columns, (k'_8/k'_3), the calculated film thickness of the PVB15C5 column (d_{f8}) and the inner radius of the two columns (r_{c8} and r_{c3}), an estimated film thickness of 0.08 μm can be calculated for column 3 using Equation 67.

$$d_{f3} = \frac{k'_3}{k'_8} \cdot \frac{r_{c3}\, d_{f8}}{r_{c8}} \tag{67}$$

TABLE VII

PARTITION RATIOS (k'), RETENTION INDICES (I), MCREYNOLDS' CONSTANTS (ΔI), AND AVERAGE POLARITY FOR COLUMN 3 AND RATIO OF PARTITION RATIOS FOR COLUMN 3 AND COLUMN 8

	Benzene	n-Butanol	2-Pentanone	Nitropropane	Pyridine	Average
ΔI	287	499	379	558	523	449
I	940	1089	1006	1210	1222	-
k'	0.014	0.035	0.021	0.068	0.073	-
$\frac{k'_8}{k'_3}$	16.1	12.2	12.5	14.1	12.6	13.5 ± 1.4

Columns 4: HCl Leached, 5: HCl Leached and MAPTMS Treated, and 6: In Situ Polymerization of Vinylmethylsila-17-crown-6

Initial column characterization was done by injecting a mixture of fourteen alcohols onto each column. (See the legend of Figure 28 for the alcohols and column conditions.) Comparison of the alcohol chromatograms obtained from the HCl leached and the HCl leached and MAPTMS silanized columns (Figure 27 (a) and (b)) with the chromatogram from the vinylmethylsila-17-crown-6 column (Figure 28) shows that it is the silacrown ether that allows the separation of the alcohols. The severe adsorption which results after the HCl leach and MAPTMS silanization is reduced after the silacrown ether treatment. Besides increasing the efficiency and column capacity, the silacrown ether may also deactivate the surface silanols left on the capillary wall after the MAPTMS treatment. Collaring of the silanol by the crown ether ring could prevent polar solutes from interacting with the surface silanol and thereby reduce tailing.

Evaluation of the VMSi17C6 column included determination of the effect of sample size on the partition ratio for 1-octanol at an oven temperature of 60°C. The first attempt at this evaluation gave very poor reproducibility in peak areas for each sample size. Relative standard deviations in peak area were decreased from ∿10% to ∿2% by changing solvent from methanol to pentane, improving the injection technique and repacking the injection port with silanized glass wool.

Figure 29 shows that as the sample size increased, a slight decrease in partition ratio occurred. This decrease in k' can be attributed to

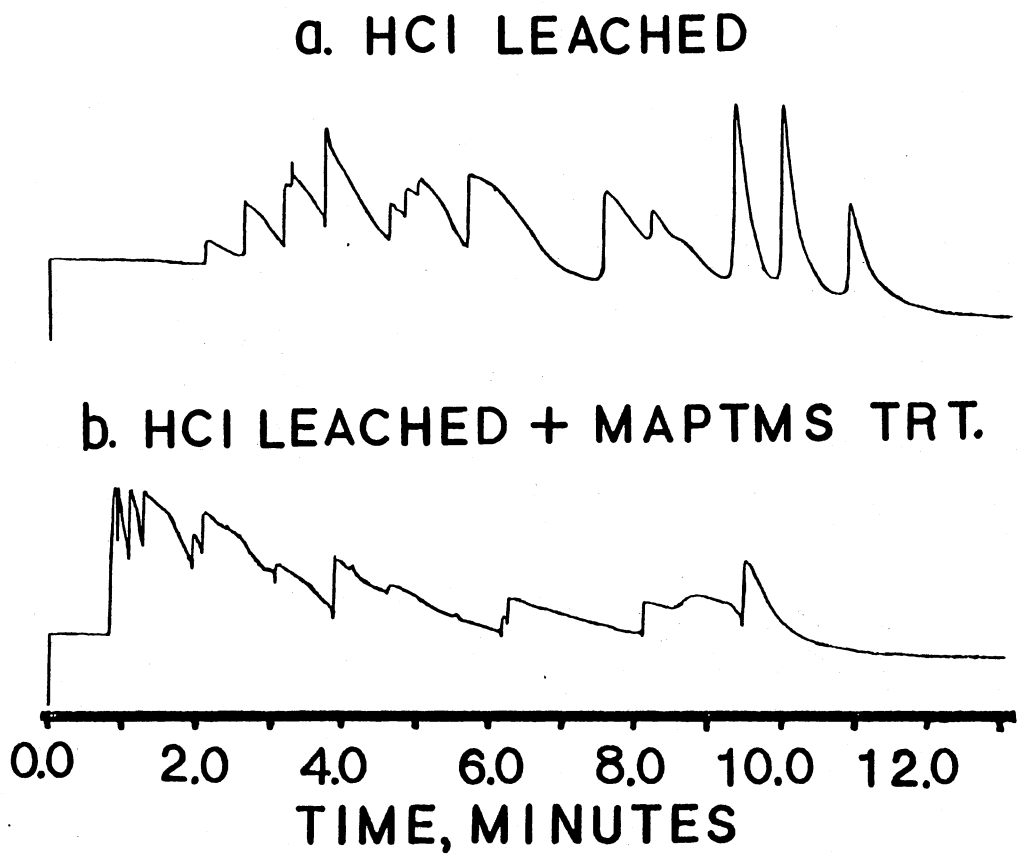

For temperature program and components of alcohol mixture see Figure 28.

Figure 27. Chromatogram of an Alcohol Mixture on HCl Leached Capillary (Column 4) and HCl Leached and MAPTMS Treated Capillary (Column 5)

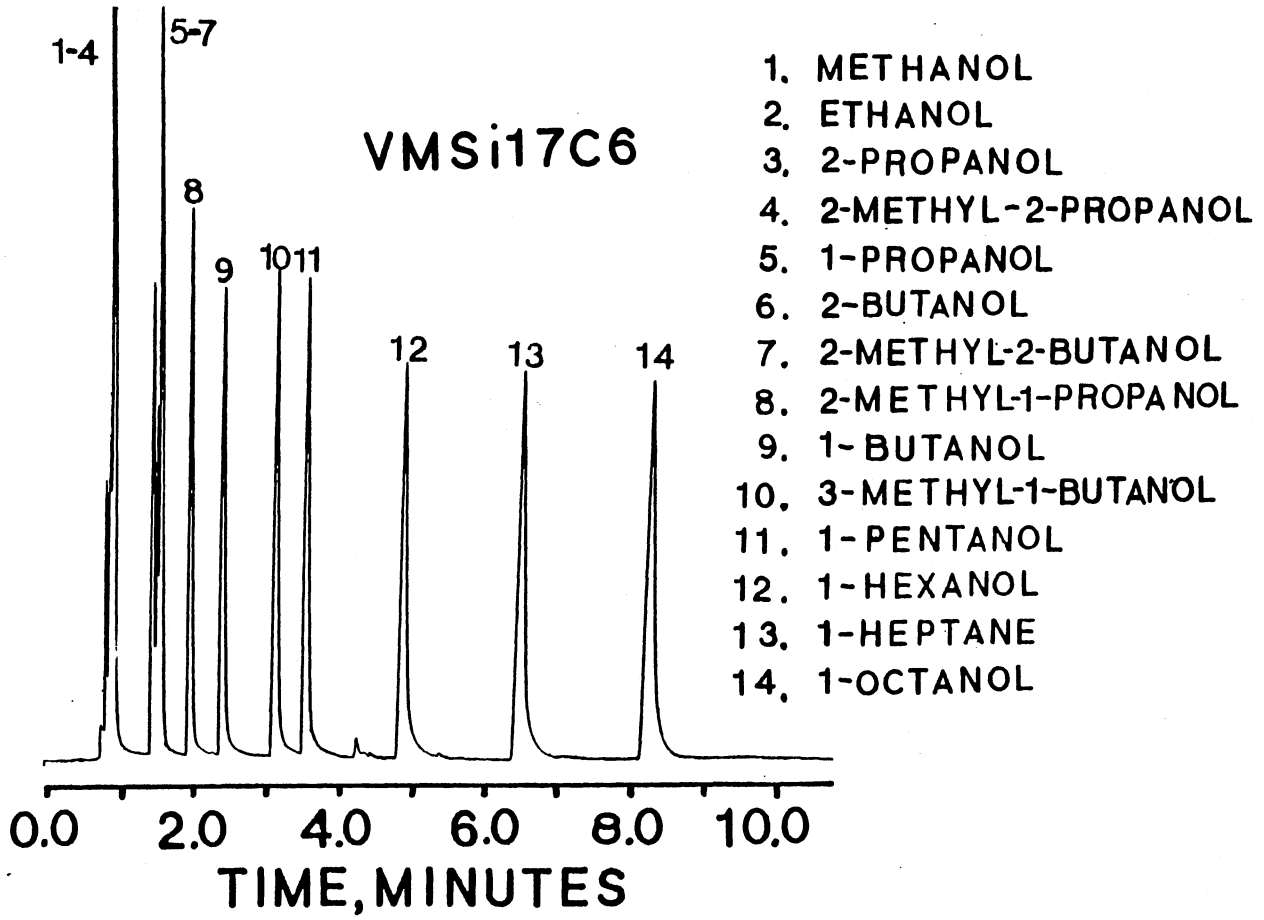

Volume injected: 0.1 µl of 7.1% v/v alcohol mixture Attenuation: 2^6
$\bar{v}(60^{\circ}C)$: 38.4 cm/s Split ratio: 1/31 Temperature program: -10°C for 3 min then 10°C/min to 30°C, 5°C/min to 65°C, 30°C/min to 100°C for 10 min

Figure 28. Chromatogram of an Alcohol Mixture on VMSi17C6 Capillary (Column 6)

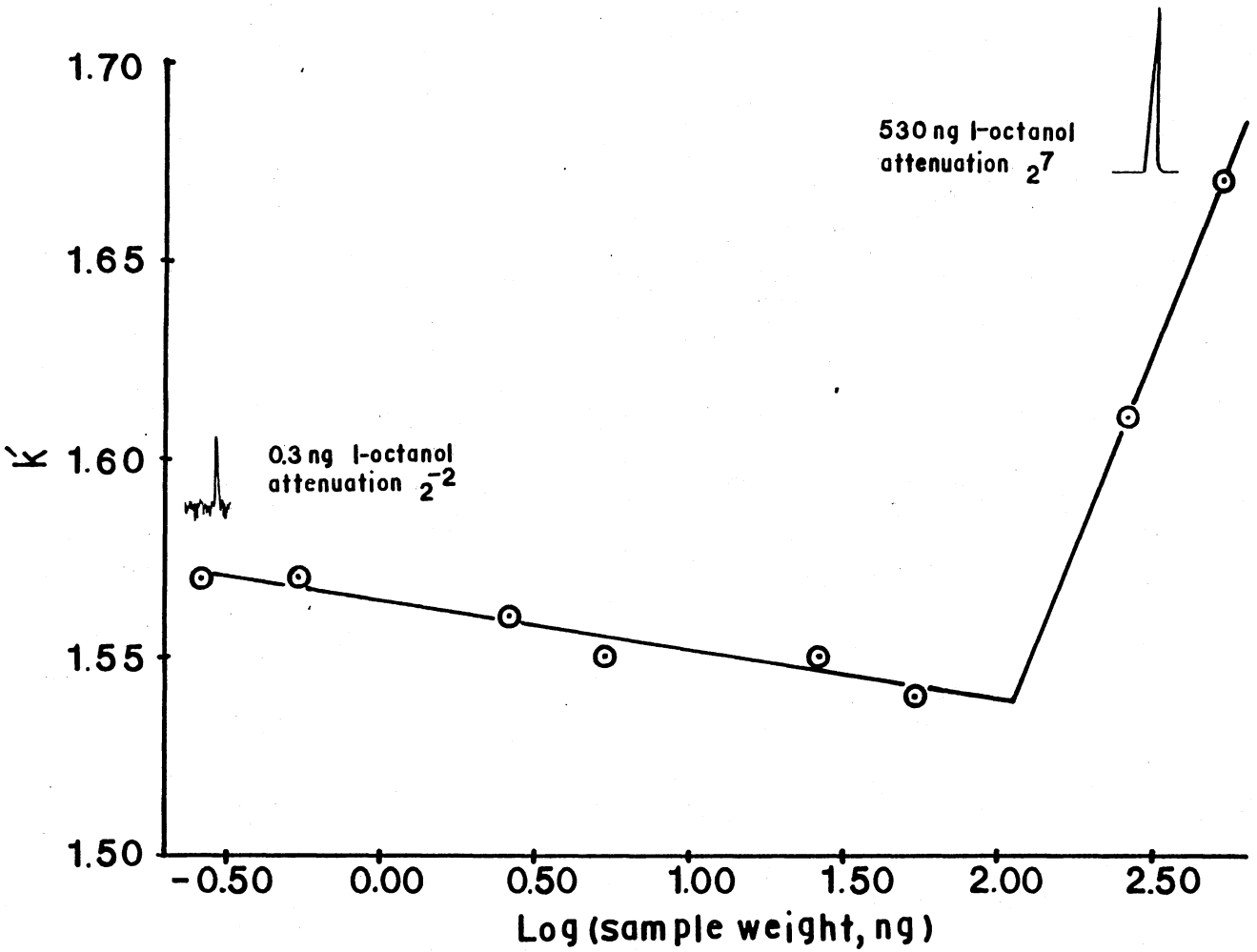

Figure 29. Relationship of k' and log of Sample Weight of 1-Octanol for VMSi17C6 Capillary (Column 6)

loss of stationary phase during the period of the experiment. This apparent dependence occurs because the sample size was increased as the experiment progressed. Figure 30 shows that the partition ratio of 1-octanol determined over a period of ten days decreased from one day to the next and that the change in k' was independent of sample size when the sample weight was below 5 ng. (During this period, the column temperature was not taken above 100°C.) Figure 29 also shows that when the amount of 1-octanol injected on the column exceeded 50 ng, the partition ratio started to increase. The peak shape of 1-octanol above this sample size exhibited fronting which can be attributed to overload of the column. This column overload was also confirmed in Figure 31. Deviation from linearity in each of these plots started at approximately 50 ng of 1-octanol. The linearity of the plot of log(area) versus log(weight), Figure 31, shows that over the sample size range of 0.4 to 500 ng irreversible adsorption of 1-octanol does not occur. If this type of adsorption occurred the peak area would decrease at lower sample sizes. Such adsorption might be occuring at sample sizes less than 0.4 ng.

Comparison of the plots in Figure 31 shows that the two slopes are approximately equal for sample weights below 50 ng. This implies that the area of each peak is proportional to the peak height or that the width of each peak is constant. The relation between these two plots can then be expressed as

$$\log(\text{area}) = \log(\text{height}) + \log(\text{width at half height}). \qquad (68)$$

The efficiency of column 6 was determined by constructing van Deemter plots for n-dodecane, n-undecane and n-decane. Figure 32 shows the plot of HETP versus linear velocity for these alkanes at a column temperature

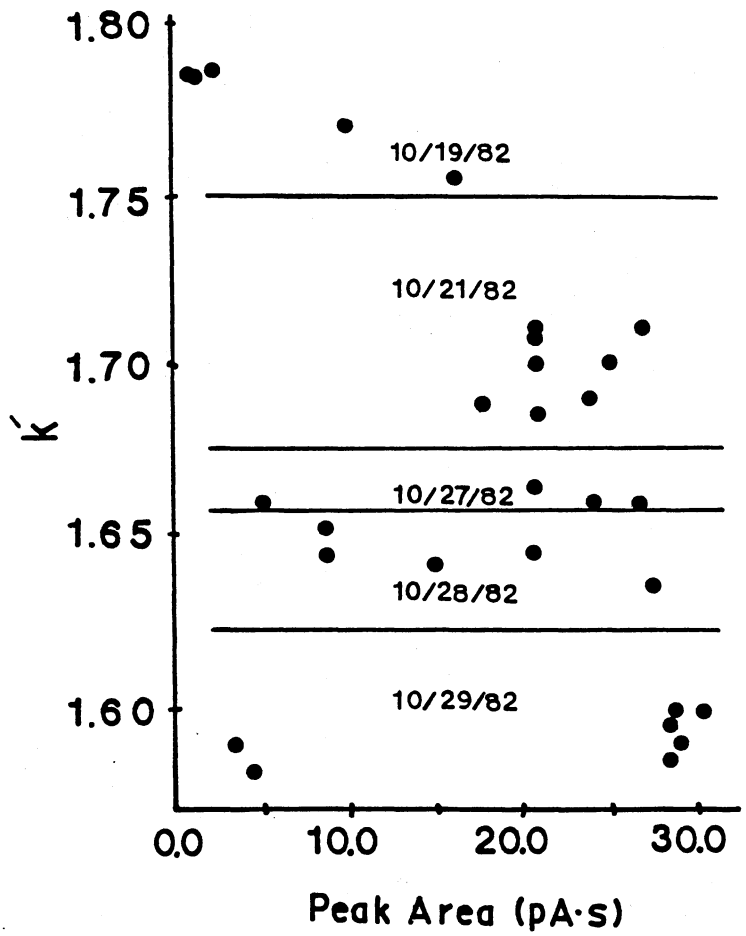

Figure 30. Relationship of k' and Peak Area of 1-Octanol for VMSi17C6 Capillary (Column 6) with Date of Observation Indicated

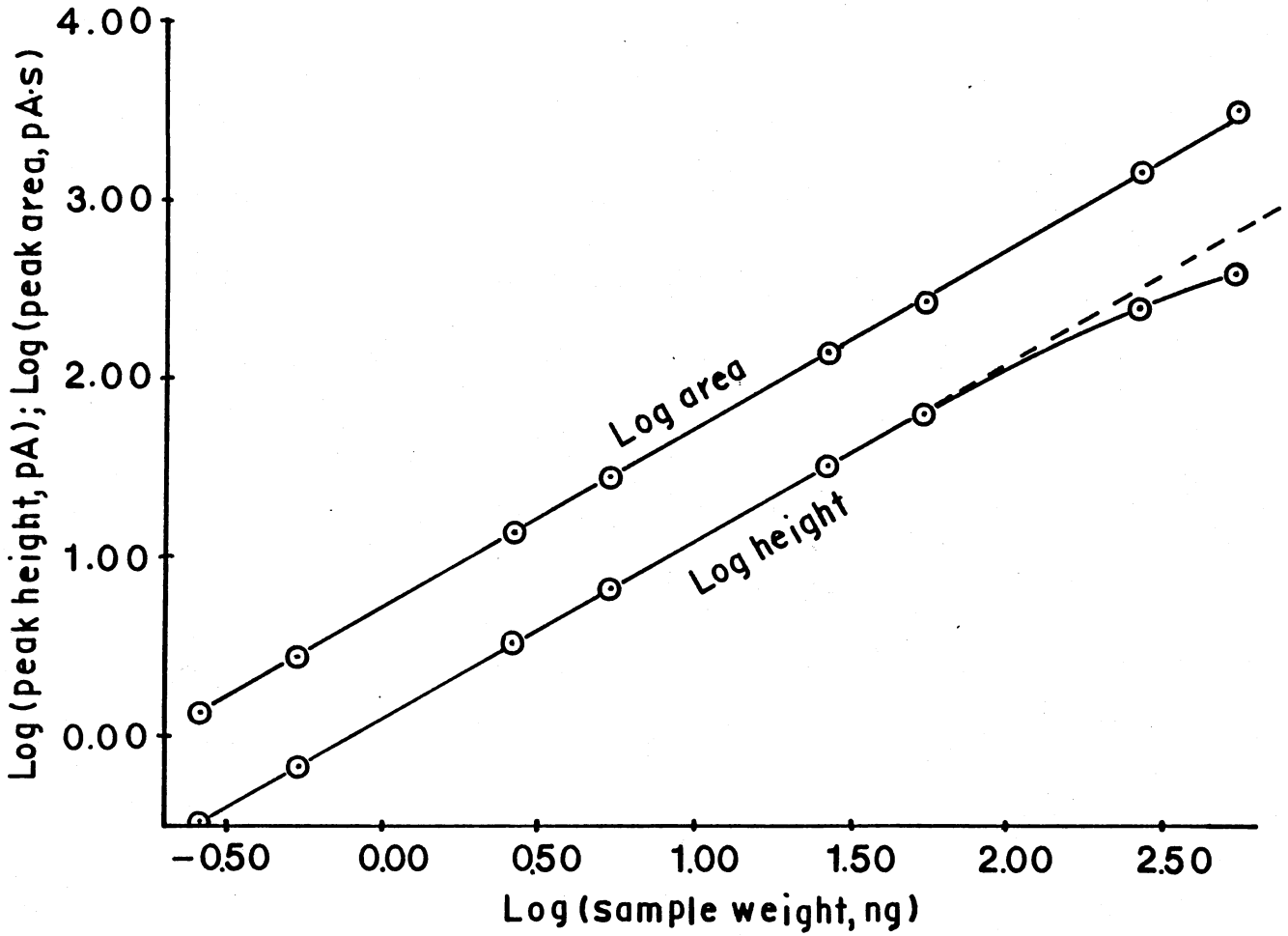

Figure 31. Relationship of log of Peak Height or Peak Area and log of Sample Weight of 1-Octanol for VMS117C6 Capillary (Column 6)

Column length: 18 m I. D.: 0.42 mm T_C: 35°C
Volume injected: 0.9 µl of 0.2% v/v $nC_{7,8,9,10,11,12}$ in pentane
Attenuation: 2^3 Split ratio: 1/48

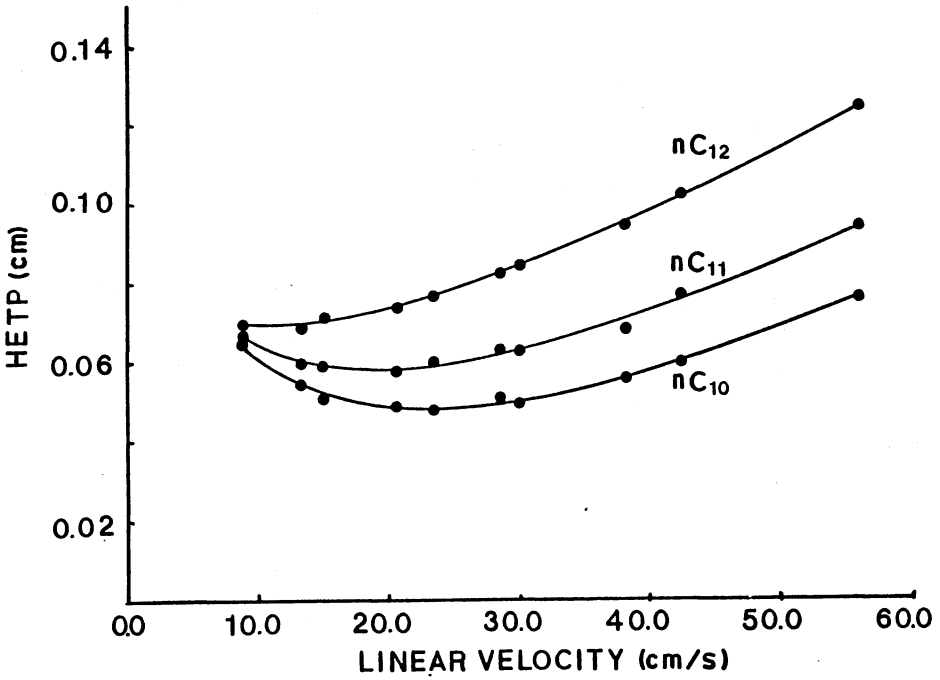

Figure 32. Relationship of HETP and Linear Velocity for n-Decane, n-Undecane and n-Dodecane on VMSi17C6 Capillary (Column 6)

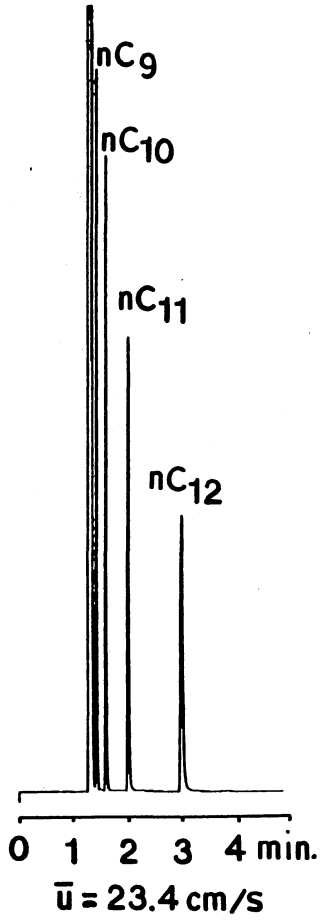

Figure 33. Chromatogram of Four Alkanes on VMSi17C6 Capillary (Column 6)

of 35°C. The minimum HETP value for decane, 0.48 mm, occurred at an optimum linear velocity of 23.4 cm/s. Figure 33 shows the separation of these alkanes at this optimum linear velocity. The %UTE for n-decane, 36%, was considerably better than for the styrene columns. Figure 34 shows the plots of the theoretical and effective plate numbers versus the partition ratio for the three alkanes. These plate numbers were calculated at the optimum linear velocity for n-decane. As the carbon number in each alkane increased, the number of plates (both theoretical and effective) converge to the value of the real plate number (84). This value, 15,700 plates, was calculated from Equation 20.

In order to further characterize the column, plots of log k' versus 1/T for n-dodecane, n-butylbenzene, n-amyl acetate, 1-pentanol, and 2-octanone were constructed. Figures 35a through 35e were obtained by determining partition ratios at column temperatures which decreased from 100°C to 10°C. The five log k' versus 1/T plots revealed that each probe interacts differently with the stationary phase as phase changes occur on the capillary surface. Instead of linear plots which change slope at the temperature which would be characteristic of a glass, melting or liquid transition of a thin film, the plots exhibit change with the functional group on each probe. Such behavior could be due to the presence of two transition temperatures in the polymer which are indicated according to the polarity of the probe or to differences in the solubility of each probe in the silacrown ether.

Additional evaluation of the VMSi17C6 column including the McReynolds' constants, column bleed and column efficiency will be considered later in the section which compares the three different crown ether columns.

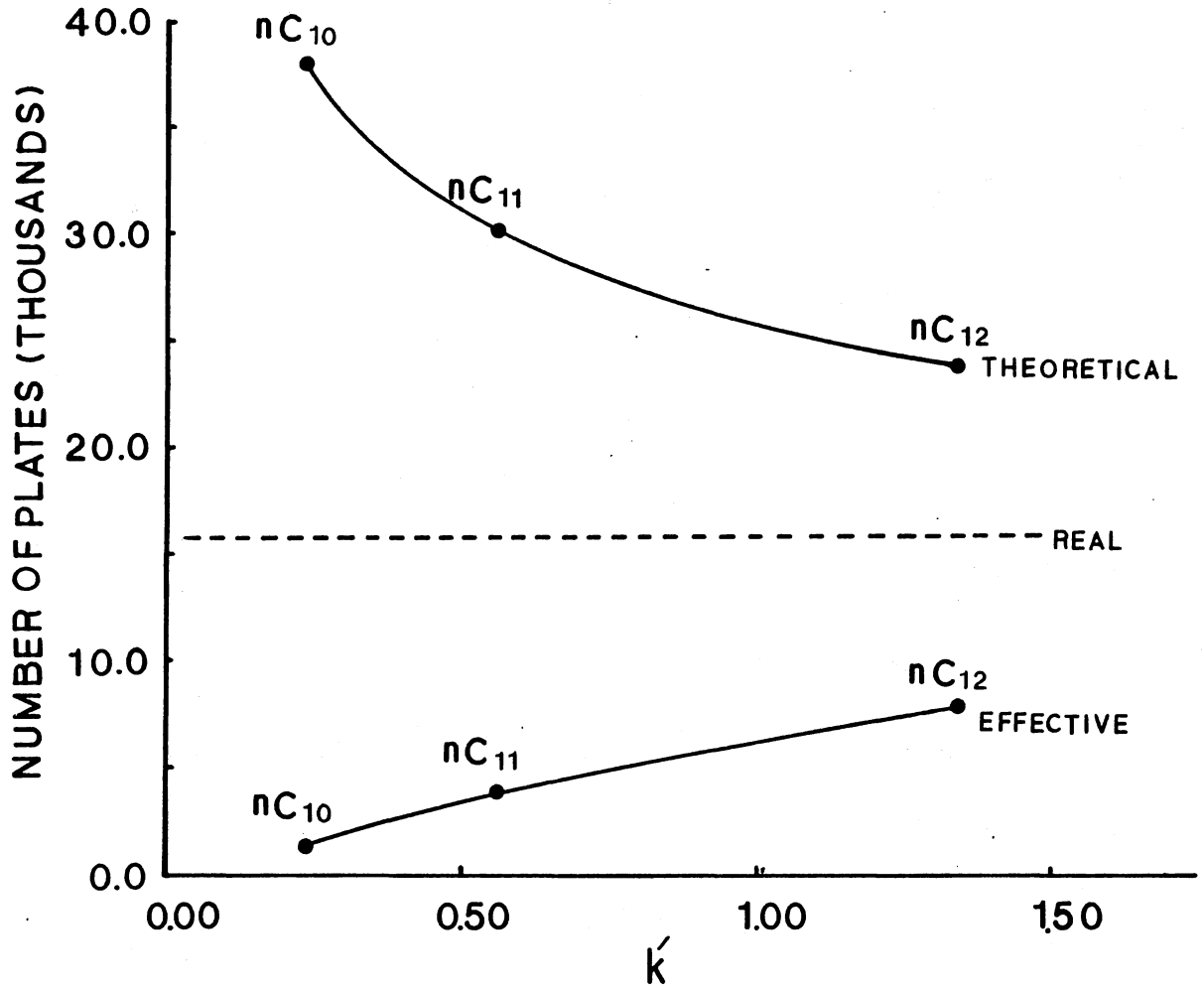

Figure 34. Relationship of n, N, and n_{real} Plates and k' for n-Decane, n-Undecane and n-Dodecane on VMSi17C6 Capillary (Column 6)

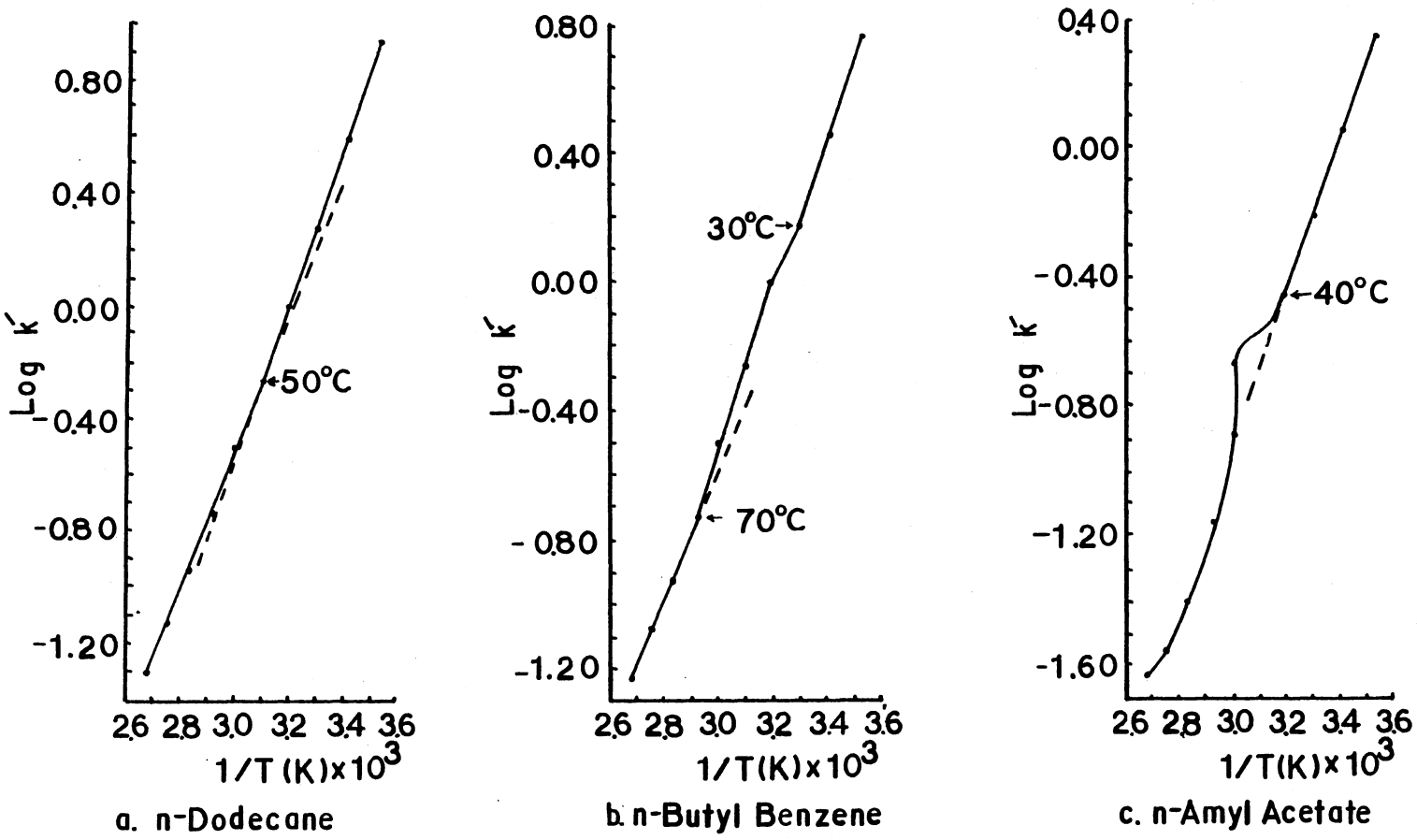

Figure 35. Relationship of log k' and 1/T for Several Probes on VMSi17C6 Capillary (Column 6)

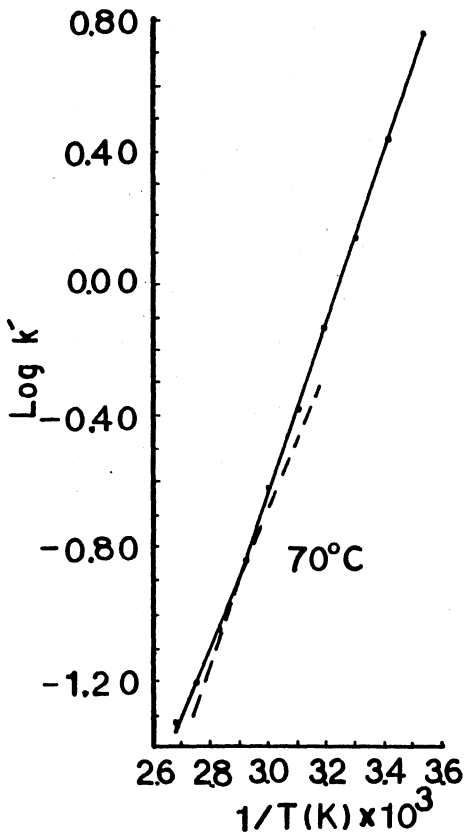

d. 1-Pentanol

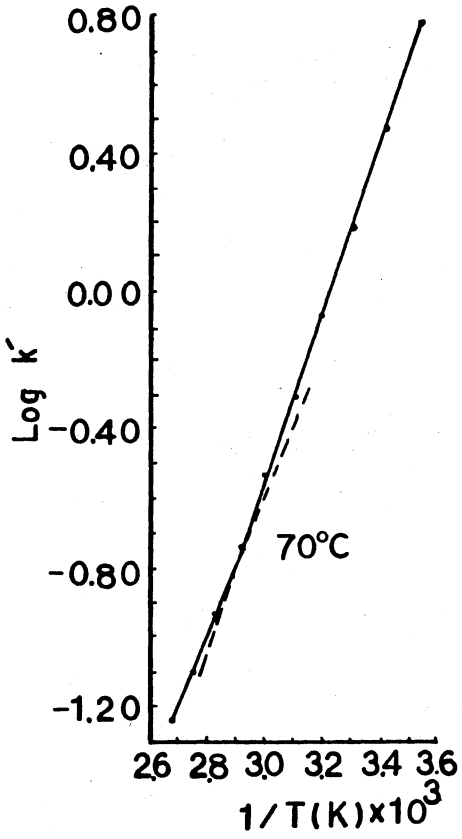

e. 2-Octanone

Figure 35. (Continued)

Column 7: In Situ Polymerization of Vinylmethylsila-14-crown-5

Column 7 was evaluated by following the changes in partition ratio, peak shape, effective plate number and slope of log k' versus 1/T plots before and after the column was rinsed with two solvents and conditioned three times at 160°C. Table VIII indicates when column evaluation was done and gives details about the column rinse and temperature conditionings.

Figure 36 shows the chromatogram of a mixture of fourteen alcohols which was obtained after the initial column conditioning. Comparison of this chromatogram with the one obtained from VMSi17C6, Figure 28, shows that the VMSi14C5 column causes more broadening of the early eluting alcohols. As the retention of the alcohols increased the difference in broadening decreased until the last peak in each chromatogram had comparable peak shape. Several factors concerning these two columns make it difficult to determine the cause for this difference in band broadening. Since the carrier linear velocities for each column were different, 37.4 cm/s for Column 6 and 26.2 cm/s for Column 7, each alcohol experienced different temperature ranges in the multilevel temperature program. Also, the difference in phase transition temperatures, 40°C and 80°C for Column 7 (See Page 127) and 70°C for Column 6 (See Figure 35d), and column efficiency as will be seen later make rationalization of the band broadening even more difficult.

Table VIII shows how the partition ratios for n-dodecane, n-undecane, n-decane, n-butylbenzene and n-pentanol changed after each of the column treatments. Column conditions were maintained throughout each evaluation with an oven temperature of 60°C and the linear velocity varying slightly

TABLE VIII

PARTITION RATIOS FOR FIVE PROBES BEFORE AND AFTER EACH OF FOUR COLUMN TREATMENTS

Probe	Column Temperature: 60°C									
	After Initial Conditioning	Solvent Wash		First Condition		Second Condition		Third Condition		
		Before	After	Before	After	Before	After	Before	After	4 Days Later
Dodecane (C_{12})	2.00	2.45	2.57	2.13	2.98	2.38	3.69	2.98	4.13	3.16
Undecane (C_{11})	0.89	1.06	1.11	0.93	1.24	1.03	1.52	1.25	1.67	1.33
Decane (C_{10})	0.39	0.46	0.48	0.41	0.52	0.44	0.63	0.53	0.68	0.56
n-Butyl Benzene	1.51	1.67	1.69	1.57	1.78	1.67	2.05	1.92	2.22	2.06
n-Pentanol	0.64	0.65	0.67	0.64	0.67	0.65	0.69	0.67	0.70	0.69

Solvent Wash: 10 ml each of methanol and methylene chloride

First Condition: 60°C to 160°C at 5°C/min then isothermal at 160°C for 10 min

Second, Third Condition: Temperature program (~30°C/min) up to 160°C; isothermal at 160°C for 1 hr

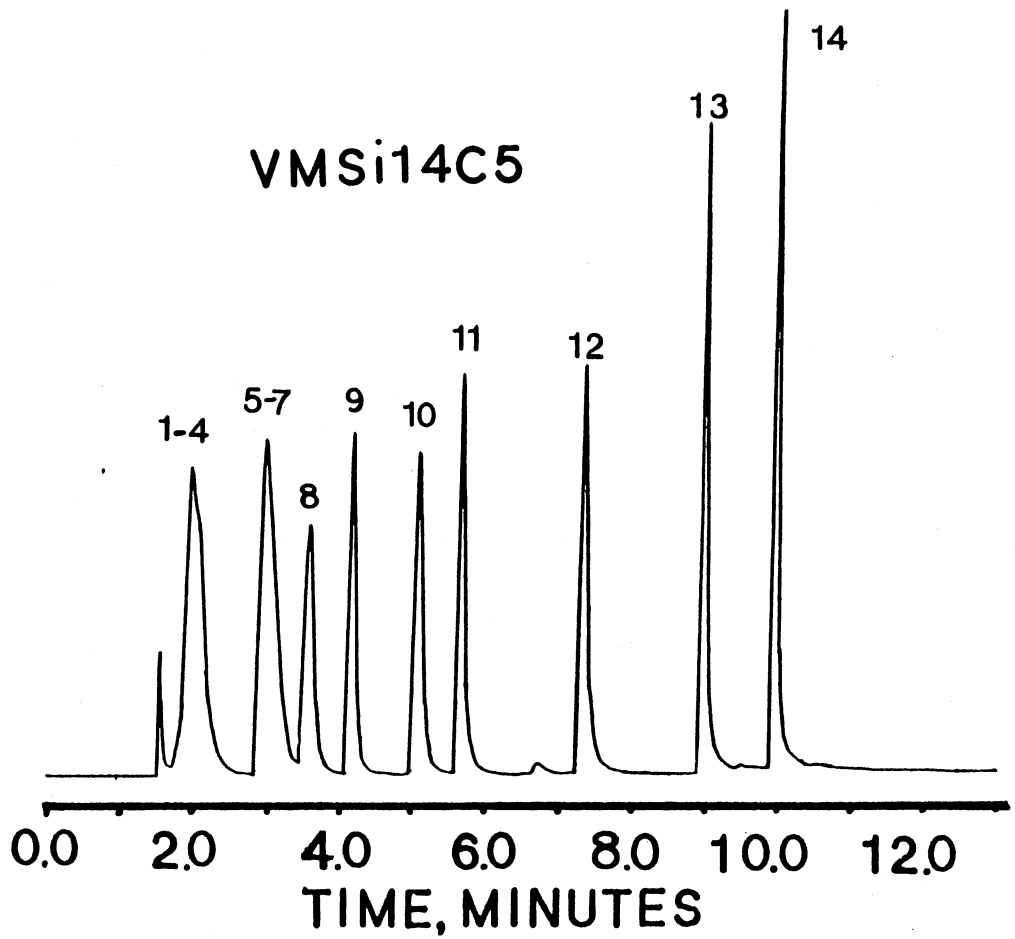

Column length: 16 m I. D.: 0.40 mm Volume injected: 0.10 µl Split ratio: 1/57
Attenuation: 2^6 (For temperature program and alcohol mixture see Figure 28.)

Figure 36: Chromatogram of an Alcohol Mixture on VMSi14C5 Capillary (Column 7)

from 28.5 to 30.0 cm/s. The partition ratios show the same pattern of change for each probe with an increase after each treatment and a decrease upon reevaluation. It can also be seen that there is an overall increase above the original k' value. From the definition of k'

$$k' = K \frac{V_L}{V_M} \tag{69}$$

it appears that the solvent rinse and temperature conditionings have caused an increase in the stationary phase volume, V_L, and/or the partition coefficient. The partition coefficient would increase if a chemical change occurred in the stationary phase or if after some of the stationary phase was rinsed off the column, adsorption processes caused an increase in solute retention. An increase in the stationary phase volume could be due to swelling of the stationary phase after the solvent rinse. An additional increase in the stationary phase volume due to thermal expansion could occur at the high conditioning temperatures. If the return to the equilibrium volume at 60°C was slow, larger k' values would first be observed. Decreases in k' would then occur upon reevaluation. This physical behavior could also effect the chemical nature of the column by causing an increase in the partition coefficient. With increased stationary phase volume, more sites of the crown ether would be available for partitioning or adsorption.

Additional information regarding the increase in retention is provided from the log k' versus 1/T plots (Figures 37 through 41) for the probes: n-dodecane, amyl acetate, n-butylbenzene, n-pentanol and 2-octanone. These plots show the log k' versus 1/T response obtained before the solvent rinse and after the third conditioning. All the probes

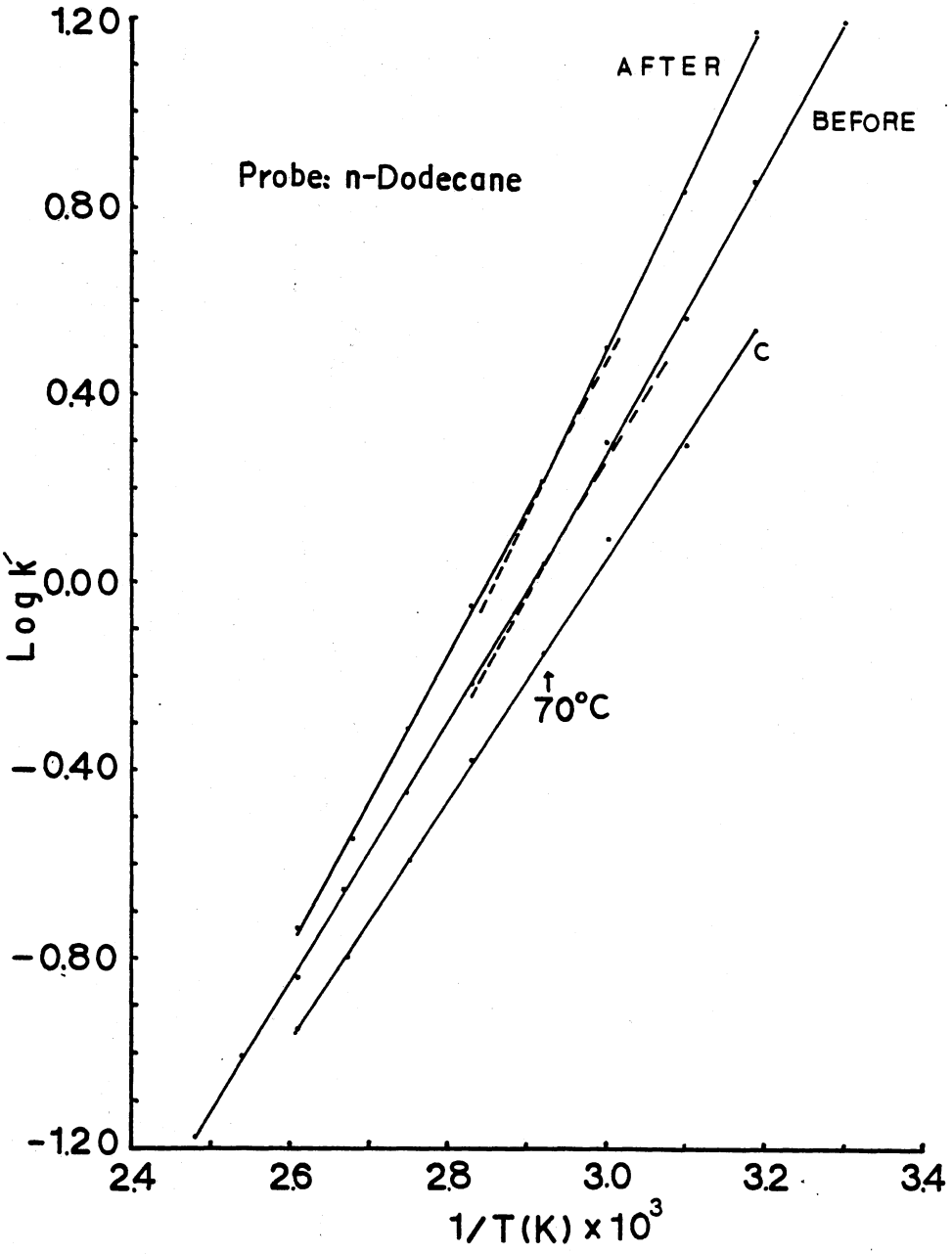

Figure 37. Relationship of log k' and 1/T for n-Dodecane on VMSi14C5 Capillary (Column 7)

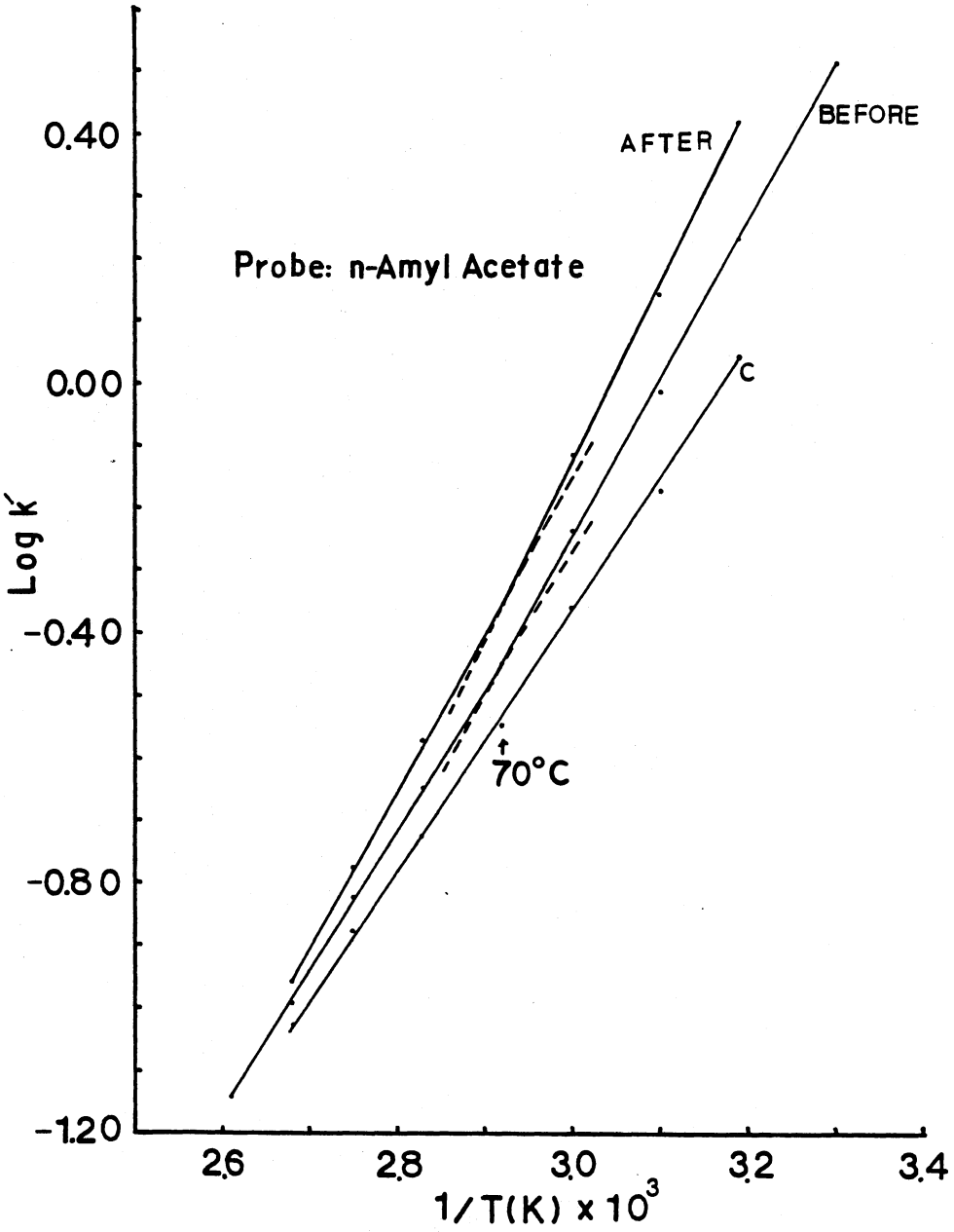

Figure 38. Relationship of log k' and 1/T for n-Amyl Acetate on VMSi14C5 Capillary (Column 7)

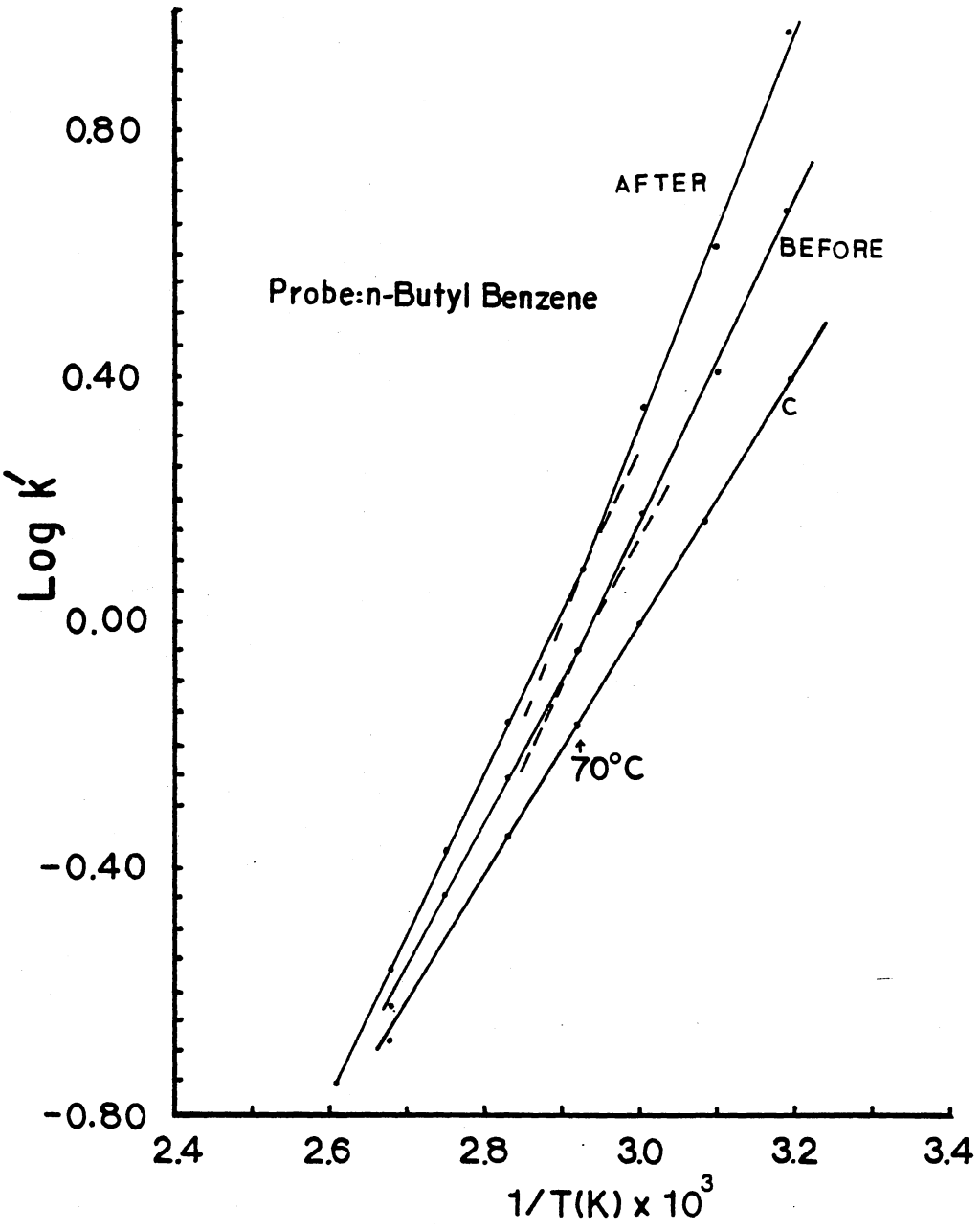

Figure 39. Relationship of log k' and 1/T for n-Butylbenzene on VMSi14C5 Capillary (Column 7)

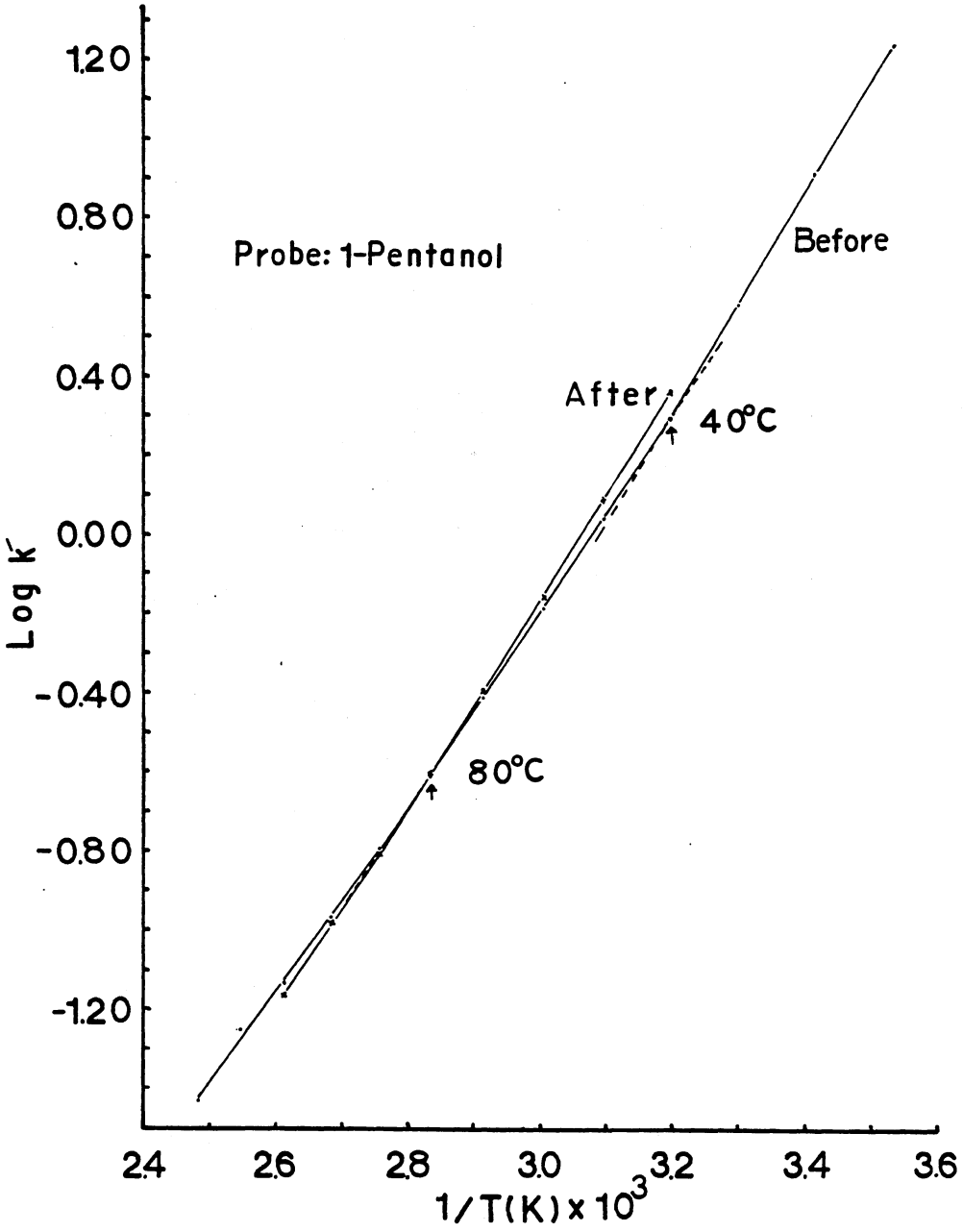

Figure 40. Relationship of log k' and 1/T for 1-Pentanol on VMSi14C5 Capillary (Column 7)

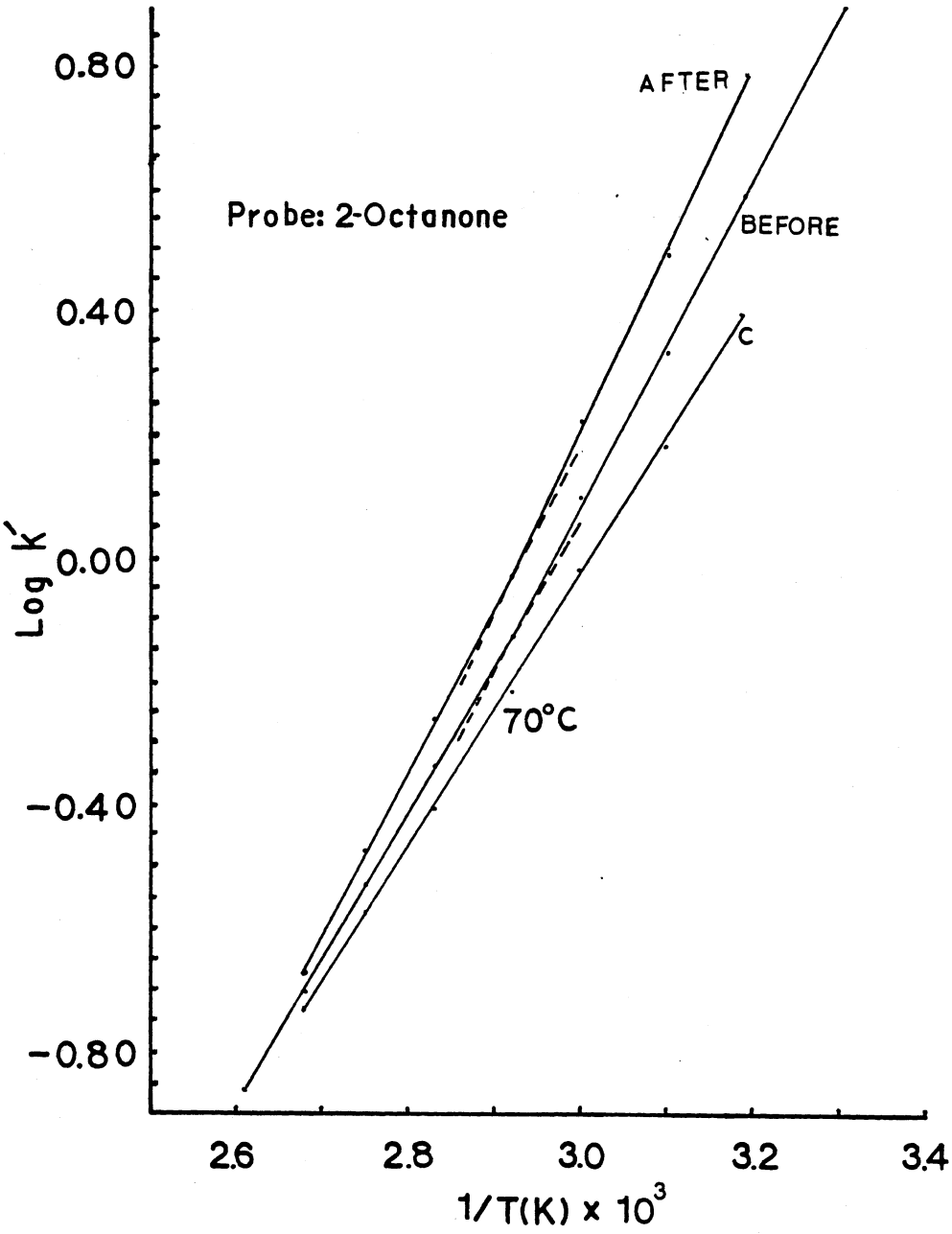

Figure 41. Relationship of log k' and 1/T for 2-Octanone on VMSi1405 Capillary (Column 7)

except n-pentanol exhibited an increase in retention after the column treatments for each temperature evaluated. In addition, a phase transition temperature at approximately 70°C occurs on each plot. The transition temperature for each probe and an estimate of the enthalpy for each solute/stationary phase interaction are given in Table IX. These enthalpies are obtained from the slopes of log k' versus 1/T on each side of the phase transition. The theoretical expression used to calculate ΔH° from these slopes is derived below (152,153).

$$k' = \frac{V_L}{V_M} K = \frac{V_L}{V_M} \exp \frac{\Delta G^\circ}{RT} = \frac{V_L}{V_M} \exp \frac{-\Delta S^\circ}{RT} \exp \frac{\Delta H^\circ}{RT} \tag{70}$$

$$\log k' = \log \frac{V_L}{V_M} - \frac{\Delta S^\circ}{R} + \frac{\Delta H^\circ}{RT} \tag{71}$$

ΔH° is the heat of evaporation of the dilute solute from the solution and can be expressed as (152)

$$\Delta H^\circ = \Delta H^\circ_{vap} - (b_1 \Delta H^\circ_{ads1} + b_2 \Delta H^\circ_{ads2}) - \Delta H^\circ_{mix} \tag{72}$$

where ΔH°_{vap} is the enthalpy of vaporization of the pure liquid probe, ΔH°_{ads1} is the enthalpy of adsorption of the probe at the stationary phase-support interface, ΔH°_{ads2} is the enthalpy of adsorption of the probe at the gas-stationary phase interface, ΔH°_{mix} is the enthalpy of mixing of the probe with the stationary phase, and b_1 and b_2 are constants related to the surface to volume ratio of the stationary phase at the two interfaces.

Since ΔH°_{vap} is a characteristic quantity of each probe, an increase in ΔH° would occur if the value of ΔH°_{ads} or ΔH°_{mix} decreased. The effect

TABLE IX

TRANSITION TEMPERATURES AND ESTIMATED ENTHALPIES OF FIVE PROBES BEFORE AND AFTER COLUMN TREATMENT

	Dodecane		n-Butyl Benzene		1-Pentanol		2-Octanone		Amyl Acetate	
	Before	After	Before	After	Before	After	Before	After	Before	After
ΔH Calculated Below Transition Temperature (kcal/mole)	13.7	14.1	12.0	14.5	11.5	12.2	12.1	13.7	11.5	12.9
Transition Temperature	70°C	70°C	70°C	70°C	40°C, 80°C	80°C	70°C	70°C	70°C	70°C
ΔH Calculated Above Transition Temperature (kcal/mole)	12.6	14.4	10.9	12.0	10.8	11.4	10.0	12.3	10.3	11.6

of b_1 or b_2 on ΔH° depends on the sign of ΔH°_{ads}. If ΔH°_{ads} is negative, an increase in b would cause ΔH° to increase. If ΔH°_{ads} is positive then a decrease in b_1 or b_2 would cause ΔH° to increase. Decreases in ΔH°_{ads} or ΔH°_{mix} would mean that the stationary phase has changed in a way such that less energy is required for the probe to be adsorbed onto the surface or mixed into the bulk of the stationary phase. ΔH° would also decrease if additional adsorption processes occurred in the column. The most significant increases in slope occurred for n-dodecane, amyl acetate and 2-octanone on both sides of the transition temperature.

This increased adsorption or mixing above and below the transition temperature may result from two possible sources. The temperature conditioning of the stationary phase may have caused re-orientation of the crown ether so that more sites were available for interaction with the probes. Since n-dodecane, 2-octanone and amyl acetate show more significant changes in ΔH°, it could be suggested that the temperature conditioning caused the ethylene groups of the crown ether or polymer backbone to become more available for interaction with the alkyl substituents of these probes. The small change in slope for n-pentanol might imply that there is little change in the hydrogen bonding character of the stationary phase.

Besides changes in orientation of the crown ether, increased polymerization of the vinyl groups on the VMSil4C5 could be occurring. This rationale does not appear possible since the transition temperature would be expected to increase as the chain length and average molecular weight of the stationary phase increased. Table IX shows that four of the probes detect identical transition temperatures before and after the treatments.

By expressing Equation 72 in the form below

$$\log k' = \log \frac{V_L}{V_M} - \frac{\Delta S^\circ}{R} + \frac{\Delta H^\circ_{vap}}{RT} - \frac{\Sigma b \Delta H^\circ_{ads}}{RT} - \frac{\Delta H^\circ_{mix}}{RT} \qquad (73)$$

and making several reasonable assumptions, the change in slope and intercept of the log k' versus 1/T plots for n-dodecane, amyl acetate, n-butylbenzene and 2-octanone can be explained (154). The first assumption is that ΔH°_{ads} does not change at the phase transition temperature. This is reasonable if the surface area does not change within the time required for the log k' versus 1/T plot. The contribution of adsorption to log k' would then be linear with respect to 1/T over the entire temperature. The second assumption is that ΔH°_{mix} changes at the transition temperature. This is possible since a solid-liquid or liquid-liquid transition would cause the solute to have different solubilities in each of the different phases. This contribution, that due to adsorption, and their combined effect would give Figure 42. The log k' versus 1/T plots exhibit this adsorption-mixing combination. Before conditioning, Figures 37, 38, 39 and 41 resemble plot B. As a result of the solvent wash and temperature conditioning, an adsorption or mixing process not effected by the transition was initiated or increased and a plot resembling C results. When log k' values before and after conditioning were subtracted and the difference subtracted from B, a linear plot across the transition temperature resulted. A least square fit of each line labelled C gives a determination of correlation which is greater than 0.998 for each case.

The log k' versus 1/T plot for n-pentanol does not show the same character as the plots for the other four probes. Instead of an increase in retention after the solvent wash and temperature conditionings, a de-

crease in the retention of 1-pentanol occurs above the transition temperature at 80°C. The plot also reveals a transition temperature at 40°C. From these plots it is seen that the change in the column which was caused by the solvent wash and temperature conditioning does not effect the retention of 1-pentanol as much as it effects the other probes. This is also evident from Table VIII where the partition ratio of 1-pentanol changes only slightly after each treatment.

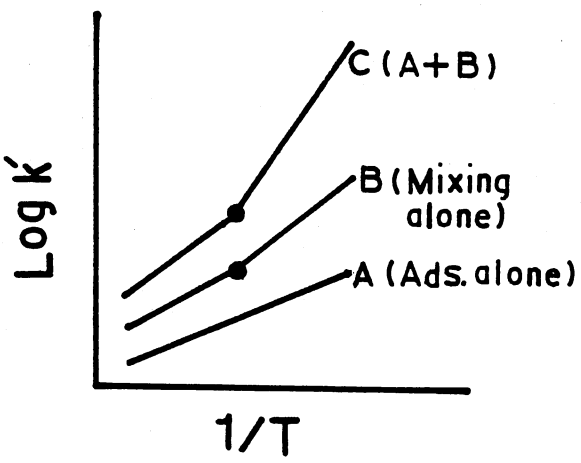

Figure 42. Theoretical Relationship of log k' and 1/T Showing the Effect of Increased Adsorption

Figures 43, 44 and 45 show the chromatograms of an alkane mixture, an aromatic mixture and n-pentanol. These chromatograms were obtained before and after the solvent rinse and after the third temperature conditioning. Comparison of the alkane and aromatic separations show that

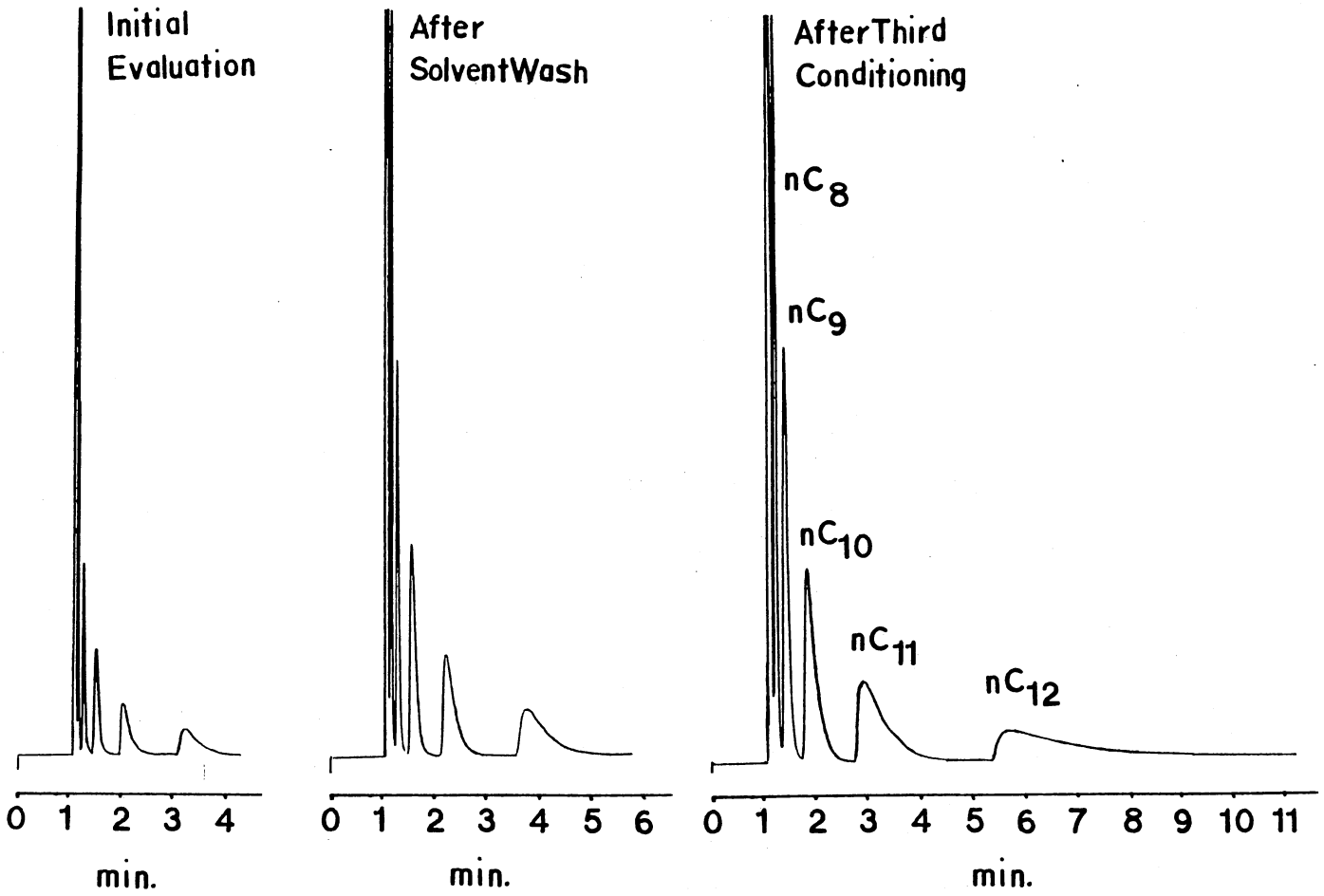

Alkane mixture: 0.2% v/v $nC_{7,8,9,10,11,12}$ in pentane Sample size: 0.4 µl

Split ratio: 1/49 T_C: 60°C Attenuation: 2^4 $\bar{v}$: 30.0 cm/s

Figure 43. Chromatograms of an Alkane Mixture on VMSi14C5 Capillary (Column 7)

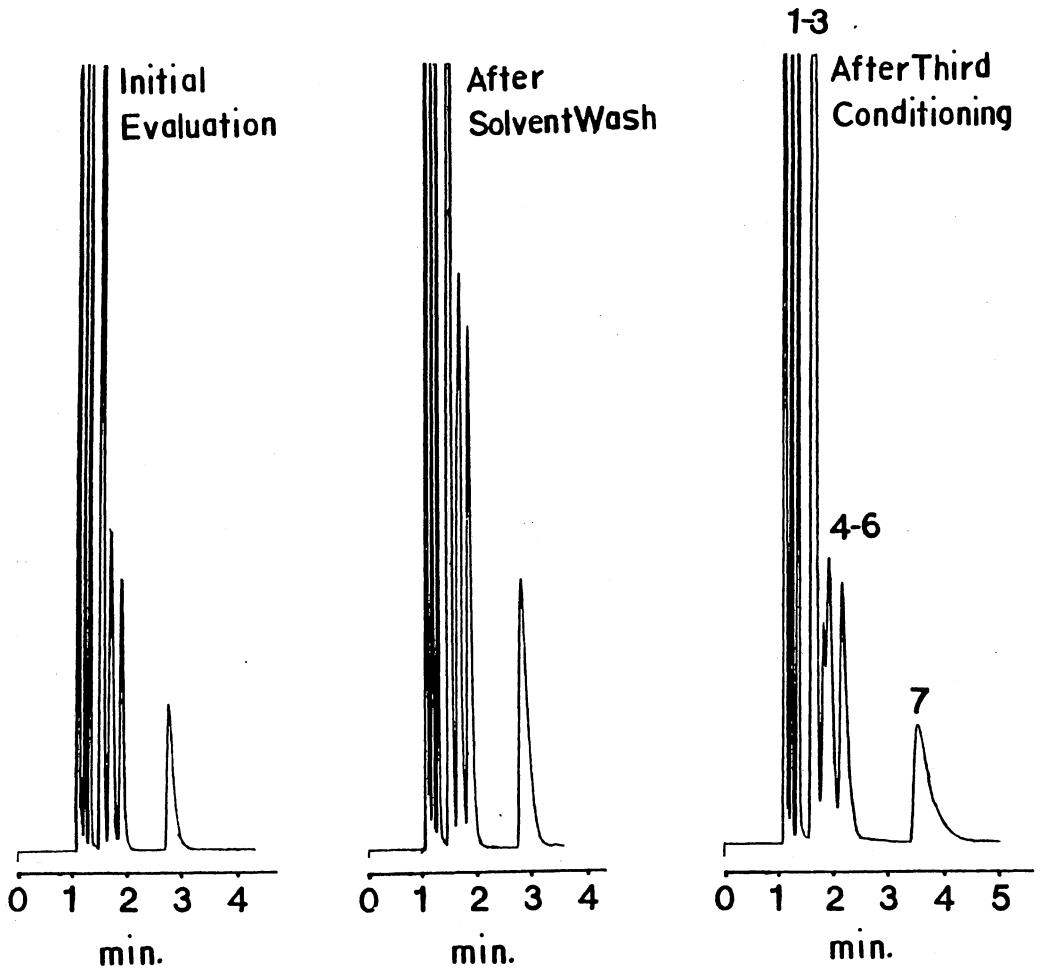

Aromatic mixture: 0.2% v/v 1) toluene, 2) ethyl benzene, 3) m-xylene, 4) p-xylene, 5) isopropyl benzene, 6) n-propyl benzene, 7) n-butyl benzene in pentane
Sample size: 0.4 µl Split ratio: 1/49 T_C: 60°C Attenuation: 2^4 $\bar{v}$: 30 cm/s

Figure 44. Chromatograms of an Aromatic Mixture on VMSi14C5 Capillary (Column 7)

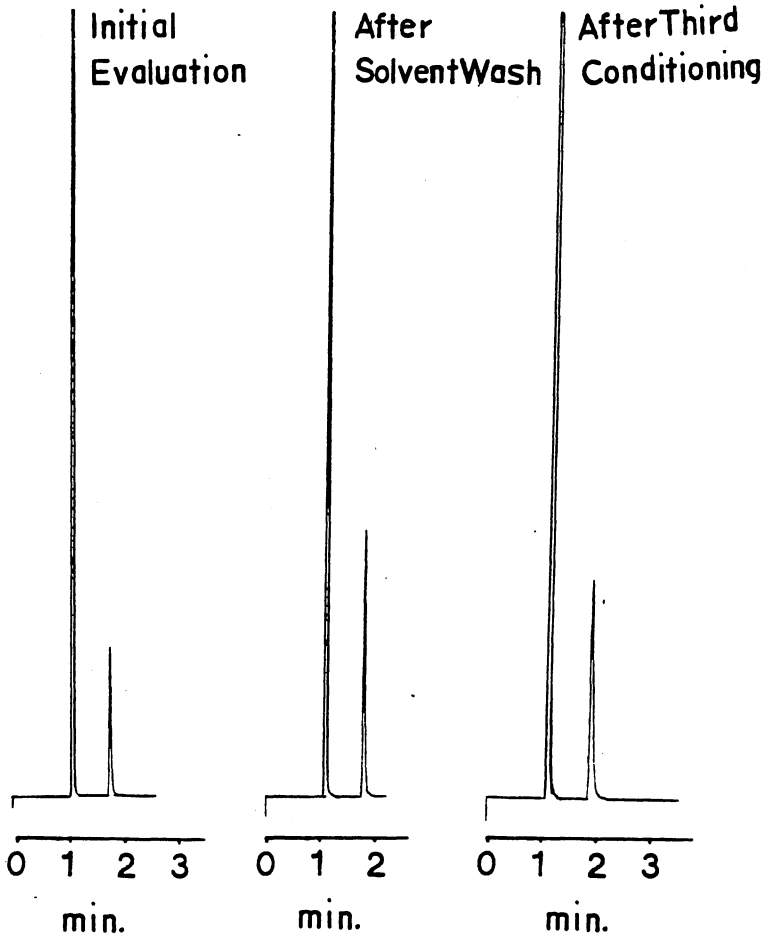

Sample size: 0.4 µl of 0.2% v/v 1-pentanol in pentane
Split ratio: 1/49 T_C: 60°C Attenuation: 2^4 $\bar{v}$: 30 cm/s

Figure 45. Chromatograms of 1-Pentanol on VMSi14C5 Capillary (Column 7)

along with increased retention, an increase in tailing has occurred. This would be expected if increased adsorption was present. 1-Pentanol shows only slight peak broadening after the temperature conditioning.

Table X provides the number of effective plates for each probe at 60°C. After each of the treatments, a decrease in the efficiency occurred as would be expected if adsorption processes increased. The increase in efficiency upon reevaluation follows the same pattern as was observed for the partition ratios with the exception of 1-pentanol. The efficiency of 1-pentanol increased after the solvent wash and first conditioning but decreased when the heat treatment was maintained for longer periods of time.

Comparison of the behavior of 1-pentanol with the four other probes shows that after the column treatments 1-pentanol exhibited less change in retention over the temperature range, higher efficiency and less tailing than alkanes with the same retention. This difference in behavior may be due to the higher solubility of 1-pentanol in the crown ether stationary phase. Since the column temperature at which the chromatograms and efficiency measurements were obtained, 60°C, was below the phase transition temperature at 70-80°C, the tailing of nonpolar probes would be due to adsorption on the stationary phase surface. The alcohol which has higher solubility in the polar crown ether stationary phase would not exhibit adsorption as its retention would still be due to partitioning.

Column 8: Statically Coated PVB15C5

A temperature program of the fourteen component alcohol mixture on the PVB15C5 column over the temperature range used in the silacrown ether

TABLE X

NUMBER OF EFFECTIVE PLATES FOR FIVE PROBES AFTER EACH TREATMENT

Probe	Column Temperature: 60°C								
	After Initial Conditioning	Solvent Wash		First Condition		Second Condition		Third Condition	
		Before	After	Before	After	Before	After	Before	After
Decane (C_{10})	129	114	130	168	94	139	79	102	68
Undecane (C_{11})	163	110	173	190	110	155	90	109	61
Dodecane (C_{12})	206	124	145	251	99	206	97	106	76
n-Butyl Benzene	793	650	666	912	566	893	416	541	345
1-Pentanol	1770	1800	1850	1680	1970	1801	1130	899	978

columns was not possible due to the severe broadening and tailing that occurred at low temperatures. Isothermal chromatograms at 130°C and 180°C (Figure 46) showed that column temperatures above 130°C are required to obtain efficient peaks. Possible reasons for this temperature effect can be found in the phase transitions observed in the column.

Figure 47 shows the log k' versus 1/T plot for acetonitrile on the PVB15C5 column. Acetonitrile was chosen as a phase transition probe because it is soluble in polystyrene and polyethylene glycol. It also provides acidic methyl protons which can interact with several of the crown ether oxygens at the same time (145). Changes in retention behavior of acetonitrile on PVB15C5 occur at 75°C, 110°C and 150°C. These changes occur at temperatures which may correspond to a glass phase transition and two liquid-liquid transitions. The transition at 75°C may be related to the softening (glass transition) temperatures for two PVB15C5 polymers prepared by Kopolow (146). The glass transition temperatures for his polymers occurred at 113-117°C and 122-128°C for polymers with number-average molecular weights ($\bar{M}_n$) of ∿28,000 and ∿113,000, respectively. Differences in the glass transition temperatures are due to a dependence on the inverse of the $\bar{M}_n$ (155). Equation 74 where T_g^∞ is the glass transition temperature at infinite molecular weight and k is a constant, shows this relationship.

$$T_g = T_g^\infty - \frac{k}{\bar{M}_n} \qquad (74)$$

Since the T_g of the polymer prepared here was lower than the T_g of the polymers prepared by Kopolow, it might be assumed that its $\bar{M}_n$ was also lower. From the T_g and $\bar{M}_n$ values provided by Kopolow and the transition temperature determined from column 8, an estimate of 7000 for $\bar{M}_n$ was

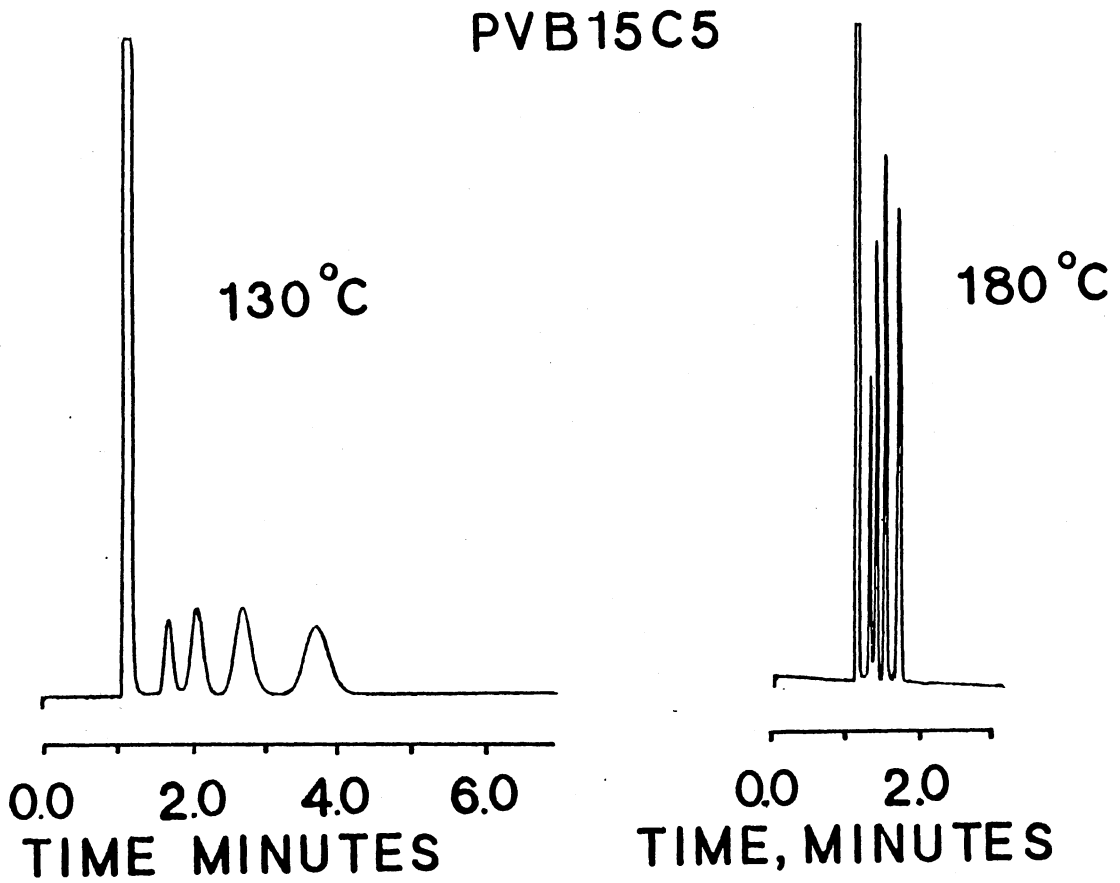

Column length: 20 m I. D.: 0.32 mm Sample size: 0.2 µl
Alcohol mixture: 0.1% v/v of 1-pentanol, 1-hexanol, 1-heptanol and 1-octanol
Split ratio: 1/140 at 180°C Attenuation: 2^2 $\bar{v}$: 29.0 cm/s Film thickness: 1 um

Figure 46. Chromatograms of an Alcohol Mixture on PVB15C5 Capillary (Column 8)

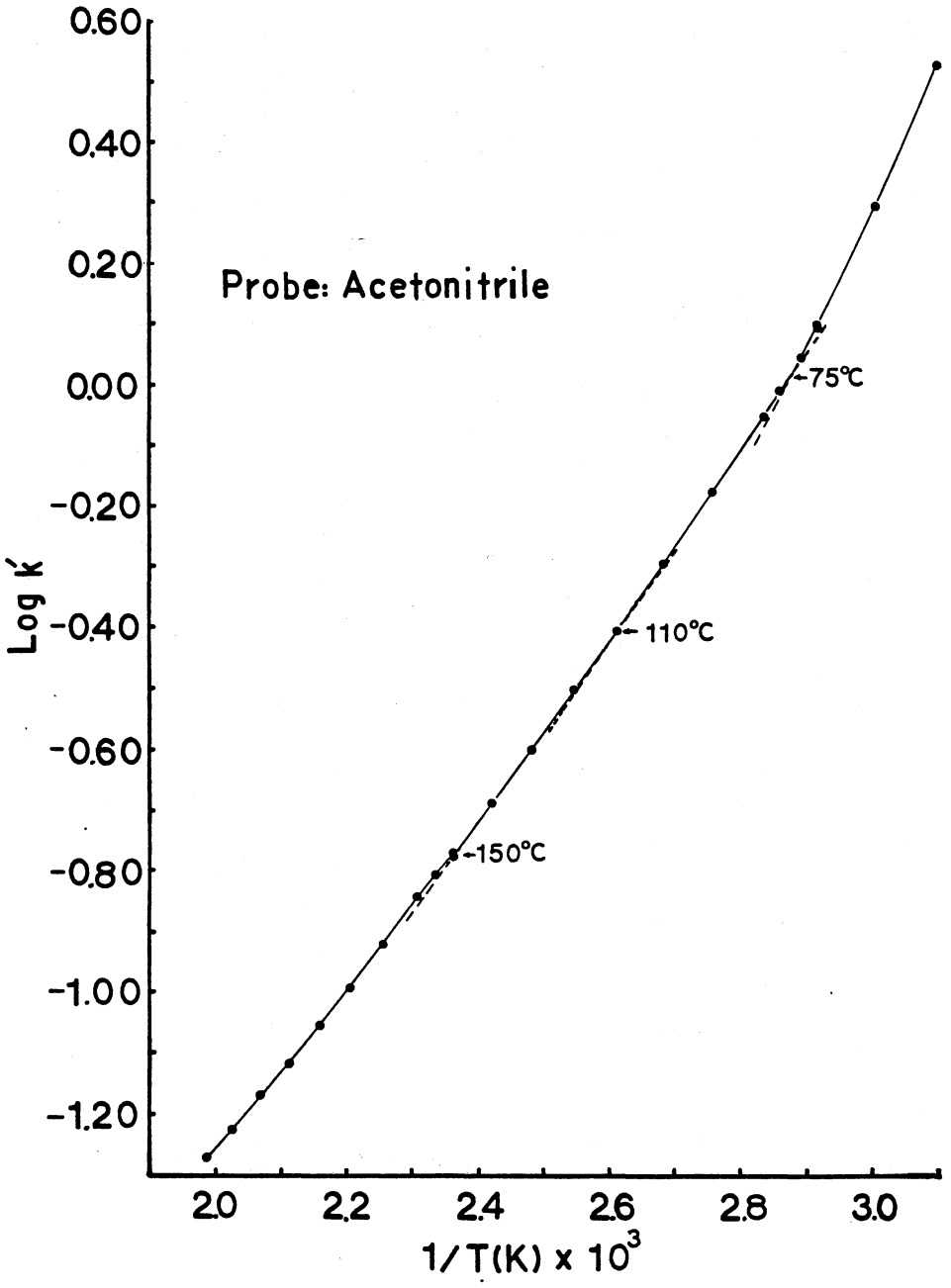

Figure 47. Relationship of log k' and 1/T for Acetonitrile on PVB15C5 Capillary (Column 8)

calculated.

The transitions at 110°C and 150°C may correspond to liquid-liquid transitions which have been designated as $T_{\ell\ell}$ and $T'_{\ell\ell}$ (156,157). Such transitions which have been observed in atatic polymers including polystyrene by fourier transform infrared spectroscopy and differential scanning calorimetry may be related to temperatures where the liquid of fixed structure becomes a true liquid, $T_{\ell\ell}$, and where barriers to conformation become negligible, $T'_{\ell\ell}$. General values of $T_{\ell\ell}$ for many atatic polymers occur in the range of 1.1 to 1.3 T_g. The T_g and $T_{\ell\ell}$ of PVB15C5 at 75°C and 110°C occur near this range.

The transition at 150°C was also confirmed with plots of log k' versus 1/T (Figure 48) and real plate numbers versus column temperature (Figure 49) for four linear alcohols. These figures show transitions which occur at 145°C and 150°C. A log k' versus 1/T plot for acetonitrile on a second PVB15C5 column confirmed the three transition temperatures (Figure 50).

Differential scanning calorimetry (DSC) of the PVB15C5 polymer (Figures 51, 52, 53 and 54) shows evidence of the glass transition temperature. Figure 52 shows an endothermic change in the polymer with an extrapolated onset temperature at 67°C and a minimum of the endotherm at 80°C. Although endotherms are not characteristic of glass transitions, Wunderlich (158) and Gillham (159) have reported that polymers which have experienced fast heating and slow cooling rates show endotherms which contain first and second order transition character. DSC tracings which were reported by Gillham for heat treated polystyrene show glass transitions which resemble the tracings in Figure 52. Before the DSC in Figure 52 was obtained, the polymer was heated to remove solvents used

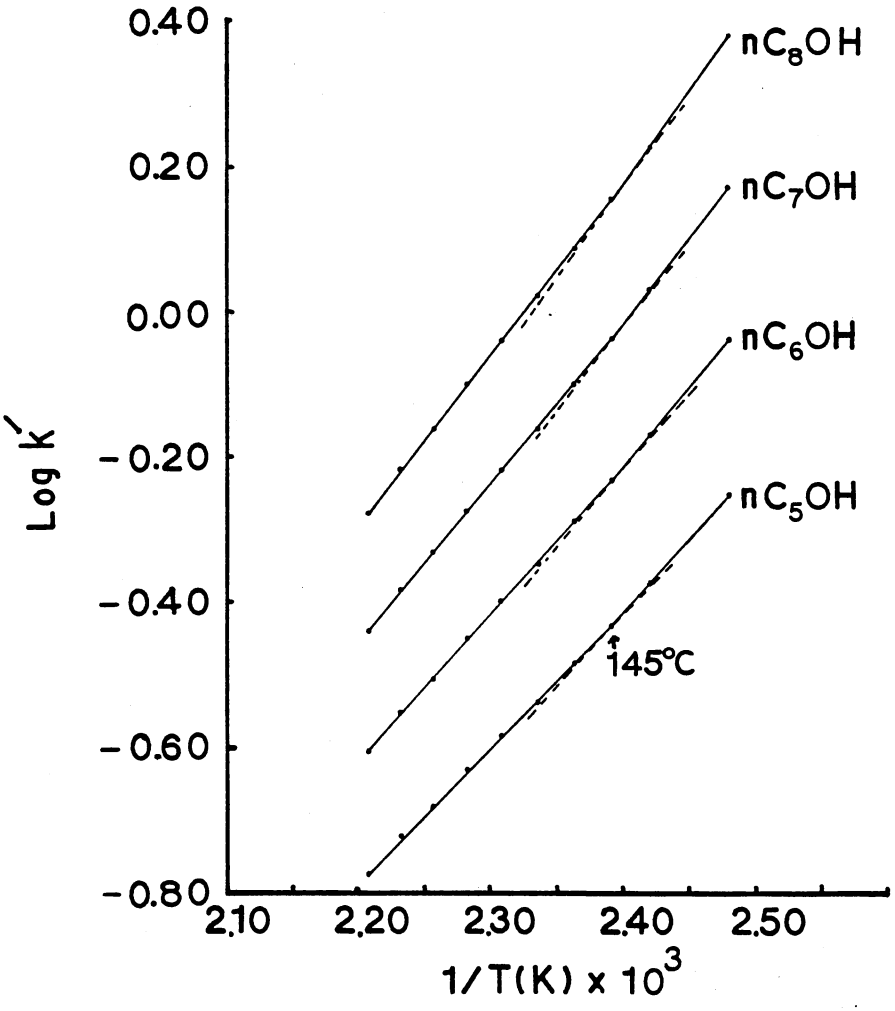

Figure 48. Relationship of log k' and 1/T for Four Alcohols on PVB15C5 Capillary (Column 8)

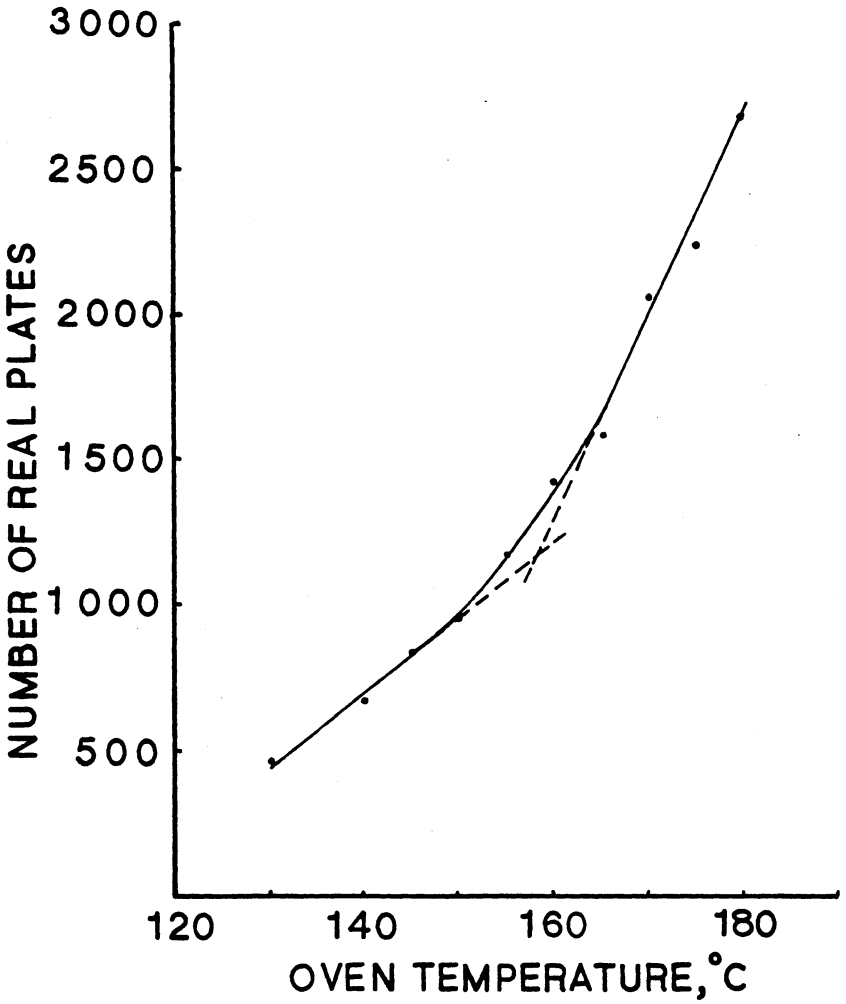

Figure 49. Relationship of the Number of Real Plates and Column Temperature for a Series of Alcohols on PVB15C5 Capillary (Column 8)

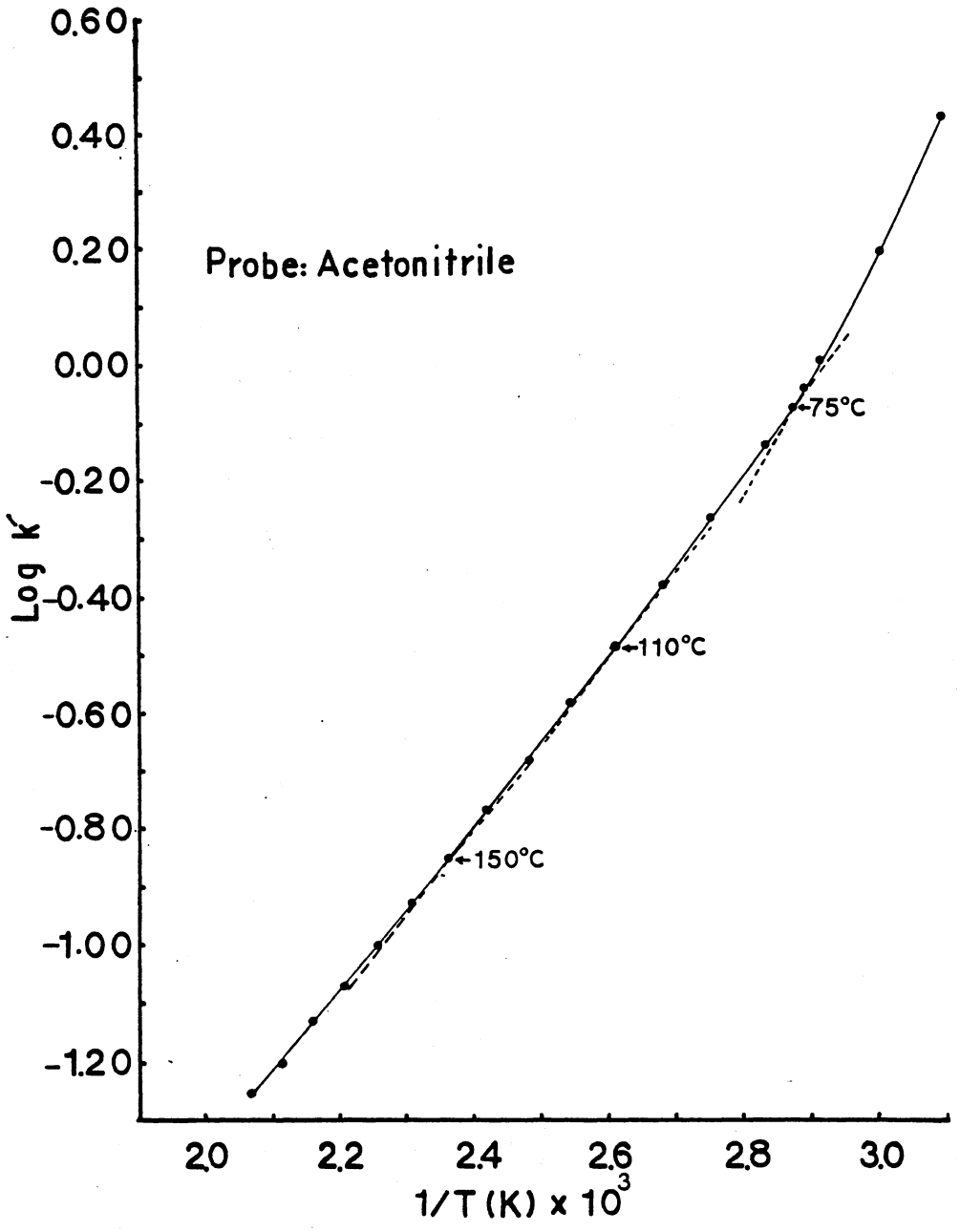

Figure 50. Relationship of log k' and 1/T for Acetonitrile on a Second PVB15C5 Column

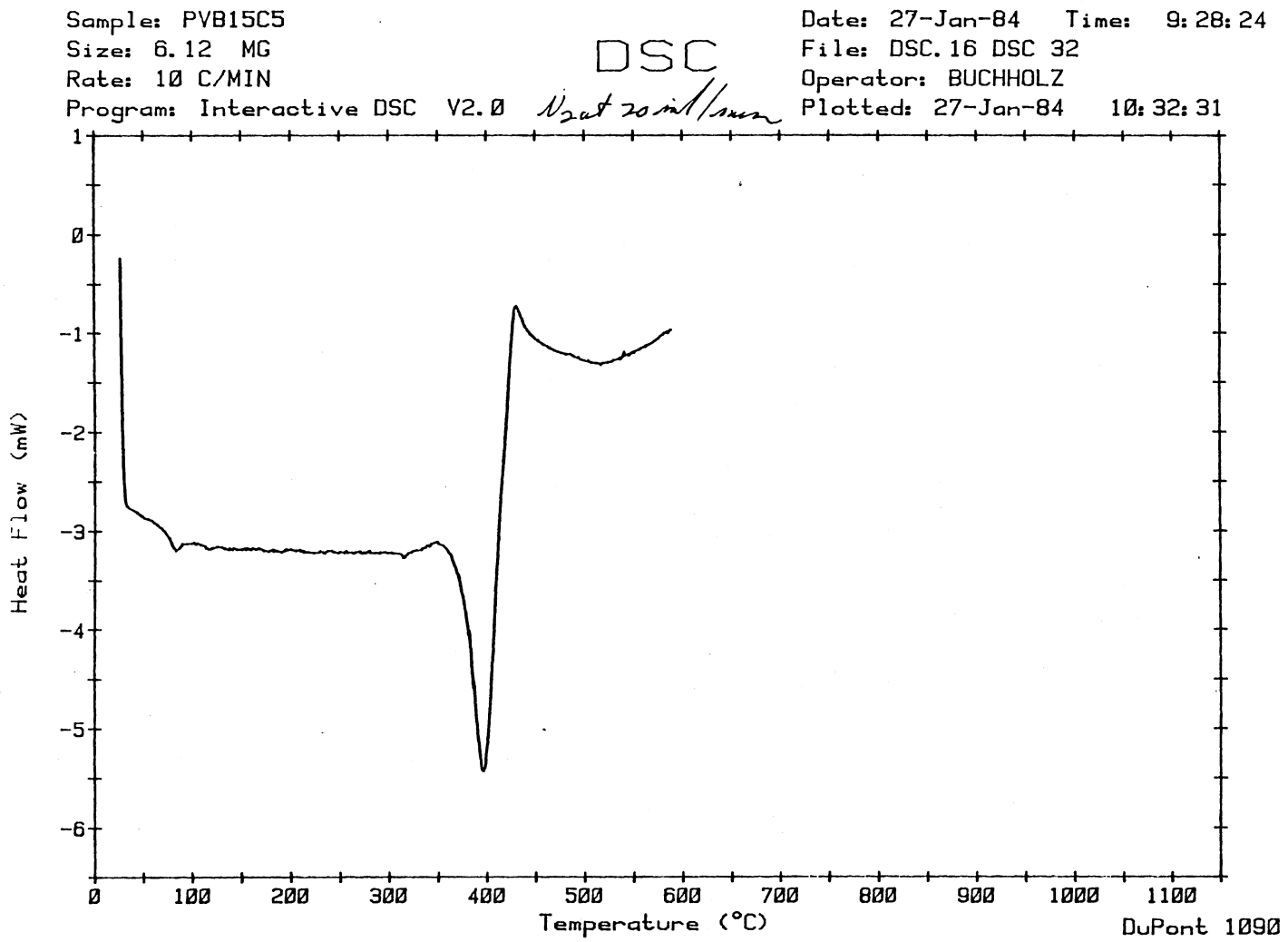

Figure 51. Differential Scanning Calorimetry of PVB15C5

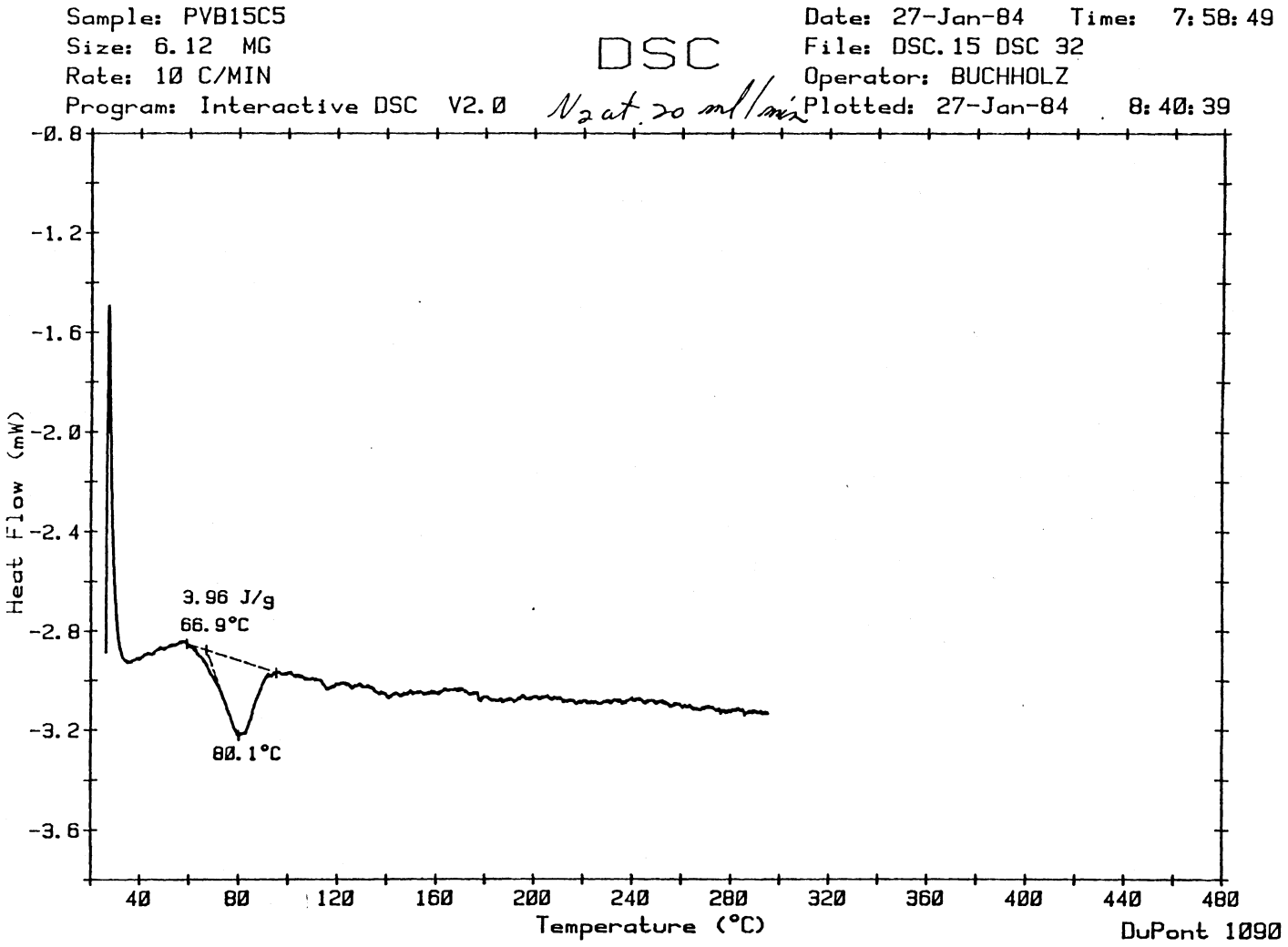

Figure 52. Differential Scanning Calorimetry of PVB15C5

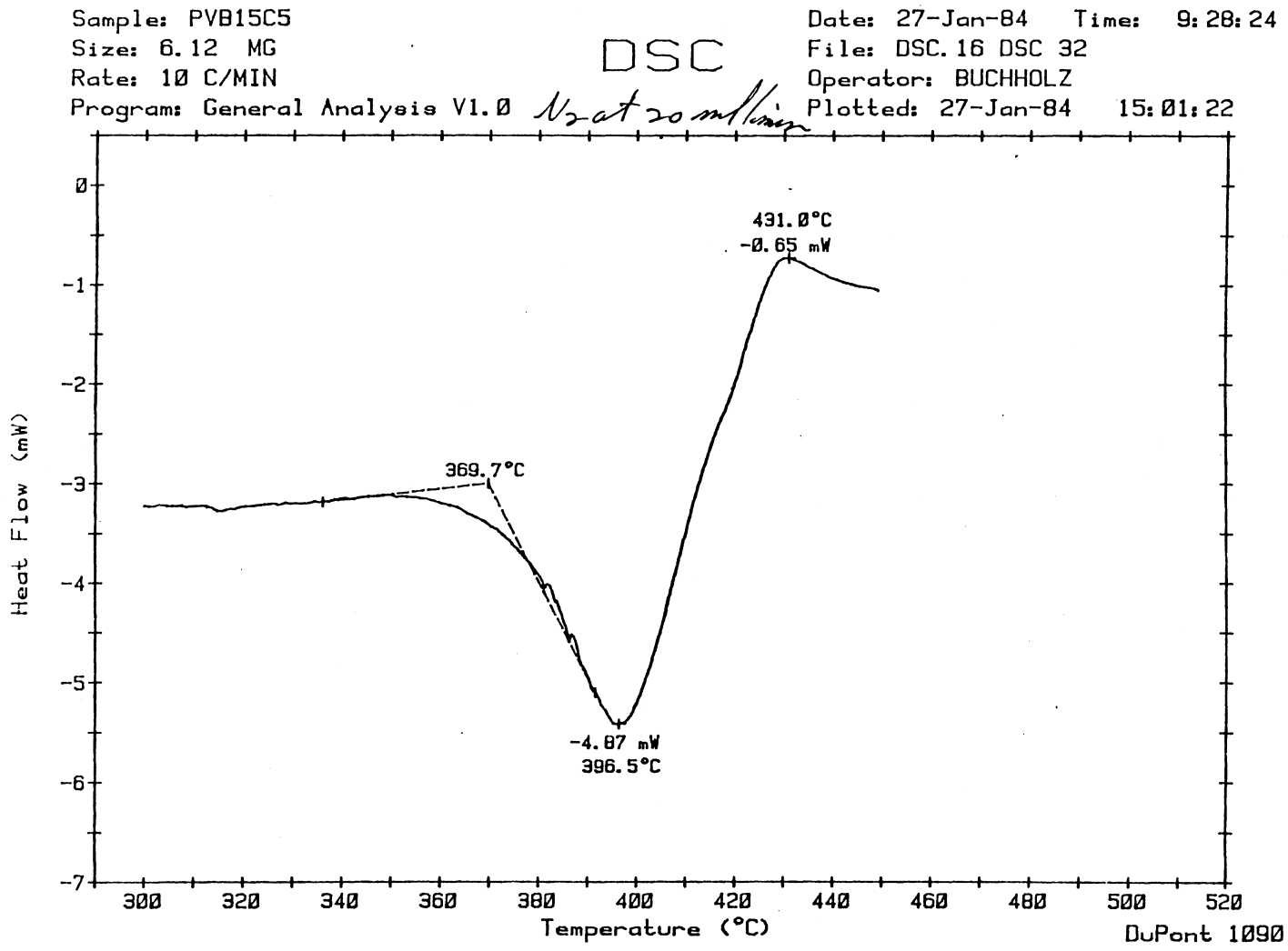

Figure 53. Differential Scanning Calorimetry of PVB15C5

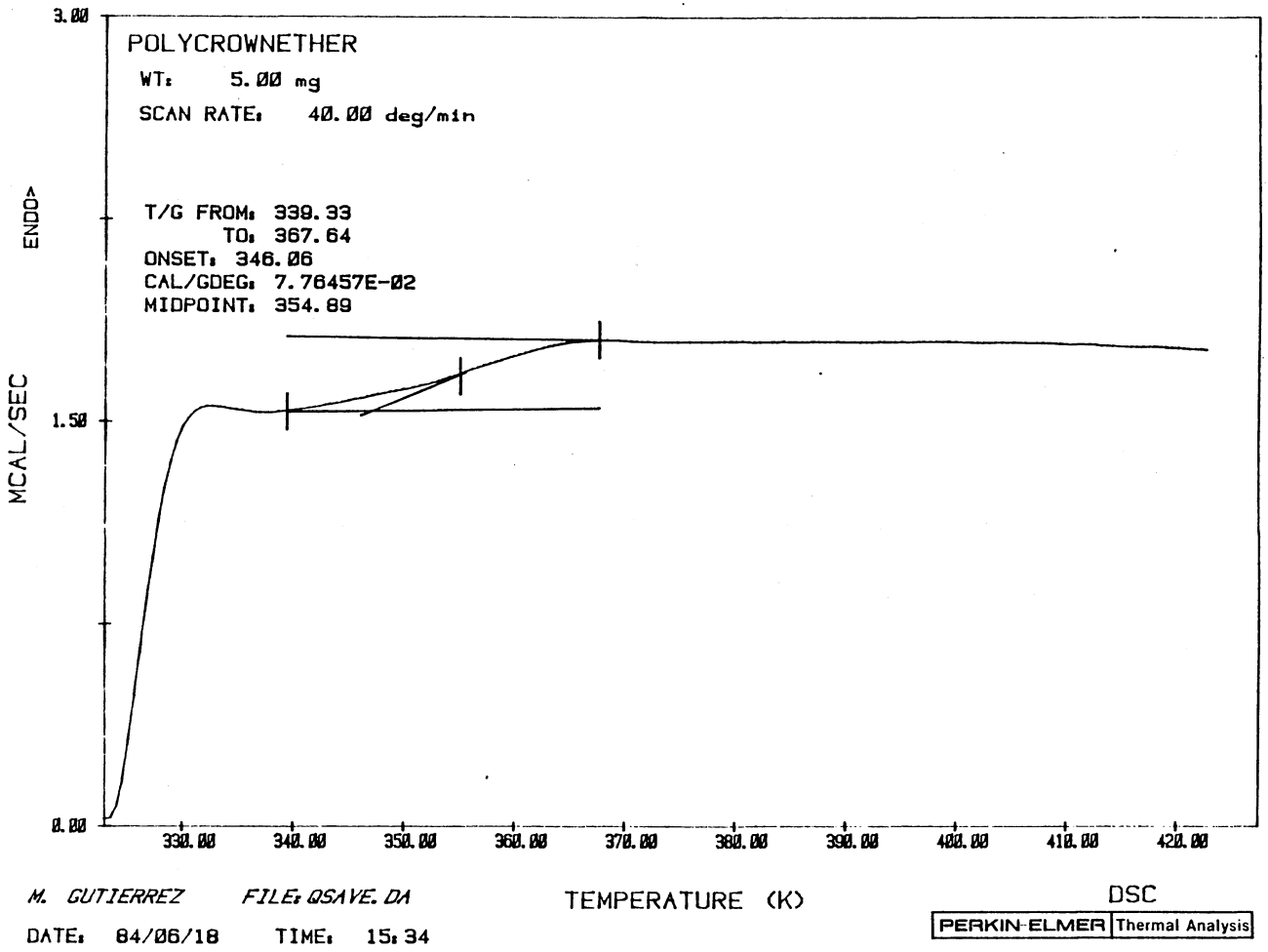

Figure 54. Differential Scanning Calorimetry of PVB15C5

for reprecipitation and may not have reached thermal equilibrium before the DSC experiment was started. The DSC tracing in Figure 54 was obtained five months later and shows no evidence of thermal history. Here a second order phase transition which is characteristic of a glass transition was observed which had an onset temperature of 73°C and a midpoint temperature of 83°C. The glass phase temperatures from the two DSC experiments correlates well with the phase transition temperature, 75°C, which was determined by gas chromatography. The DSC did not reveal, however, a transition at 110°C and 150°C. A possible explanation for the absence of the transition could be that the change in heat capacity of the polymer that occurs at these transitions was too small to be detected by DSC. The gas chromatographic experiment used changes in retention of a chemical probe to detect changes in the physicochemical nature of the polymer. Transitions in the polymer that result in small changes in heat capacity could cause changes in the solubility of the probe in the polymer. These changes would be detected by changes in retention.

In addition to the DSC of PVB15C5, thermogravimetric analysis (TGA) of PVB15C5 and DSC and TGA of Carbowax 20M were also performed. Comparison of the DSC of Carbowax 20M (Figure 55) with PVB15C5 (Figure 52) shows that the Carbowax 20M endotherm at 66°C absorbs about 40 times more energy per gram than PVB15C5. This difference in energy absorption probably occurs because more energy is absorbed by the Carbowax 20M polymer as it goes through its melting transition. For PVB15C5, only part of the polymer, the ethyleneoxy groups of the crown ether gain energy. The endotherms at 370°C which are followed by exotherms are due to absorption of energy before the polymers start to decompose.

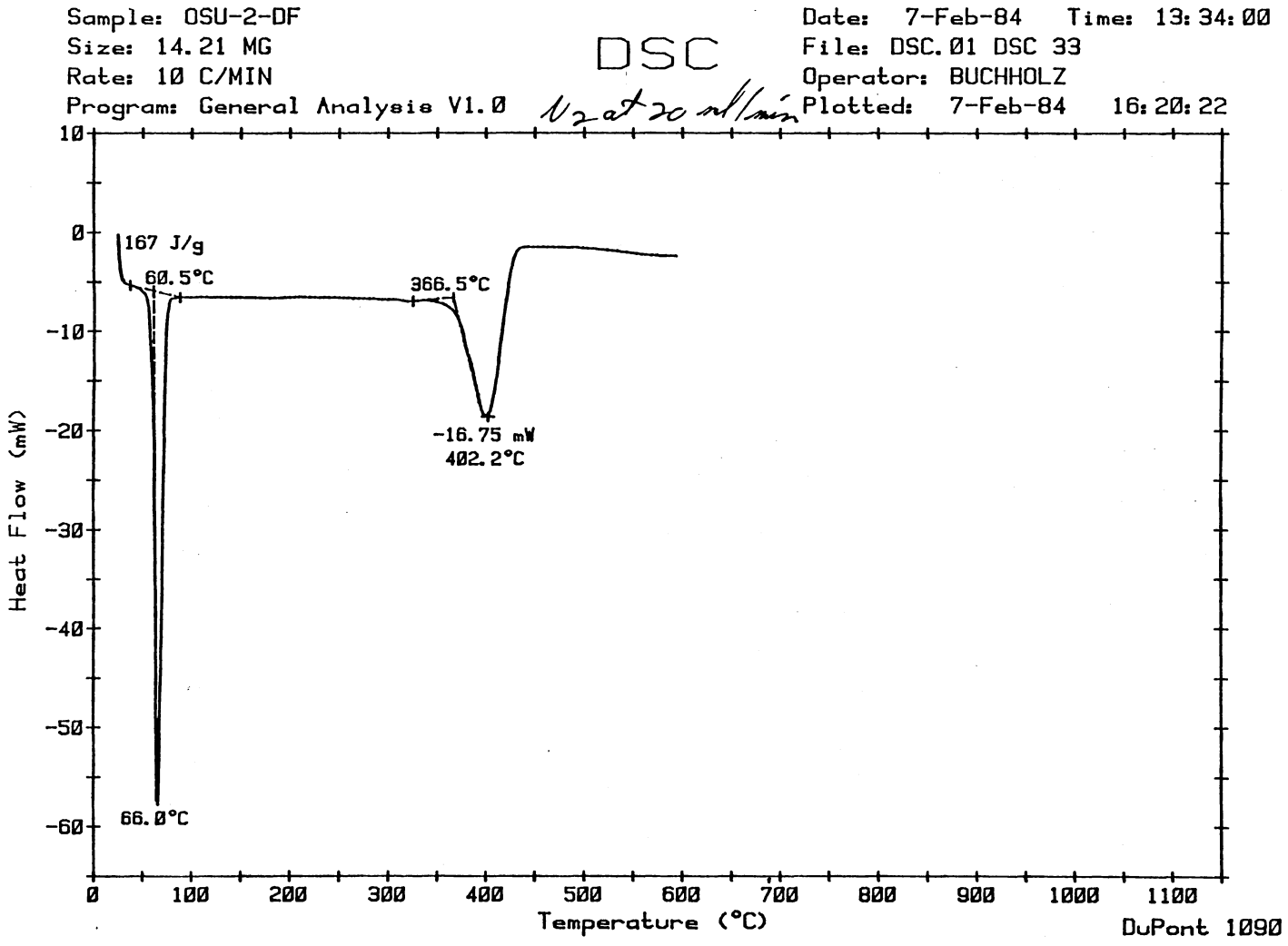

Figure 55. Differential Scanning Calorimetry of Carbowax 20M

To determine how oxygen affects the DSC of Carbowax 20M, the nitrogen atmosphere in the DSC cell which contained 1-2 ppm oxygen was replaced with air. Figure 56 shows that an increasing exotherm which is due to oxidation started at 171°C.

Thermogravimetric analysis of PVB15C5 and Carbowax 20M (Figures 57 and 58) reveal similar results with discernable weight losses beginning at 360°C for PVB15C5 and 330°C for Carbowax 20M. Although these temperatures might be taken as maximum operating temperatures in gas chromatography, it has been recommended that capillary columns containing Carbowax 20M not be used at temperatures above 280 to 300°C (75). This difference could be due to the gas chromatography detectors responding to much lower amounts of stationary phase bleed, or catalytically induced decomposition of the stationary phase by the glass or fused silica capillary.

Comparisons of Columns 6, 7 and 8

Tables XI and XII show comparisons of various column parameters. The inner diameter and column lengths of the two silacrown ether columns are approximately the same while the PVB15C5 column has a smaller inner diameter. The minimum operating temperature for each of the three columns was determined at the highest phase transition temperature. While this temperature provides a good lower limit for the PVB15C5 column as shown in Figure 46, the silacrown ether columns exhibit reasonable chromatography below the observed transition temperature. This is evident from the alcohol chromatograms in Figures 28 and 36. For each of these columns, the lower limit is therefore less than the observed transition temperature.

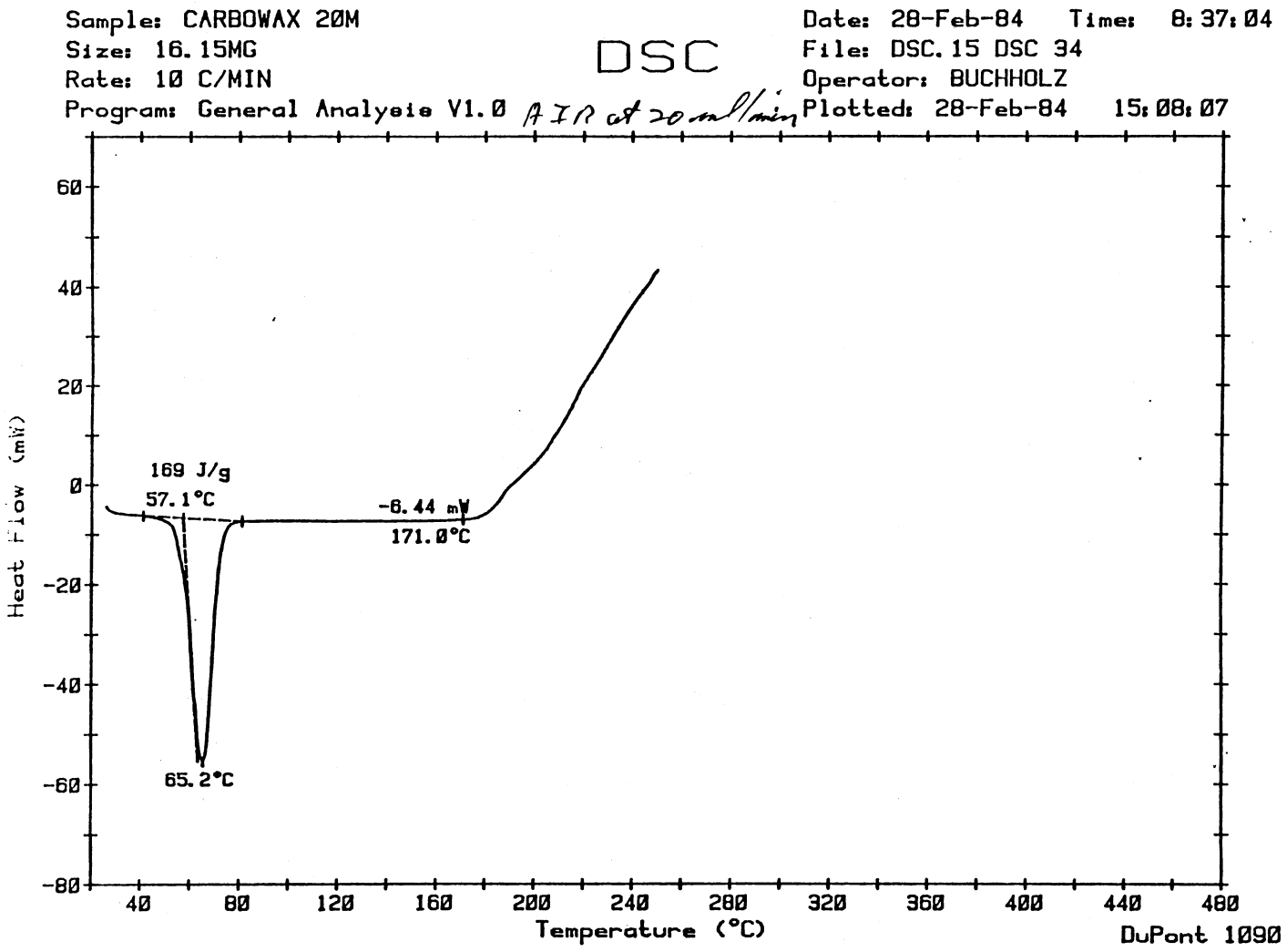

Figure 56. Differential Scanning Calorimetry of Carbowax 20M

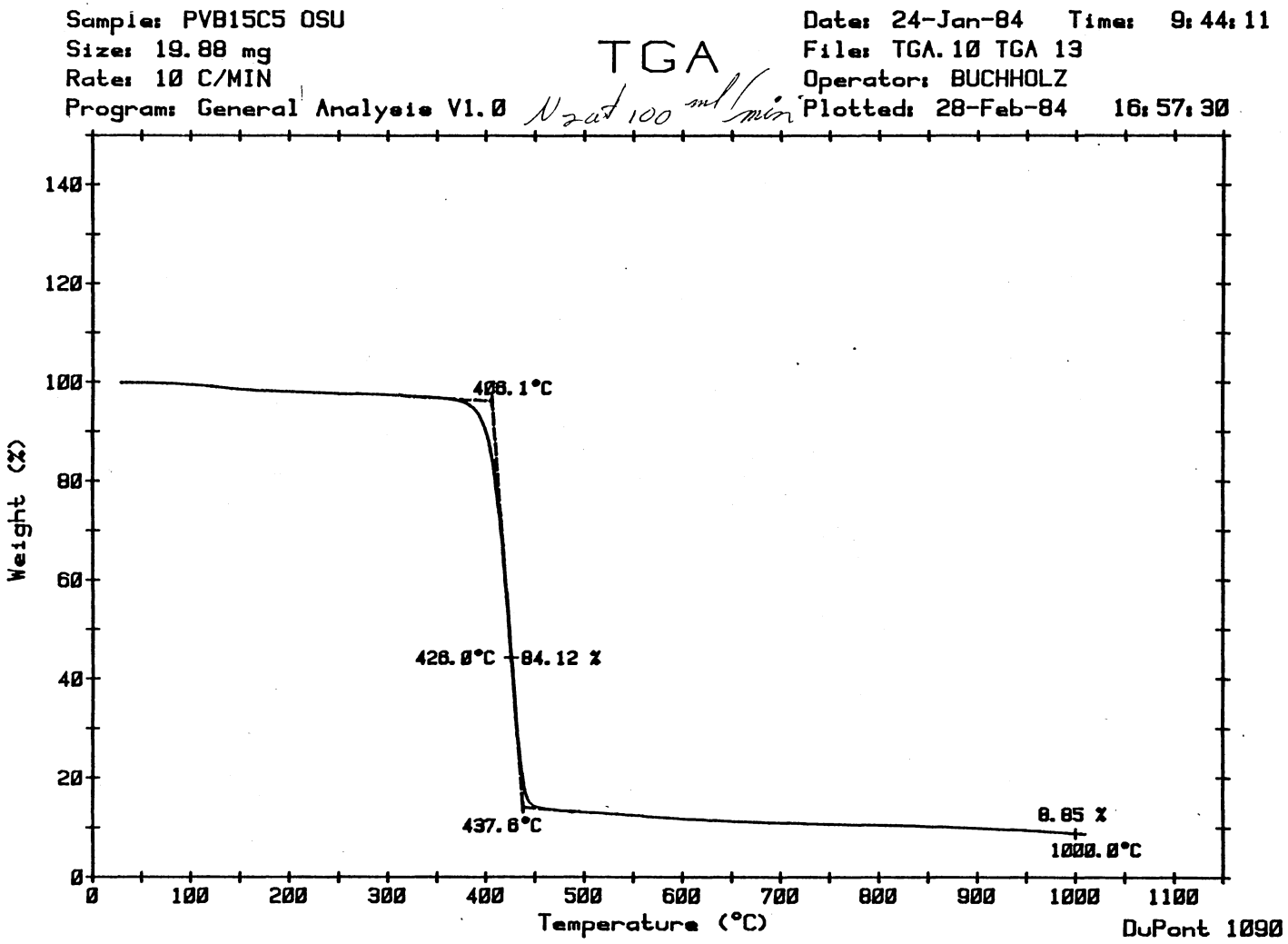

Figure 57. Thermogravimetric Analysis of PVB15C5

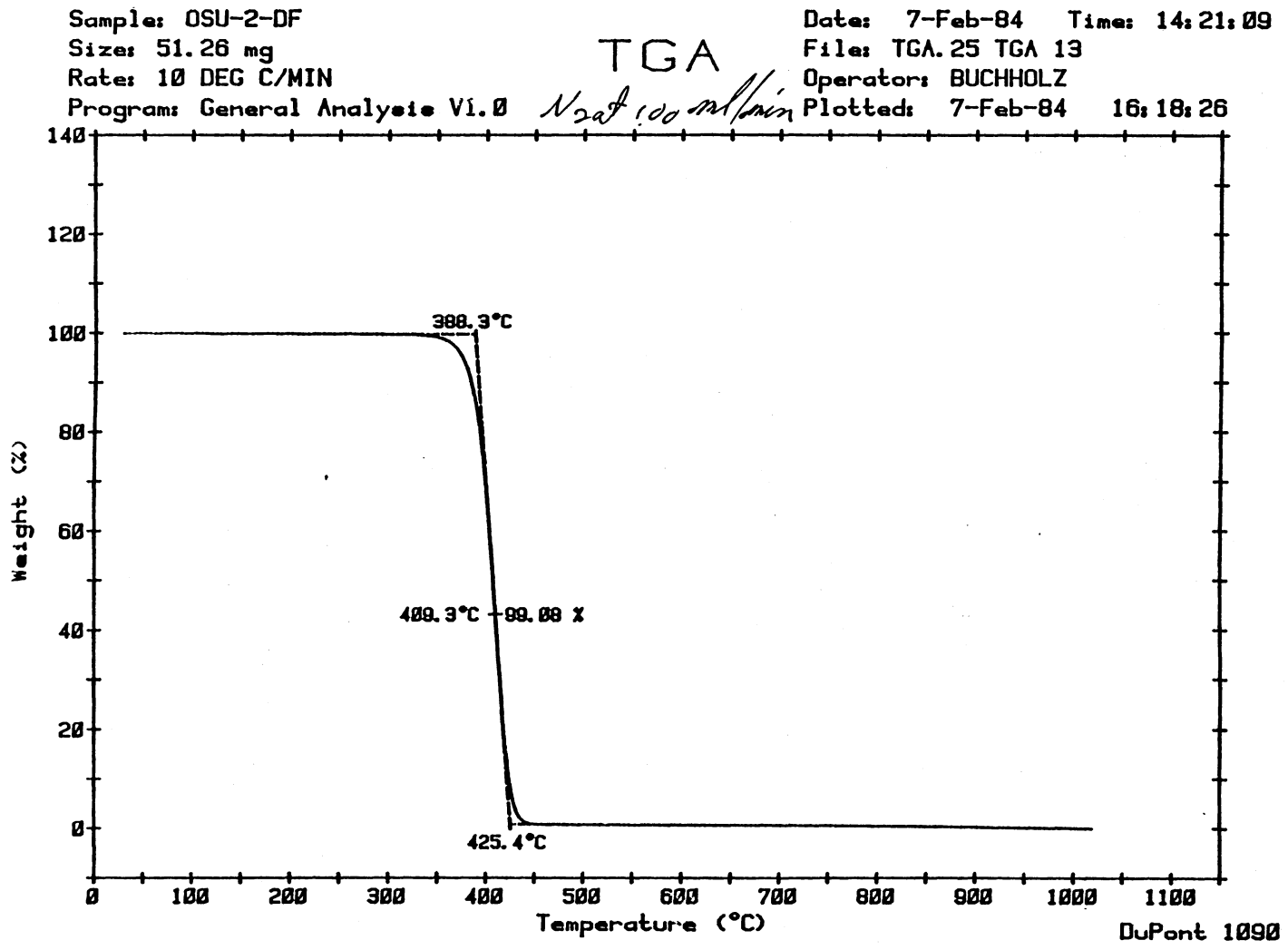

Figure 58. Thermogravimetric Analysis of Carbowax 20M

TABLE XI

COMPARISON OF COLUMN DIMENSIONS, PHASE TRANSITION TEMPERATURES, MINIMUM AND MAXIMUM OPERATING TEMPERATURES, % UTILIZATION OF THEORETICAL EFFICIENCY AND NUMBER OF THEORETICAL PLATES PER METER FOR THE CROWN ETHER CAPILLARY COLUMNS

Stationary Phase	I.D.(mm)/ Length (m)	Phase Transition Temperatures	Min./Max. Operating Temperatures	% U.T.E./ Plates per meter (Column temperatures)
Vinylmethylsila-17-crown-6	0.42/18	40°C-70°C	>70°C/100°C	20%/943(75°C)
Vinylmethylsila-14-crown-5	0.40/16	40°C, 70°C-80°C	>70°C/154°C	16%/794(109°C)
Poly(vinylbenzo-15-crown-5)	0.32/20	75°C(67°C,73°C)* 110°C,150°C	150°C/220°C	13%/667(180°C)

* Phase transition determined by DSC.

TABLE XII

PARTITION RATIOS (k'), RETENTION INDICES (I), MCREYNOLDS' CONSTANTS (ΔI) AND AVERAGE POLARITY FOR THE MCREYNOLDS' PROBES ON EACH OF THE CROWN ETHER CAPILLARY COLUMNS ALONG WITH THE RETENTION INDICES AND MCREYNOLDS' CONSTANTS FOR CARBOWAX 20M (139)

		Benzene	n-Butanol	2-Pentanone	Nitropropane	Pyridine	Average Polarity
	ΔI	347	553	373	491	477	448
VMSi17C6	I	1000	1143	1000	1143	1176	
	k'	0.008	0.030	0.008	0.030	0.038	
	ΔI	243	398	280	378	359	327
VMSi14C5	I	896	988	907	1030	1058	
	k'	0.019	0.036	0.020	0.048	0.056	
	ΔI	382	564	439	648	595	526
PVB15C5	I	1035	1154	1066	1300	1294	
	k'	0.225	0.426	0.264	0.959	0.923	
	ΔI	322	536	368	572	510	462
Carbowax 20M	I	975	1126	995	1224	1209	

The maximum allowable operating temperature (MAOT) of each column was determined during a temperature program where a shift in baseline of 12 picoamps occurred. For the flame ionization detector of the Hewlett Packard 5880A gas chromatograph this corresponds to a 10% baseline shift at an attenuation of 2^3 where the sensitivity is 1.2×10^{-10} amps full scale. A carrier linear velocity of 25 cm/s and temperature program starting at 60°C with a 5°C/min temperature ramp were used for each column. This method is based on an arbitrary baseline shift which is set as a minimum of acceptable bleed. The MAOT for the silacrown ether columns at 100°C and 154°C were lower than expected. This could be due to incomplete polymerization of the vinyl groups in the silacrown ether. Thus the low MAOT results from bleed of the unpolymerized silacrown ether. Although NMR spectroscopy of the monomer solution emptied from the VMSi17C6 column after heat treatment showed no evidence of a polyethylene backbone, this, however, does not preclude copolymerization with MAPTMS on the column wall. The PVB15C5 column showed a much higher MAOT due to the polystyrene backbone which was confirmed by NMR spectroscopy.

To determine the utilization of theoretical efficiency and the number of plates per meter, van Deemter plots using 1-octanol as a probe were constructed (Figure 59). For each column, the oven temperature was adjusted so that the partition ratio of 1-octanol was as close as possible to 0.5. In each case this temperature was above the highest phase transition temperature. The values determined for the %UTE and the number of plates per meter were low when compared to values typical for commercially available polar columns. One possible cause for this low efficiency could be the numerous interaction sites present in the columns.

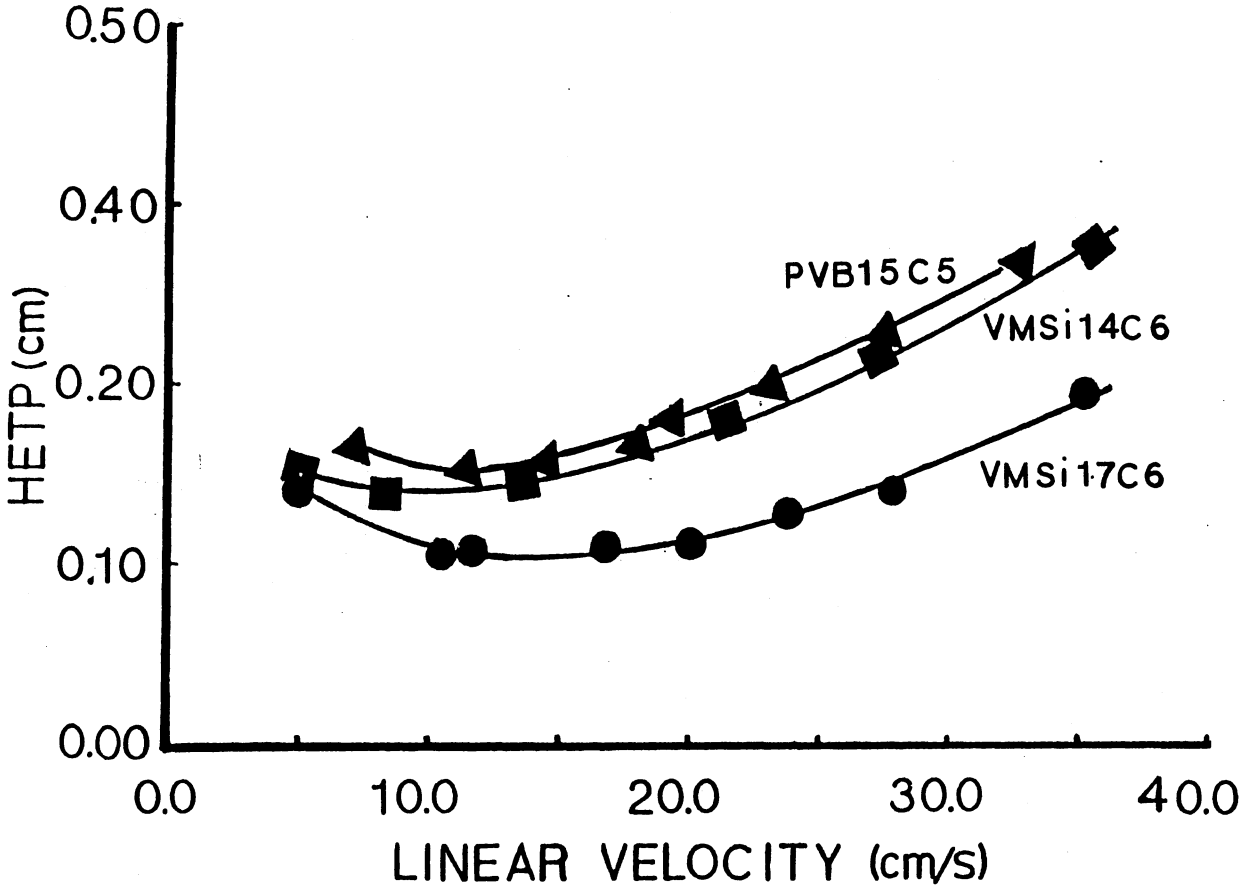

A column temperature of 180°C in the PVB15C5 column, 109°C in the VMSi14C5 column and 75°C in the VMSi17C6 column was used to obtain a partition ratio of 0.5 for 1-octanol in each column.

Figure 59. Relationship of HETP and Linear Velocity for 1-Octanol on VMSi17C6 Capillary (Column 6), VMSi14C5 Capillary (Column 7) and PVB15C5 Capillary (Column 8)

PVB15C5 has aromatic, aliphatic and polar sites which can interact with the probe used for the efficiency evaluation. In the silacrown ether columns, MAPTMS was added to copolymerize with the silacrown ether and bond it to the glass surface. From the adsorption of alcohols shown in Figure 27, this silane may have contributed more to band broadening and tailing than to stationary phase stability.

The choice of probe to evaluate efficiency can also be important. Figure 60 shows that on the PVB15C5 column, alkanes, the usual probe selected for column efficiency evaluation, did not exhibit the highest number of plates. For both theoretical and effective plate numbers, the more polar compounds, diols, provided higher numbers of plates than alcohols or alkanes. The column efficiency for each homologous series increased with each addition of a hydroxy group. This behavior could be due to the hydroxy groups interacting with the flexible crown ether which is located on the outside of the polymer and the methyl groups interacting with the more rigid aliphatic backbone within the polymer. This difference in flexibility at different sites and preference of sites by hydroxy or methyl groups could result in lower diffusion coefficients in the stationary phase for molecules containing methyl groups. If the diffusion coefficients for alkanes in PVB15C5 is lower than alcohols and diols, nonpolar solutes would exhibit lower efficiencies due to an increase in resistance to mass transfer in the liquid phase.

Measures of selectivity and polarity of the crown ether columns are given by the McReynolds' constants (ΔI), retention indices (I), partition ratios (k'), and average polarity in Table XII. The column temperature for these retention parameters was 120°C for the VMSi14C5 and PVB15C5 columns and 100°C for the VMSi17C6 column. The lower column

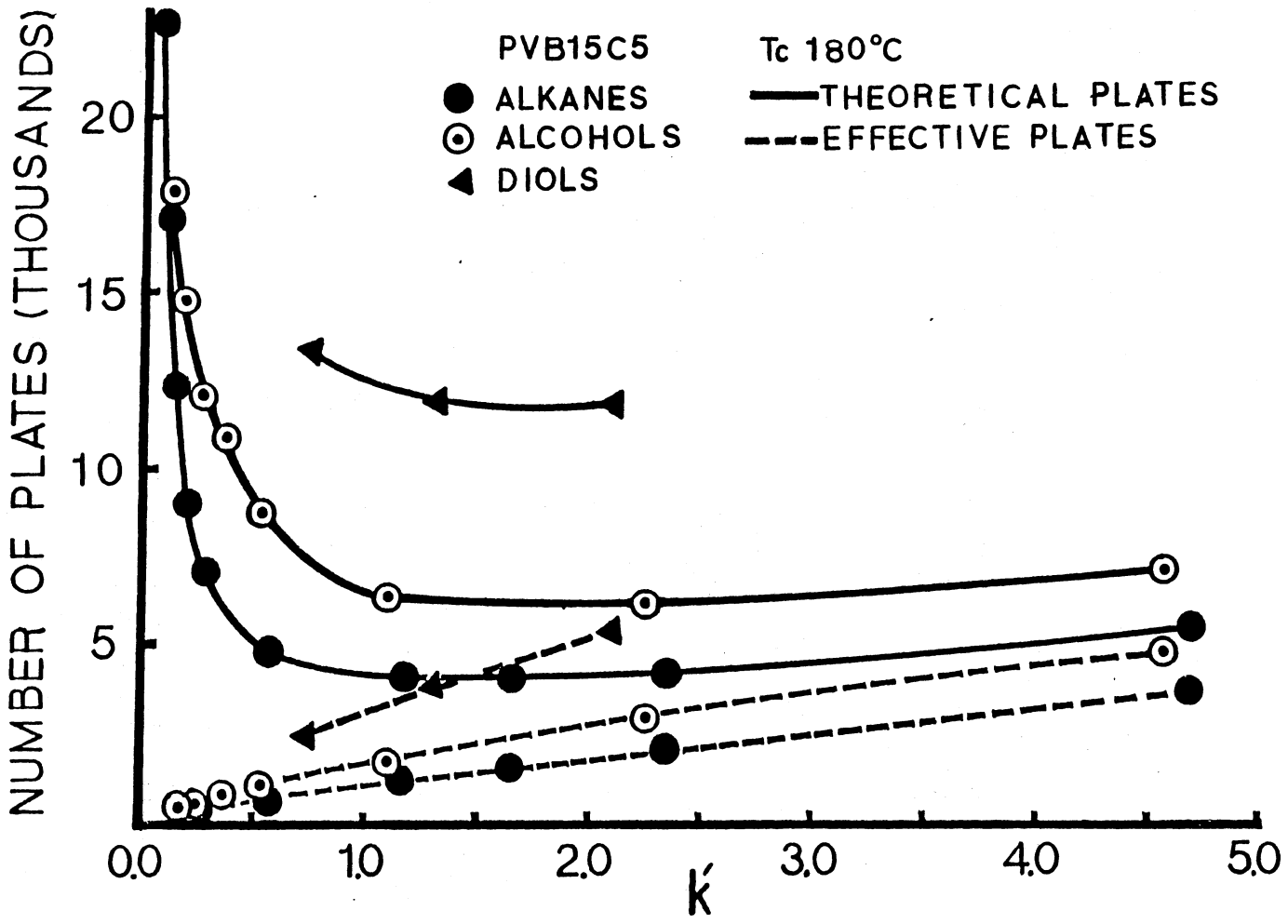

Figure 60. Relationship of Number of Theoretical and Effective Plates and k' for Alkanes, Alcohols and Diols on PVB15C5 Capillary (Column 8)

temperature was necessary in order to obtain a measurable partition ratio for the McReynolds' probes. Calculation of the McReynolds' constants for this column using the absolute retention indices of squalane at 120°C instead of 100°C should introduce errors of only 1-3% in each ΔI value (135-138). While the temperature for the retention indices determination of VMSi17C6 and VMSi14C5 columns were above their transition temperatures, the temperature for the indices determination of PVB15C5 was between the phase transition temperature at 110°C and 150°C. This means that the McReynolds' constants were determined when PVB15C5 was in a semi-liquid state which lacked the rapid backbone motion of the $T'_{\ell\ell'}$ state. The determination of McReynolds' constants for PVB15C5 at temperatures above the phase transition at 150°C requires retention indices for the probes from a squalane column at this temperature. This may not be possible as the recommended maximum operating temperature for squalane is 150°C on a packed column and 100°C on a capillary column.

Comparison of the values of the McReynolds' constants and the average polarity for the three crown ether columns with other stationary phases in McReynolds' table (139) shows that the crown ether phases have an average polarity which is similar to that of Carbowax 20M. The McReynolds' constants, retention indices and average polarity of Carbowax 20M are given in Table XII for comparison. Of the three crown ether columns, the PVB15C5 column has the highest polarity. This is due to the induced dipole interactions which the aromatic ring contributes to the overall polarity. The lower polarity of the silacrown ether columns is due to the weaker induction interactions of any nonpolymerized vinyl groups which may be present and weak dispersion interactions of the methyl groups. The higher polarity of the VMSi17C6 column over the VMSi14C5 is

due to the increased number of ethyleneoxy linkages in the crown ring.

The retention indices also indicate that the PVB15C5 column elutes the McReynolds' probes in the same sequence as Carbowax 20M. The sila-crown ether columns differ from this sequence in that 1-nitropropane and pyridine switch elution order. The polarity and selectivity of the PVB15C5 column is also evident in Figure 61 where log k' versus boiling point is plotted for homologous series of diols, alcohols, and alkanes. In addition to the expected linearity within each homologous series, the plot shows selective retention of compounds which have the same boiling point but differ in increasing polarity. This behavior is typical of polar columns where retention of compounds is determined more by their polarity than by their boiling point.

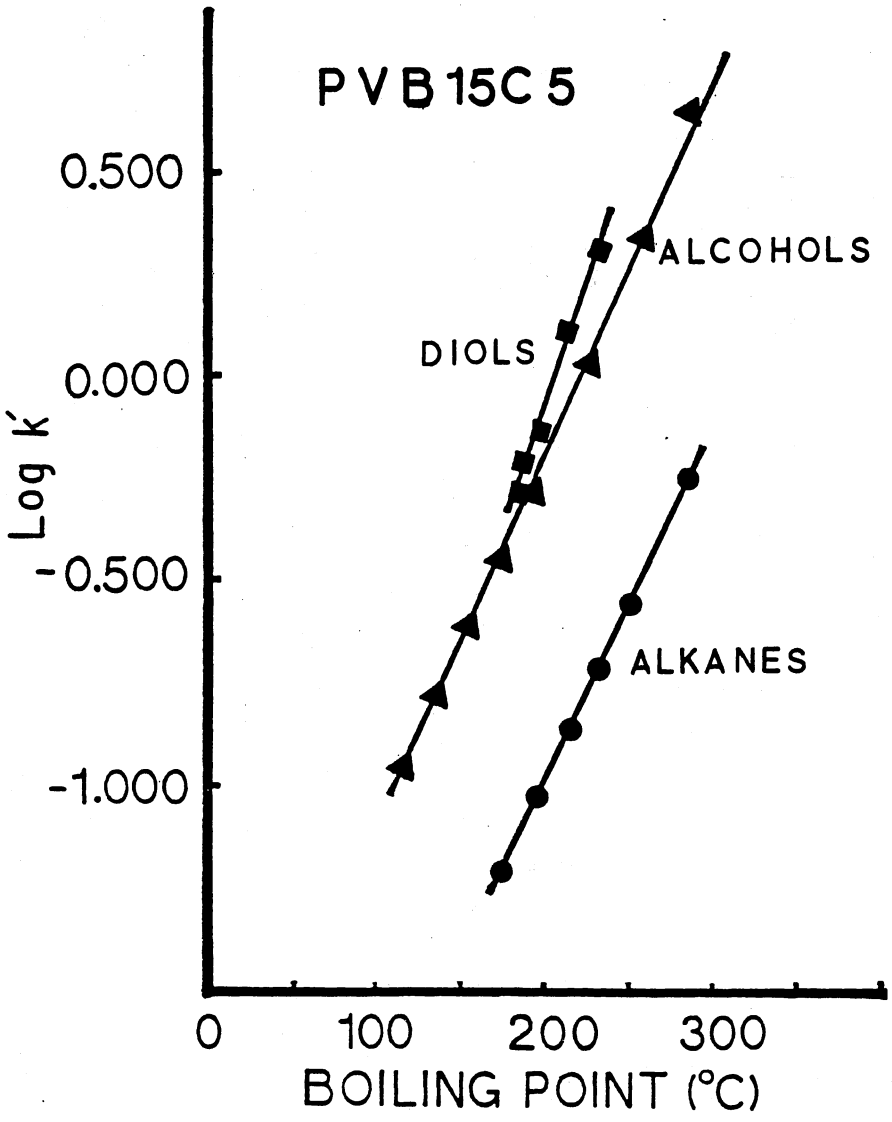

Figure 61. Relationship of log k' and Boiling Point of Alkanes, Alcohols and Diols for PVB15C5 Capillary (Column 8)

CHAPTER VI

SUMMARY AND CONCLUSIONS

The preparation and characterization of glass capillary columns containing polystyrene, vinylmethylsila-17-crown-6, vinylmethylsila-14-crown-5 and polyvinylbenzo-15-crown-5 has been presented. The characterization of the crown ether columns using McReynolds' constants and retention indices revealed that the crown ether columns had an average polarity which was similar to Carbowax 20M. The polarity of PVB15C5 was also evident in the comparison of partition ratios and boiling points of different classes of compounds. Here, diols, alcohols and alkanes which had similar boiling points exhibited different retention with the more polar compounds having the higher retention. Although the diols and alcohols had higher retention than the alkanes, the efficiency of the diols and alcohols was higher than the alkanes. This behavior which was also observed in the VMSi14C5 column can be attributed to the difference in solubility of the probes in the crown ether stationary phase. When the solubility is high as in the case of the diols, retention is dominated by partitioning. With low solubility, adsorption at the gas-liquid interface occurs and increased band broadening results.

Characterization of the capillaries using log k' versus 1/T plots revealed much about the temperatures of the phase changes in the crown ethers. The transitions for VMSi17C6 and VMSi14C5 which occurred at temperatures between 30°C and 70°C were probably liquid-liquid transi-

tions of the ethyleneoxy linkages in the crown ether. The first transition in PVB15C5 at 75°C may be due to a second order glass phase transition. The transition at 110°C and 145 - 150°C could be due to liquid-liquid transitions of the polystyrene backbone of the polymer.

Differential scanning calorimetry of PVB15C5 confirmed only one of the three phase transitions which were observed during the gas chromatography experiment. This showed that gas chromatography could be used not only as a complimentary technique to determine phase transitions but also to reveal phase changes which were not observable with DSC.

Although the crown ethers which were chosen were less than ideal, the separation of alcohols and alkanes which were obtained from capillaries containing these phases showed that crown ethers do have potential as stationary phases in gas chromatography. Liabilities which were observed could be eliminated by incorporating crown ethers into polymers which have low melting points such as polysiloxanes or polyethylene glycols. Structures of these polymers and a linear polymeric crown ether which may have potential are given in Figure 62.

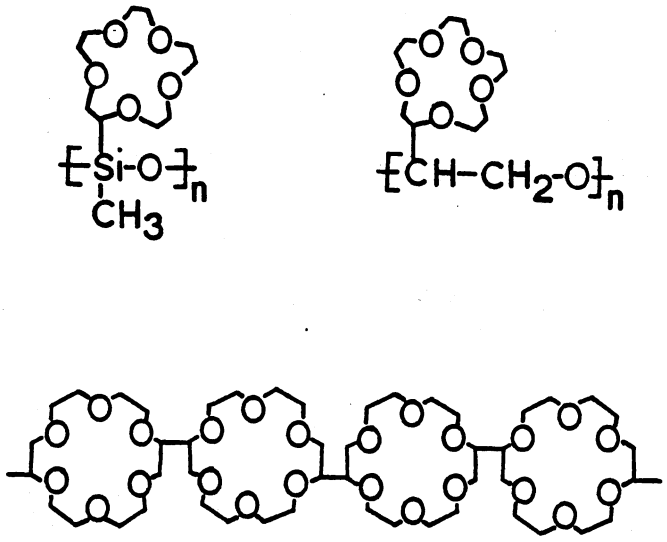

Figure 62. Proposed Crown Ether Stationary Phases

BIBLIOGRAPHY

1. Golay, M. J. E., Progress Report on Gas Chromatographic Experimental Work for September and October 1956, Perkin-Elmer Corp., Norwalk, Conn.

2. Golay, M. J. E., in Gas Chromatography 1958, D. E. Desty (Ed.), Butterworths, London, 1958, p. 36.

3. Karger, B. L., Snyder, L. R., and Horvath, C., An Introduction to Separation Science, Wiley Interscience, New York, New York, 1973.

4. Schomburg, G., Behlau, H. Dielmann, R., Weeke, F. and Husmann, H., J. Chromatogr., 142, 87 (1977).

5. Grob, K. and Grob, Jr., K., J. High Resolut. Chromatogr. Chromatogr. Commun., 1, 57 (1978).

6. Grob, K., J. High Resolut. Chromatogr. Chromatogr. Commun., 1, 263 (1978).

7. Purcell, J. E., Chromatographia, 15, 548 (1982).

8. Grob Jr., K. and Neukom, J. High Resolut. Chromatogr. Chromatogr. Commun., 2, 15 (1979).

9. Grob, K. and Grob, G., J. High Resolut. Chromatogr. Chromatogr. Commun., 6, 133 (1983).

10. Supelco, Inc., G. C. Bulletin 814, Supelco Park, Bellefonte, Pa., 1984.

11. Bombick, D. and DiNunzio, J., Chromatographia, 14, 19 (1981).

12. Ettre, L. S., Open Tubular Columns in Gas Chromatography, Plenum Press, New York, New York, 1965.

13. Desty, D. H., Haresnape, J. N., Whyman, B. H. F., Anal. Chem., 32, 302 (1960).

14. Dandeneau, R. D. and Zerenner, E. H., J. High Resolut. Chromatogr. Chromatogr. Commun., 2, 351 (1979).

15. Wright, B. W., Lee, M. L., Graham, S. W., Phillips, L. V., Hercules, D. M., J. Chromatogr., 199, 355 (1980).

16. Armistead, C. G., Taylor, A. J., Hambleton, F. H., Mitchell, S. A., Hockey, J. A., J. Phys. Chem., 73, 3947 (1967).

17. Zhuravlev, L. T. and Kisselev, A. V., Russ. J. Phys. Chem., 39, 236 (1965).

18. Bather, J. M. and Gray, R. A. C., J. Chromatogr., 122, 159 (1976).

19. Onuska, F. I., Afghan, B. K., Wilkinson, R. J., J. Chromatogr., 158, 83 (1978).

20. Simon, J. and Szepesy, L., J. Chromatogr., 119, 495 (1976).

21. Heckman, R. A., Green, C. R., Best, F. W., Anal. Chem., 50, 2157 (1978).

22. Kiselev, A. V., in Gas Chromatography 1962, M. van Swaay (Ed.), Butterworths, London, 1962.

23. Mohnke, H. and Saffert, W., in Gas Chromatography 1962, M. van Swaay (Ed.), Butterworths, London, 1962.

24. Bruner, F. A. and Cartoni, G. P., Anal. Chem., 36, 1522 (1964).

25. Peters, T. L., Nestrick, T. J., Lamparski, L. L., Anal. Chem., 54, 2397 (1982).

26. Onuska, F. I., Comba, M. E., Bistricki, T., Wilkinson, R. J., J. Chromatogr., 142, 117 (1977).

27. Schieke, J. D., Comins, N. R., Pretorius, V., J. Chromatogr., 112, 97 (1975).

28. Masada, A. Y., Hashimoto, K., Inoue, T., Sumida, Y., Sishi, T., Suwa, Y., J. High Resolut. Chromatogr. Chromatogr. Commun., 2, 400 (1979).

29. Tesarik, K. and Novotny, M., in Gas Chromatographie 1968, H. G. Struppe (Ed.), Akademie-Verlag, Berlin, 1968.

30. Watanbe, C. and Tomita, H., J. Chromatogr. Sci., 13, 123 (1975).

31. Franken, J. J., Rutten, G. A. F. M., Rijks, J. A., J. Chromatogr., 126, 117 (1976).

32. Grob, K. and Grob, G., J. Chromatogr., 125, 471 (1976).

33. Vidal-Madjar, C., Bekassy, S., Gonnord, M. F., Arpino, P., Guiochon, G., Anal. Chem., 49, 768 (1977).

34. German, A. L. and Horning, E. C., J. Chromatogr. Sci., 11, 76 (1973).

35. Pellizzari, E. D., J. Chromatogr., 92, 299 (1974).

36. Badings, H. T., van der Pol, J. J. G., Wassink, J. G., J. High Resolut. Chromatogr. Chromatogr. Commun., 2, 297 (1979).

37. Schulte, E., Chromatographia, 9, 315 (1976).

38. Torline, P. and Schnautz, N., J. High Resolut. Chromatogr. Chromatogr. Commun., 1, 301 (1978).

39. Grob, K., Grob, G., Grob Jr., K., Chromatographia, 10, 181 (1977).

40. Lee, M. L., Vassilaros, D. L., Phillips, L. V., Hercules, D. M., Azumaya, H., Jorgenson, J. W., Maskarinec, M. P., Novotny, M., Anal Lett., 12, 191 (1979).

41. Metcalfe, L. D. and Martin, R. J., Anal. Chem., 39, 1204 (1967).

42. Rutten, G. A. F. M. and Luyten, J. A., J. Chromatogr., 74, 177 (1972).

43. Sandra, P. and Verzele, M., Chromatographia, 10, 419 (1977).

44. Cronin, D. A., J. Chromatogr., 97, 263 (1974).

45. Blomberg, L., J. Chromatogr., 115, 365 (1975).

46. Verzele, M., J. High Resolut. Chromatogr. Chromatogr. Commun., 2, 647 (1979).

47. Schomburg, G., Husmann, H., Borwitzky, H., Chromatographia, 12, 651 (1979).

48. Novotny, M., Blomberg, L., Bartle, K. D., J. Chromatogr. Sci., 8, 390 (1970).

49. Welsch, T., Engewald, W., Klaucke, C., Chromatographia, 10, 22 (1977).

50. Grob, K., Grob, G., Grob Jr., K., J. High Resolut. Chromatogr. Chromatogr. Commun., 2, 31 (1979).

51. Lee, M. L., Wright, B. W., Graham, S. W., Hercules, D. M., ExpoChem, Houston, October 22nd, 1979.

52. Dijkstra, G. and de Goey, J., in Gas Chromatography 1958, D. H. Desty (Ed.), Academic Press, New York, 1958.

53. Levy, R. L., Murray, D. A., Gesser, H. D., Hougen, F. W., Anal. Chem., 40, 459 (1968).

54. McConnell, M. L. and Novotny, M., J. Chromatogr., 112, 559 (1975).

55. Schomburg, G. and Hussmann, H., Chromatographia, 8, 517 (1975).

56. Fairbrother, F. and Stubbs, A. E., J. Chem. Soc., 527 (1935).

57. Roeraade, J., Chromatographia, 8, 511 (1975).

58. Blomberg, L., J. Chromatogr., 138, 7 (1977).

59. Grob, K. and Grob, G., Chromatographia, 4, 422 (1971).

60. Golay, M. J. E., in Gas Chromatography 1958, D. H. Desty (Ed.), Academic Press, New York, 1958.

61. Giabbai, M., Shoults, M., Bertsch, W., J. High Resolut. Chromatogr. Chromatogr. Commun., 1, 277 (1978).

62. Grob, K., J. High Resolut. Chromatogr. Chromatogr. Commun., 1, 93 (1978).

63. Grob, K. and Grob, G., J. High Resolut. Chromatogr. Chromatogr. Commun., 5, 119 (1982).

64. Jennings, W. G., Yabunoto, K., Wohleb, R. H., J. Chromatogr. Sci., 12, 344 (1974).

65. Onuska, F. I., J. Chromatogr., 289, 207 (1984).

66. Harrison, I. T., Anal. Chem., 47, 1211 (1975).

67. Grob, K., J. Chromatogr., 211, 243 (1981).

68. Grob, K. and Grob, G., J. Chromatogr., 213, 211 (1981).

69. Wright, B. W., Peaden, P., Lee, M. L., Stark, T. J., J. Chromatogr., 248, 17 (1982).

70. Richter, B. E., Kuel, J. C., Park, N. J., Crowley, S. J., Bradshaw, J. S., Lee, M. L., J. High Resolut. Chromatogr. Chromatogr. Commun., 6, 371 (1983).

71. Schomburg, G., Husmann, H., Ruthe, S., Herraiz, M., Chromatographia, 15, 599 (1982).

72. Bertsch, W., Pretorius, V., Pierce, M., Thompson, J. C., Schnautz, N. G., J. High Resolut. Chromatogr. Chromatogr. Commun., 5, 432 (1982).

73. Supina, W. R., "Columns and Column Selection in Gas Chromatography", in Modern Practice of Gas Chromatography, R. L. Grob (Ed.), Wiley-Interscience, New York, New York.

74. Jennings, W. J., Gas Chromatography with Glass Capillary Columns, Academic Press, New York, New York, 1978.

75. Lee, M. L., Yang, F. J., Barlte, K. D., Open Tubular Column Gas Chromatography: Theory and Practice, Wiley-Interscience, New York, New York, 1984.

76. Martin, A. D. J. and Synge, R. L. M., J. Biochem., 35, 1358 (1941).

77. Gueuckauf, E., Trans. Faraday Soc., 51, 34 (1955).

78. Purnell, H., Gas Chromatography, Wiley and Sons, Inc., N. Y., 1967.

79. Purnell, H., J. Chem. Soc. (London), 1268 (1960).

80. Guiochon, G., J. Gas Chromatog., 2, 139 (1964).

81. James, A. T. and Martin, A. T. P., J. Biochem., 50, 679 (1952).

82. Giddings, J. C., Seager, S. L., Stucki, L. R., Stewart, G. M., Anal. Chem., 32, 867 (1960).

83. Desty, D. H., Goldup, A., Swanton, W. T., in Gas Chromatography (1951 Lansing Symposium), N. Brenner, J. E. Callen and M. D. Weiss (Eds.), Academic Press, New York, 1962.

84. Kaiser, R. E., Chromatographia, 9, 337 (1976).

85. Kaiser, R. E., Chromatographia, 9, 463 (1976).

86. Kaiser, R. E., Chromatographia, 9, 644 (1976).

87. Kaiser, R. E., Chromatographia, 10, 323 (1977).

88. Kaiser, R. E., Chromatographia, 10, 455 (1977).

89. Kaiser, R. E., Chromatographia, 11, 257 (1978).

90. Kaiser, R. E., J. High Resolut. Chromatogr. Chromatogr. Commun., 2,

91. Nilsson, O., J. High Resolut. Chromatogr. Chromatogr. Commun., 2, 720 (1979).

92. Said, A. S., J. High Resolut. Chromatogr. Chromatogr. Commun., 1, 203 (1978).

93. Franken, J. J., Chromatographia, 9, 643 (1976).

94. Sternberg, J. C., in Advances in Chromatography, Vol. 2, J. C. Giddings and R. A. Keller (Eds.), Dekker, N. Y., 1966.

95. Guiochon, G., Chromatographia, 11, 249 (1978).

96. Smuts, T. W., Buys, T. S., de Clerk, K., du Toit, T. G., J. High Resolut. Chromatogr. Chromatogr. Commun., 1, 41 (1978).

97. Smuts, T. W., Buys, T. S., de Clerk, K. and du Toit, T. G., J. High Resolut. Chromatogr. Chromatogr. Commun., 2, 456 (1979).

98. Nilsson, O., J. High Resolut. Chromatogr. Chromatogr. Commun., 2, 147 (1979).

99. Nilsson, O., J. High Resolut. Chromatogr. Chromatogr. Commun., 2, 191 (1979).

100. Nilsson, O., J. High Resolut. Chromatogr. Chromatogr. Commun., 2, 605 (1979).

101. Giddings, J. C., Dynamics of Chromatography, Part I, Dekker, N. Y., 1965.

102. Golay, M. J. E., in Gas Chromatography, 1958, D. H. Desty (Ed.), Butterworth, London, 1959.

103. Desty, D. H. and Goldup, A., in Gas Chromatography, 1960, R. B. Scott (Ed.), Butterworth, London, 1959.

104. Ettre, L. S. and Purcell, J. E., Advan. Chromatogr., 10, 1 (1974).

105. Cramers, C. A., Wijnheijmer, F. A., Rijks, J. A., Chromatographia, 12, 643 (1979).

106. Cramers, C. A., Wijnheijmer, F. A., Rijks, J. A., J. High Resolut. Chromatogr. Chromatogr. Commun., 2, 329 (1979).

107. Giddings, J. C., Anal. Chem., 36, 741 (1964).

108. Ettre, L. S., Chrom. Rev., 165, 235 (1979).

109. Said, A. S., J. Gas Chromatogr., 2, 60 (1964).

110. Knox, J. H., J. Chem. Soc., 433 (1961).

111. Said, A. S., J. Sep. Science & Tech., 13, 647 (1978).

112. Said, A. S., J. High Resolut. Chromatogr. Chromatogr. Commun., 2, 193 (1979).

113. Kaiser, R. E., Z. Analyt. Chem., 189, 1 (1962).

114. Ettre, L. S. and March, E. W., J. Chromatogr., 91, 5 (1974).

115. Kaiser, R. E., J. High Resolut. Chromatogr. Chromatogr. Commun., 2, 91 (1979).

116. McNair, H. M. and Bonelli, E. J., Basic Gas Chromatography, Varian Aerograph, Walnut Creek, Ca., 1968.

117. Schieke, J. D. and Pretorius, V., J. Chromatogr., 132, 223 (1977).

118. Said, A. S., J. High Resolut. Chromatogr. Chromatogr. Commun., 2, 253 (1979).

119. Grubner, O., Anal. Chem., 43, 1934 (1971).

120. Grubner, O., Advances in Chromatography Vol. 6, J. Giddings and R. Keller (Eds.), Dekker, N. Y., 1968.

121. Gruska, E., Myers, M. N., Schettler, P. D., Giddings, J. C., Anal. Chem., 41, 889 (1969).

122. Chesler, S. N. and Cram, S. P., Anal. Chem., 43, 1922 (1971).

123. Chesler, S. N. and Cram, S. P., Anal. Chem., 44, 2240 (1972).

124. Cram, S. P., Yang, F. J., Brown, A. C., Chromatographia, 10, 397 (1977).

125. Grob Jr., K., Grob, G., Grob, K., J. Chromatogr., 156, 1 (1978).

126. Onuska, F. I. and Comba, M. E., Chromatographia, 10, 498 (1977).

127. Grob, K. and Grob, G., Chromatographia, 4, 422 (1971).

128. Schomburg, G., Husmann, H., Weeke, F., Chromatographia, 10, 580 (1977).

129. Grob, K. and Grob, G., J. High Resolut. Chromatogr. Chromatogr. Commun., 1, 302 (1978).

130. Hartigan, M. J. and Ettre, L. S., J. Chromatogr., 119, 187 (1976).

131. Hartigan, M. J., Billieb, K., Ettre, L. S., Chromatographia, 10, 571 (1977).

132. Guillet, J. E., Advances in Analytical Chemistry and Instrumentation V. 11, New Developments in Gas Chromatography, H. Purnell (Ed.), John Wiley & Sons, New York, 1973.

133. Lavoie, A. and Guillet, J. E., Macromolecules, 2, 443 (1969).

134. Blomberg, L. and Wannman, T., J. Chromatogr., 148, 379 (1978).

135. Ettre, L. S., Chromatographia, 6, 489 (1973).

136. Ettre, L. S., Chromatographia, 7, 39 (1974).

137. Ettre, L. S., Chromatographia, 7, 261 (1974).

138. Kovats, E., Helv. Chim. Acta, 41, 1915 (1958).

139. McReynolds, W. O., J. Chromatogr. Sci., 8, 685 (1970).

140. Kolthoff, I. M., Anal. Chem., 51, 1R (1979).

141. Yoshio, M. and Noguchi, H., Anal. Lett., 15(A15), 1197 (1982).

142. Kimura, K. and Shono, T., J. Liq. Chromatogr., 5, 223 (1982).

143. Elbasyouny, A., Brügge, H. J., von Deuten, K., Dickel, M., Knöchel, A., Koch, K. U., Kopf, J., Melzer, D., Rudolph, G., J. Am. Chem. Soc., 105, 6568 (1983).

144. Watson, W. H., Galloy, J., Grossie, D. A., Vögtle, F., Müller, W. M., J. Org. Chem., 49, 347 (1984).

145. van Zon, A., de Jong, F., Reinhoudt, D. N., Torny, G. J., Onwezen, Y., Recveil, J. Royal Neth. Chem. Soc., 100/12, 453 (1981).

146. Kopolow, S., Hogen Esch, T. E., Smid, J., Macromolecules, 6, 133 (1973).

147. Odian, G., Principles of Polymerization, Wiley-Interscience, New York, 1983.

148. Parish, W. W., Stott, P. E., McCausland, C. W., Bradshaw, J. S., J. Org. Chem., 43, 4577 (1978).

149. Dow Corning. Information About Organofunctional Chemicals. Z-6030 Silane. Form No. 23-230-76.

150. Gearhart, H., Bruke, M., J. Chrom. Sci., 15, 1 (1977).

151. Laub, R. J. and Pecsok, R. L., Physicochemical Applications of Gas Chromatography, J. Wiley & Sons, New York, New York, 1978.

152. Goedert, M. and Guiochon, G., Anal. Chem., 42, 962 (1970).

153. Guillet, J. E. and Stein, A. N., Macromolecules, 3, 102 (1970).

154. Courval, G. and Gray, D. G., Macromolecules, 8, 326 (1975).

155. Billmeyer Jr., F. W., Textbook of Polymer Science, Wiley-Interscience, New York, New York, 1971.

156. Boyer, R. F., J. Macromol. Sci. Phys., B18(3), 461 (1980).

157. Enns, J. B., Boyer, R. F., Ishida, H., Koenig, J. L., Polymer Eng. Sci., 19, 756 (1979).

158. Wunderlich, B., "The Basis of Thermal Analysis", in Thermal Characterization of Polymeric Materials, E. A. Turi (Ed.), Academic Press, New York, New York, 1981.

159. Gillham, J. K., J. Macromol. Sci. Phys., B13(3), 497 (1977).

VITA 2

Dennis Dale Fine

Candidate for the Degree of

Doctor of Philosophy

Thesis: THE PREPARATION AND CHARACTERIZATION OF GLASS CAPILLARY GAS CHROMATOGRAPHY COLUMNS CONTAINING CROWN ETHER STATIONARY PHASES

Major Field: Chemistry

Biographical:

Personal Data: Born in Sallisaw, Oklahoma, October 22, 1950, the son of Harold D. and Madeleine Fine. Married to Anne E. Scott on June 9, 1979. Benjamin T. Fine was born to Anne and Dennis on September 21, 1980.

Education: Graduated from Sallisaw High School, Sallisaw, Oklahoma, in May, 1968; received Bachelor of Science Degree in Chemistry from Oklahoma State University in July, 1977; completed requirements for the Doctor of Philosophy Degree at Oklahoma State University in December, 1984.

Professional Experience: Personnelman, U. S. Navy, Navy Recruiting Command, Arlington, Virginia, 1972 to 1976; Teaching Assistant, Department of Chemistry, Oklahoma State University, August, 1977, to May, 1984; Member of Phi Lambda Upsilon and American Chemical Society.